Politecnico di Milano
Department of Mechanical Engineering
Doctoral Programme In Mechanical Engineering

Modeling of tank vehicle dynamics by fluid sloshing coupled simulation

Doctoral Dissertation of:
Vincenzo D'Alessandro

Supervisor:
Prof. Federico Cheli

Tutor:
Prof. Alfredo Cigada

The Chair of the Doctoral Program:
Prof. Gianpiero Mastinu

2011 – XXIV

Contents

List of Figures

List of Tables

Sommario

Le forze generate dal movimento del liquido trasportato all'interno di un'autocisterna possono avere un'influenza significativa sulla stabilità e sulla dinamica di marcia del veicolo: lo sloshing in direzione laterale e gli improvvisi cambi di corsia sono la causa principale per l'abbassamento della soglia del ribaltamento mentre lo sloshing del fluido in direzione longitudinale, a seguito di una manovra di frenata o di accelerazione, può causare la perdita di controllo del veicolo.

Le interazioni tra la dinamica del liquido e quella del veicolo non sono state sufficientemente studiate, infatti gli studi pertinenti riportati in letteratura sono limitati o allo sviluppo di metodologie per la previsione dello sloshing del liquido in contenitori generici o all'analisi della stabilità del veicolo sulla base di modelli semplificati per il moto del liquido, come ad esempio modelli quasi-statici del movimento del fluido o modelli basati sull'analogia del pendolo.

In questo lavoro di tesi, un modello CFD per la dinamica dello sloshing è accoppiato con un modello a parametri concentrati di un veicolo. Il modello CFD è basato sulle equazioni di Navier-Stokes 3D che incorporano la tecnica Volume Of Fluid (VOF) per modellare due fluidi immiscibili risolvendo un unico set di equazioni di continuità e determinare la frazione di volume di ciascuno dei fluidi in tutto il dominio. La tecnica Moving Mesh (MM) è utilizzata per imporre il movimento alla cisterna, fornendo le velocità lineari ed angolari ad ogni passo temporale. Un modello di veicolo a 14 gdl è accoppiato con un modello CFD per valutare il comportamento del veicolo in una manovra di cambio di corsia, per indagare il comportamento del veicolo in una manovra di frenatura. In entrambi i casi sono state effettuate prove a diverse velocità e diversi livelli di riempimento, i risultati sono stati con-

frontati con i risultati sperimentali disponibili in letteratura. Inoltre la tilt table test è stata simulata per valutare l'influenza del livello di riempimento sulla accelerazione limite di ribaltmento statico.

Abstract

The forces generated by the sloshing of bulk liquid carried in tank trucks can have a significant influence on the vehicle's driving dynamics and stability: lateral fluid sloshing during turning and sudden lane change manoeuvres is the main cause for low rollover threshold while longitudinal fluid sloshing due to braking or accelerating manoeuvres can cause yaw instability or loss of directional control. The dynamic interactions between the liquid motion and vehicle stability has not been sufficiently investigated, in fact the relevant studies reported in literature are limited either in the development of methodologies for predicting the liquid slosh in various containers or in the analysis of vehicle stability based upon simplified models of liquid cargo motion without sufficient consideration of the dynamic slosh effect, such as quasi-static fluid motion or pendulum analogy technique. In this thesis, a computational fluid dynamics slosh model is coupled with a lumped truck model. The CFD model is based on the Navier-Stokes equations incorporating the Volume Of Fluid (VOF) technique to model two immiscible fluids by solving a single set of momentum equations and tracking the volume fraction of each of the fluids throughout the domain and the Moving Mesh (MM) technique to specify the motion of the tank by providing the linear and angular velocities at every time step. A 14 degrees of freedom truck model is coupled with the CFD model to evaluate the vehicle behavior in a lane change manoeuvre in a braking maneuver. In both cases tests have been made at different velocities and different fill volumes and compared with experimental results available in literature. Moreover the tilt table test have been simulated for different fill volume in order to assess the influence of the fill volume on the Static Rollover Threshold.

Introduction

Tank trucks are well known to constitute a hazard on road safety because of their low directional stability characteristics. In fact, during evasive maneuvers, they are likely involved in rollover accidents. This is partially confirmed by the statistics surveys, but quite evident by scientific analysis. Statistical survey of the US Department of Transportation (US DOT) reports that each year 1.300 tank trucks rollovers occur, $56,0\%$ of which occur on straight road, $50,0\%$ involve leaving road, $98,0\%$ occur on dry road and only in $28,0\%$ of time the driver was driving too fast [153, 154]. Moreover the $31,0\%$ of the fatalities in rollovers of commercial vehicles occurs among tank trucks [153, 154]. In Figure 1 is reported a US road sign for tank truck driver, it warns the driver about the hazardous of driving on specific road's stretch.

In general, rollover is the most serious accident, in fact, the statistics show that in about $70,0\%$ of times a fatality occurs when a heavy vehicle rolls over [136, 166]. Furthermore, tank trucks are frequently employed on transport of hazardous material (hazmat). When they are involved in rollover accidents, in $86,0\%$ of time hazmat's release occurs and in the $50,0\%$ of time fire and explosion [166, 244]. Due to the seriousness of the tank truck rollover carrying hazmat, a lot of risk assessment projects have been issued in North America (USA, Canada) [166, 244, 186]. In contrast, in EU a fewer number of studies have been funded in the past years: [1, 9, 7, 8]; these studies mainly deal with rigid cargo accident, and all of them confirm the low reliability of data collected in the main EU databases.

The risk assessments of accidents involving tank trucks carrying hazmat are mainly based on statistical survey. In general, all the reviewed reports agree on the bad reliability of the data collected in the databases. As matter

Figure 1: Limited speed risk of rollover. This road sign is meant for tank truck drivers.

of fact, the report is done by police officer and mainly they contain information based on evidences on the accidents‘ scenario or witnesses. It has been further speculated that some carriers due to fear of legal reprisal may distort the events leading to an accident [186]. Common information reported in the databases, can be used mainly to drawn general conclusions on one of the four main causal factors:human factor; vehicle factor; infrastructure factor; or environment factor. As result, all the databases agree very well that in $85,5\%$ of time the human factor, such as the driver error [166, 1], is the main factor of accident. In some cases teams of experts have been established to investigate on the accident‘s spot the main causes of the accident, very well accident reconstruction have been shown. In contrast, a limited number of accidents can be investigated reducing so the statistical validity of the survey.

Generally statistics don‘t show a high frequency of accidents involving tank trucks, in [166] an average number of 360 fatal accident [6] is in fact reported refer to Appendix A. which correspond to the $0,1\%$ of the whole fleet of tank trucks, see Appendix B; In another European study [1] a total of 624 accidents collected over 2,5 years study is reported, among which only 14 were carrying hazmat; In a Canadian study [244] a total of 1.874 accidents

involving tank truck from 1990 to 1998 is reported. Even though, the daily news show a different scenario, in fact at least one rollover each days occurs on USA road and in the majority of them a tank truck is involved; similar situation is showed on European roads. Moreover, the high economical losses associated with each rollover, about 150.000$ [166, 244] increases rapidly the total amount of yearly economic lost. In [244] has been estimated that 84.420.800C of total economic loses, from 1990 to 1998 on Canada.

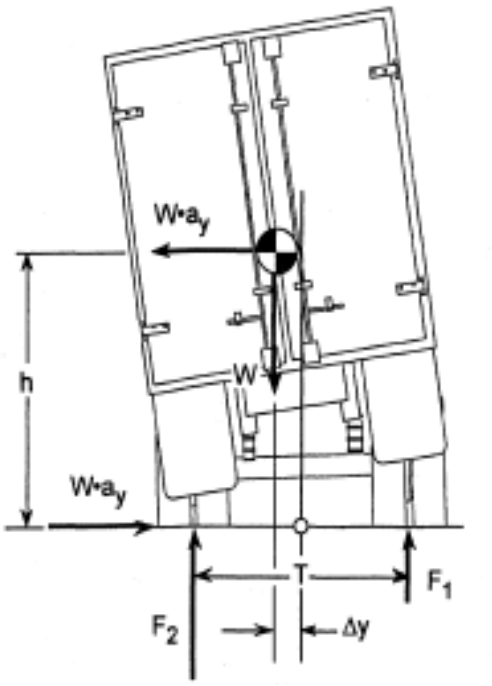

Figure 2: Simplified roll plain model of heavy vehicle, during steady turning.

Due to the low controllability limits, heavy vehicle are subject to rollover in special way during evasive maneuver. In fact, the centre of gravity of the trucks carrying rigid cargo is too high, compared to SUV or passenger car [148], this leads to a huge load transfer, in longitudinal direction as well as in lateral direction. The Static Rollover Threshold (SRT) is a measure of the lateral acceleration that leads to the lift of the inner curve side wheels during steady turning, expressed as fraction of the gravitational acceleration g. The SRT has been found to be suitable to predict the roll stability characteristics of heavy vehicles [243]. Neglecting tires and suspensions compliances a rough

estimation of the SRT is give by the Static Stability Factor ratio:

$$SSF = \frac{T}{2h}; \tag{1}$$

In Figure 2, T is the track width, h is the height of the centre of gravity; ay is the lateral acceletation; F_i is the vertical tire loads with $i = 1, 2;$, W is the weight of the vehicle and Δy is the lateral motion of the cg relative to the track. The influence of the cg height on the roll stability is clearly pointed out by the Static Stability Factor (SSF) equation (1); in fact increasing the h results in a reduction of the SSF. In many study, [148, 186, 177] has been shown the relationship between rollover crash frequency and rollover stability limits. Figure 3 shows the relationship between the SRT (Static Rollover

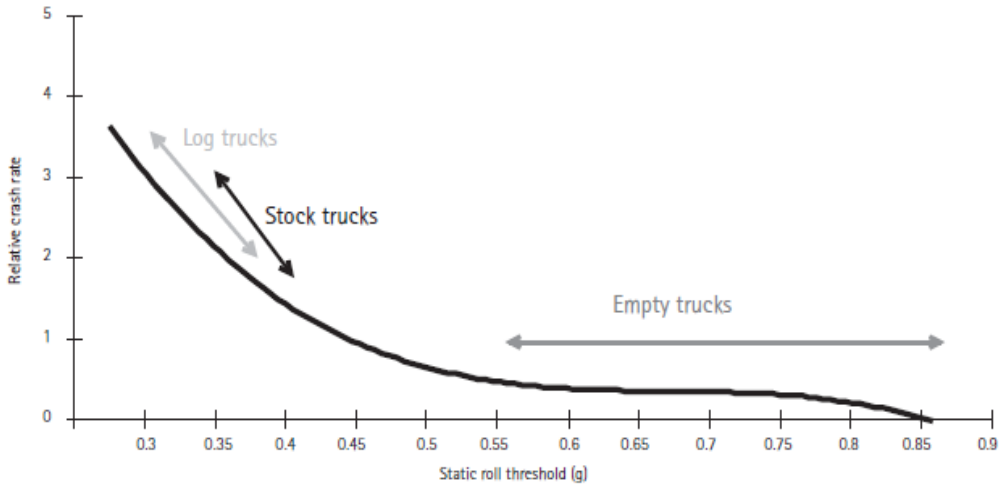

Figure 3: Relationship between rollover crash rate and Static Rollover Threshold

Threshold) and the rollover crash risk [148]. Vehicles with $0,3g$ of SRT have more than 3 times the probability of to be involved in rollover accidents, compared with vehicles with SRT of $0,5g$. A slightly increase of the SRT can improve drastically the rollover performance. A minimum value of $0,35g$ has been proposed for commercial freight to reduce the highway safety risk associated with the rollover accidents [186].

Compared to rigid cargo, the tank trucks' centre of gravity is further increased by the saddle support between the truck's chassis and the tank [166]. Moreover, due to the vehicle design, it has been found that the SRT range

Figure 4: Tanker Having Optimus Mass and Stability (THOMAS).

from $0,32g$ to $0,39g$ for tank truck carrying hazmat, showing a significant opportunity of improve vehicles stability by lowering the centre of gravity [244, 166]. Due to the significant role played by the cg height, in 1990 the Tanker Having Optimum Mass And Stability (THOMAS) see Figure 4, have been designed by the Hockney Trailers for the Australian Shell Petroleum Company [244]. In Table 1 have been reported the improvement in roll stability for the THOMAS and the European version TOPAS, compared with a standard DOT 306 used in North America. It is evident from Table 1 how an average reduction of cg height of $450mm$ can lead to an average stability improvement of the $35,0\%$. Beyond the stability other advantage like reduction of the fuel consumption, due to the drag reduction have been achieved.

Table 1: Stability comparison of tank trailers

Tanker **D**esing	**C**apacity (liters)	**C**enter of mass **h**eight (mm)	**R**ollover **t**hreshold (g)	**S**tability **I**mprovement
306 typical	38000	2100 - 2300	0.35 - 0.39	0%
TOPAS	39000	1700	0.50	35%
THOMAS	47000	1490	0.59	59%

In partly filled tank, the liquid sloshing determines an increase of the load transfer and an increase of the magnitude of the sloshing forces, so tank vehicles exhibit greater brake distance and less roll stability limits than heavy

vehicles hauling rigid cargo, or than tanker travelling in full load condition [148]. In fact, if the partly filled condition results in a reduction of the cg height, the liquid surge, in load condition between $40,0\%$ and $80,0\%$, can lead to high sloshing forces which severely reduce the rollover stability; during evasive maneuver the liquid surge can affect strongly the overall truck directional stability. While the influence of the cg height on the stability of vehicle hauling rigid loads has been widely investigated using classic mechanical models, the influence of the fluid surge on stability of tank trucks has not been completely investigated because is more complicated and so more sophisticated models have to be used [255, 186]. What make so difficult the modelling of the tank trucks dynamics is the dynamical interaction between the vehicle and the liquid cargo. In fact the dynamics of the the vehicle is strongly influenced by the sloshing force and by the shift of the liquid cg and vice versa. Vehicle and liquid cargo interact through the wetted wall exchanging mutual accelerations thus the overal dynamics cannot be modelled without modelling such mutual interaction which is really difficult to implement. Being, the equaitons of motion describing the vehicle dynamics and the one describing the liquid motion, solved in two different way doesn't exsists commericial code allowing in a easy way to implement such complicated system.

Along the years simplified model have been proposed, such like 'Quasi static model', whose main feature is to calculate with a good approximation the liquid cg shift as function of the external acceleration (see Figure 7). Many models have been proposed describing the longitudinal and the lateral dynamics. In a few cases the 3D dynamics has been modelled. Those methodology has the big advantage of to be easily implemented within vehicles equation of motion. Even though, the non-linear sloshing forces are completely neglected, moreover only simplified tank model can be considered [190]. Another methodology is based on the mechanical analogy, one degree of freedom waving mass have been used, which results agree very well with fluid behaviour. Moreover, pendulum model allowed a good description of the waving fluid under limited accelerations. In fact the main drawback presented by this methodology is a difficult in modelling the non-linear fluid

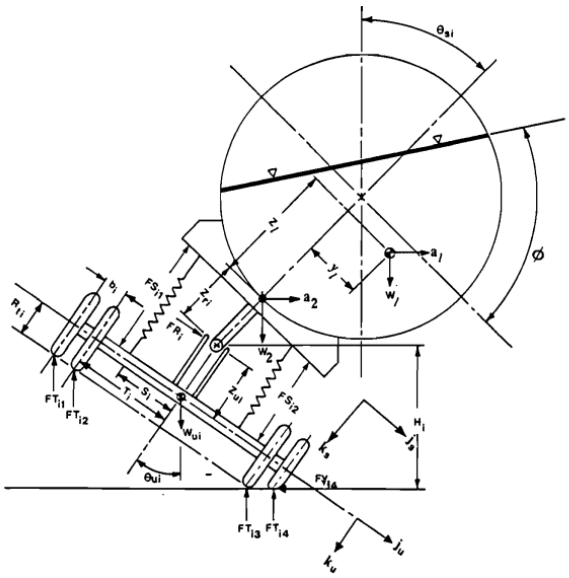

Figure 5: Schematic view of simplified Quasi Static Model of fluid sloshing in roll plane [190].

sloshing which stronglu affects the vehicle stability during evasive manoeuvre [25]. More recently with the advances in Computational Fluid Dynamics non-fluid sloshing models have been implemented to study the effects of the baffles without considering the vehicle dynamics. From those studies many insight have been gained on how to design the baffles [143].

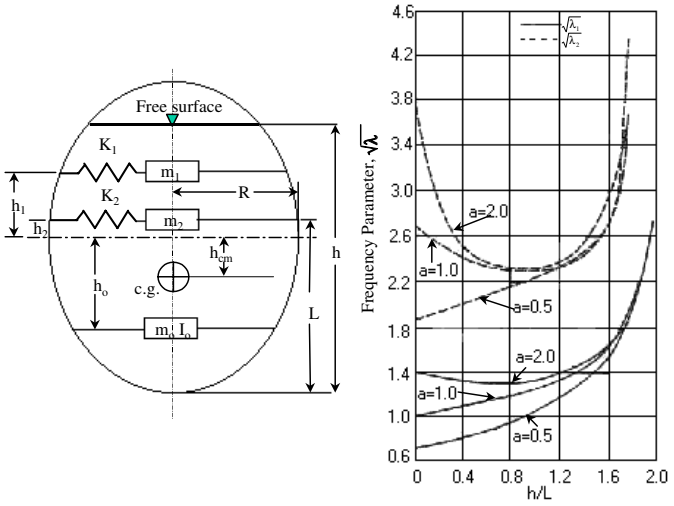

Figure 6: Schematic view of a waving masses used to Model the fluid sloshing.

Only recently a co-simulation approach has proposed to simulate the tank truck coupled dynamcs, the approach consiste in deviding into two subsistems the tank vehicle, allowing the simulation of each subsistem in a suitable computational environment, and than by an exchange process reconnects the two subsistems in order to simulate the coupled dynamics.

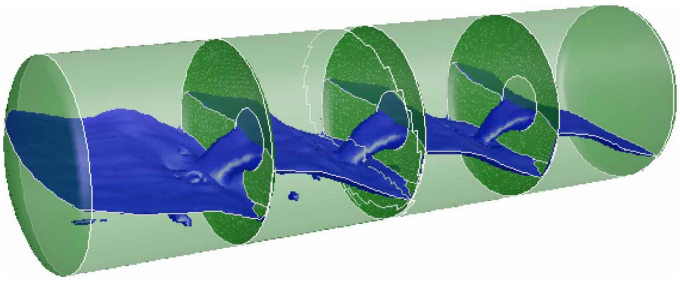

Figure 7: Pictorial view of fluid sloshing within a tank modelled by CFD.

In the present work a non-linear fluid sloshing-vehicle coupled dynamics will be investigated using a non-linear 3D fluid sloshing model in co-simulation with a 3D vehicle model (14 degrees of freedom). The application will be developed in FLUENT which is a CFD commercial code. The main puropose is to asses the influece of fluid sloshign on the vehicle dynamics, in braking as well as in cornering manoeuvre. Attention will be posed on the law limitations imposed by the standard design in order to investigate the validity of such standards, in particular on the SRT limitation imposed by ADR and on the operating conditions allowed by the ADR itself. A strong attention will be posed on the social impact of the potential hazard represented by the tank trucks travelling partialy filled.

Chapter 1

Liquid sloshing State of Arts

The liquid sloshing motion in moving containers has been widely studied since 1960s. Monograph edited by Abramson [10] presents a comprehensive view of liquid sloshing problems. However, it addresses only issues related to the space vehicle applications based on the experimental and theoretical approaches. Also, Salem et al. [204] presented a literature review of fluid-container interactions, with a particular focus on parameters that influence the stability of partly-filled tank trucks under various manoeuvres. Furthermore, Ibrahim et al. [95] performed an extensive review of research studies on sloshing phenomena in different applications such as liquid natural gas ship carriers, storage tanks, aerospace vehicles and road tankers. Since most of the available review publications in the field of liquid sloshing concern the issues associated with the aerospace and ocean vehicles as well as ground-supported structures, such as [97] and [61], theories and approaches for analysis of sloshing liquid cargo in partially-filled tank trucks along with its interaction with dynamics of such vehicles is explored in this section. Therefore, other issues related to aerospace technology (e.g. [23, 123] and [242]), low-gravity condition ([79, 235, 212] and [234]), ground storage tanks and elevated water towers (e.g. [224, 75, 132, 99] and [211]), use of liquid sloshing in structural control applications such as TLD and TMFD (e.g. [144, 210] and [156] and marine technology (e.g. [38] and [117]) are not discussed in this article. Also, for simulation of sloshing loads in tank trucks, liquid container deformations are generally negligible due to small deformations of container walls

compared to the rigid body translations ([202]). Therefore, the tank vehicle without the fluid cargo can be represented by a rigid body vehicle model in which forces and moments arising from the liquid sloshing are considered as the external forces and moments acting on the vehicle. Accordingly, research studies on liquid sloshing in flexible containers are not covered in this review (e.g. [214, 101] and [33]).

The basic problem of liquid sloshing involves the evaluation of sloshing forces and moments as well as natural frequencies of free liquid surface. In partially-filled tank trucks, these forces and moments are coupled with vehicle dynamics to illustrate the directional response and stability of heavy vehicles under external excitation. The magnitude of this external excitation is accentuated by operator-initiated manoeuvre such as lane change, braking and acceleration as well as road-induced disturbances. Fundamentally, studies on fluid sloshing in road containers involving liquid sloshing models and vehicle models can be performed by the three methods:

- quasi-static method;
- mechanical analogy method;
- dynamic liquid sloshing method.

In addition to these methods, the unique importance of experimental methods in investigation of liquid sloshing phenomenon and validation of computational methods should be taken into account. In the following sections, a brief review of those methods along with their features and limitations in the light of the results of studies on liquid sloshing in moving containers is discussed.

1.1 Quasi-Static Method

Quasi-static model is a conventional method for prediction of steady-state position of liquid free surface in moving containers. In this method, the location of the center of mass of the liquid cargo under different excitation is specified. It can be shown that the free liquid surface can be replaced

by a straight line or a flat surface. According to the lateral acceleration in the roll plane or longitudinal acceleration in the pitch plane, the free liquid surface location is calculated. Then, effect of steady state cargo load shift on directional dynamics performance of the vehicles is analyzed. Figure 1.1 shows the position of free surface in the roll plane model of a partially-filled tank truck. Conservation of momentum in the non-inertial frame of reference attached to the tank assuming incompressible homogeneous fluid under during steady turning yields:

$$-\rho g \sin\theta - \frac{\partial p}{\partial y} + (R - y\cos\theta)\omega^2 \rho \cos\theta = 0 \tag{1.1}$$

$$-\rho g \cos\theta - \frac{\partial p}{\partial z} - (R - y\cos\theta)\omega^2 \rho \sin\theta = 0 \tag{1.2}$$

Where ρ and p are the fluid density and pressure; g and ω are the gravitational and tank rotational velocity, respectively, and R is the distance between the rotational axis and origin of non-inertial frame of reference which is the bottom middle point of the tank. This set of equations contributes to a

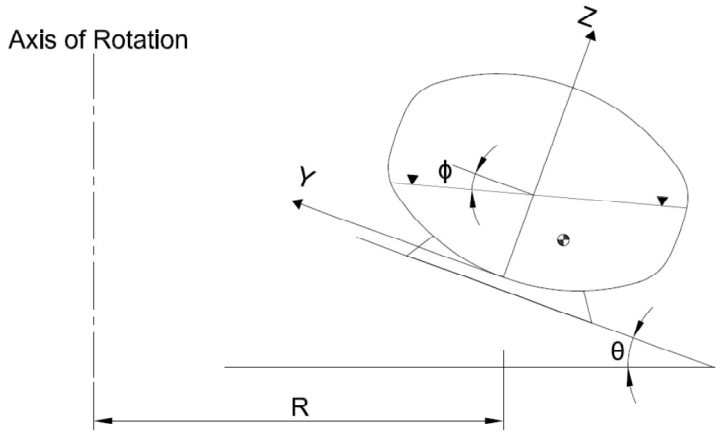

Figure 1.1: steady-state roll plane model of a partly filled tank truck.

parabolic free surface for small roll angles. However, for road containers with large radius track compared to the container width, the term $y\cos\theta$ can be neglected against R. Popov et all in [170] showed that inaccuracy caused by this approximation is negligible for evaluation of liquid free surface in tank

vehicles. Introducing lateral acceleration, ay, in equations (1.1) and (1.2) gives:

$$-\rho g \sin\theta - \frac{\partial p}{\partial y} + \rho a y \cos\theta = 0 \tag{1.3}$$

$$-\rho g \cos\theta - \frac{\partial p}{\partial z} - \rho a y \sin\theta = 0 \tag{1.4}$$

By letting $\partial p = 0$ at free surface, the following equation can be obtained for the free surface.

$$(-\rho g \sin\theta + \rho a y \cos\theta)dy + (-\rho g \cos\theta - \rho a y \sin\theta)dz = 0 \tag{1.5}$$

Two-dimensional roll plane model under steady-state turning yields the following equation for liquid free surface.

$$\frac{dz_s}{dy_s} = \frac{a y \cos\theta - g \sin\theta}{g \cos\theta + a y \sin\theta} \tag{1.6}$$

The free surface gradient assuming small roll angle can be expressed as:

$$\tan\phi = \frac{\frac{ay}{g} - \theta}{1 + \frac{ay}{g}} \tag{1.7}$$

Thus, free surface in the roll plane is a straight line with angle of Φ relative to its original position. The similar equation can be obtained for two-dimensional pitch plane under constant longitudinal acceleration.

$$\tan\phi_p = \frac{\frac{a_x}{g} - \theta_p}{1 + \frac{a_x}{g}\theta_p} \tag{1.8}$$

In which ϕ_p is the slope of liquid free surface in pitch plane, a_x is the longitudinal acceleration and θ_p is the pitch angle of tank. Based on the free surface gradient, liquid fill level and tank geometry, the translation of the center of mass of liquid bulk in longitudinal, lateral and vertical directions can be calculated. The coordinates of liquid center of mass in roll plane model can be obtained as follows:

$$Y = \frac{\int\int_\Omega y dy dz}{\int\int \Omega dy dz}, Z = \frac{\int\int_\Omega z dy dz}{\int\int \Omega dy dz}, \tag{1.9}$$

Where Ω is the liquid domain. For pitch plane model the coordinates of liquid center of mass can be computed from:

$$Y = \frac{\int\int_\Omega x dx dz}{\int\int \Omega dx dz}, Z = \frac{\int\int_\Omega z dx dz}{\int\int \Omega dx y dz}, \tag{1.10}$$

The quasi-static sloshing model is an efficient tool for evaluation of steady-state load shift due to liquid motion in tank vehicles. However, this method cannot provide the transient load shift resulted from the transient motion of liquid within the tank. Therefore, using of this method for simulation of liquid sloshing is almost limited to the studies of stability analysis of tank vehicles. In [206] and [184] the authors investigated the rollover immunity levels of articulated vehicles carrying cylindrical cleanbore and compartmented tank with partial loads during steady turning using the static roll plane model. The study concluded that partially filled cleanbore tank vehicles exhibit lower rollover threshold acceleration compared to the rigid cargo vehicles.

Ranganathan [190] and Rakheja [185] developed a quasi-static roll plane model for a partially-filled tank to calculate the forces and moments associated with the liquid movement. The vertical and lateral translation of center of mass of liquid bulk was computed during steady turning using an iterative algorithm for four different tank geometries; circular cross-section, elliptical cross-section, modified-oval cross-section and modified square cross-section. The static roll equilibrium equations were solved for small increments of roll angle until the trailer and tractor tires lift off the ground. The rollover threshold was determined by the highest lateral acceleration obtained during computation process. The proposed liquid sloshing model was used to investigate the influence of different tank geometries and liquid fill levels on rollover threshold of tank vehicles. They founded that circular tanks reveal greater stability limit with high density liquids while the modified oval and modified square tanks show higher rollover threshold with low density liquids for the same payload and composite axle loads.

Sankar [205] and Ranganathan [188] developed a three-dimensional vehicle model integrating with the quasi-static roll plane model to study the effects of liquid load shift in tank vehicles under steady steer input assuming constant speed. The equations of steady state fluid motion within two semitrailer tanks in the roll plane was integrated to the equations of yaw and roll motion of the articulated rigid cargo vehicle. The study demonstrated significant deviation in the path followed by the tank vehicle due to the liquid movement

under constant steer maneuver. Ranganathan et al. [191] employed a similar model illustrated in [188] to analyze the directional dynamics of a B-train tank vehicle considering partial load. Roll and acceleration response of the vehicle was examined under both constant and transient steer input including lane change and evasive maneuver. A simple computer program based on quasi-static analysis was developed by Southcombe et al. [220] to estimate the roll stability of partly-filled tank trailers for various tank geometries under steady state turning maneuvers. Toumi et al. [230] integrated the quasi-static model to a simplified vehicle model consisting one sprung mass and one unsprung mass with three degrees of freedom for sprung mass; lateral, yaw and roll. The results obtained from the study revealed a considerable lateral load shift in case of liquid cargo compared to rigid cargo for steady and transient steer manoeuvres.

Validation of steady-state fluid slosh model for prediction of directional response of tank vehicles was confirmed by the field test experiments performed by Rakheja et al. [183]. Their results demonstrate the capability of the two-dimensional analytical steady-state liquid sloshing model illustrated earlier by Rakheja et al., Sankar et al. and Ranganathan et al. [184, 205, 188], for prediction of the mean directional response of heavy vehicles (Figure 1.2). However, some deviations between the experimental data and analytical results can be attributed to neglecting the transient liquid motion in this method. Quasi-static model can also be employed for investigation of longitudinal load transfer in pitch plane. Ranganathan and Yang [189] studied the effect of steady state liquid load shift occurring within a partially filled cylindrical cleanbore tank on the braking characteristics of a tank vehicle. The vehicle was a five-axle tractor-tank-semitrailer unit represented by three composite axles subjected to constant deceleration and zero steer input. The effect of pitch angle on the free surface position was neglected. In addition, four different positions for liquid free surface resulted from braking maneuver were considered. An iterative numerical algorithm was developed to compute the position of liquid free surface under vehicle deceleration. According to the position of free surface, location of liquid center of mass and corresponding liquid load shift were calculated. The study showed that the load shift

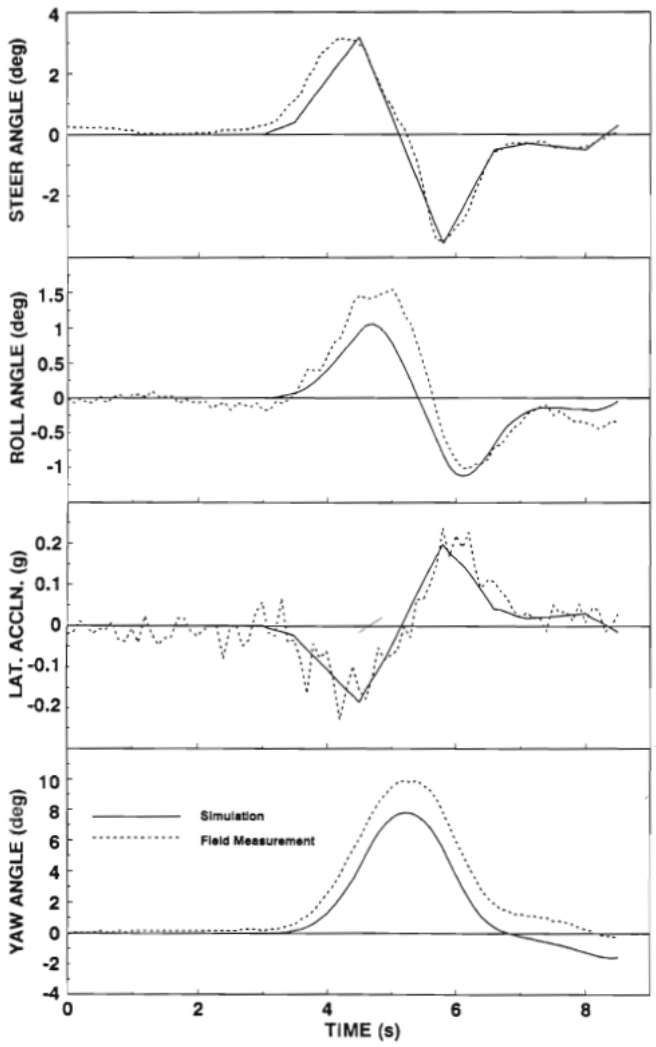

Figure 1.2: Comparison of analytical and field measured response of $70,0\%$ filled tank truck during a $21m$ lane change at $45km/h$ (Rakheja et al., [183])

from the rear to the front of the vehicle is relatively large in comparison with an equivalent rigid cargo vehicle, particularly in the range of $40,0\%$ to $60,0\%$ fill levels.

Another important application of quasi-static method is in the problems concerning optimization of design parameters of tank vehicles in order to enhance the stability and directional dynamics performance of such vehicles. In fact, effectiveness of this method in prediction of steady-state liquid load shift as well as its simplicity for implementation in vehicle equations of motion gives it an opportunity to tackle such problems efficiently. For instance, Popov et al. [172] developed an optimization technique based on the steady state solution of liquid motion in two-dimensional rectangular tanks under steady cornering manoeuvres. Overturning moment about the middle bottom point of tank resulted from the shift in the liquid center of gravity for four different positions of free surface were considered to be the objective function of the optimization technique. The study suggested an optimal tank height which varied nonlinearly from $0,707$ to $0,5$ for lateral acceleration from 0 to $1g$ regardless of liquid-fill depth. Popov et al. [173] also conducted a numerical analysis to obtain the optimal height/width ratio of elliptical road containers based on the steady-state solution. Analysis was founded on the minimization of the peak overturning moments of tank under steady turning maneuver. The effect of tank roll angle was not considered in the study. It was stated that the optimal height/width ratio decreases by increasing the magnitude of lateral acceleratio.

The other example is the work by Zhanqi et al., where steady-state fluid slosh model integrated with the vehicle pitch model was employed to compute the optimal position of compartment walls in a partially-filled ellipsoidal tank trucks subjected to constant deceleration, based on the minimization of longitudinal load transfer. The influence of pitch motion of vehicle on the coordinates of liquid center of mass was neglected. In addition, four different patterns for free surface position were considered. The study suggested equal length compartments to minimize the longitudinal load transfer under straight line braking maneuver. Quasi-static method is also used by Kang et al. [108] to obtain an optimal tank cross-section from a generic tank

cross-section including eight symmetrical circular arcs. Thirty possible free surface configurations were considered. The principle of optimization was on the minimization of height of liquid center of mass and lateral movement of liquid bulk for different fill volumes. He employed the similar procedure illustrated by Ranganathan [188] to analyze the rollover threshold of a tank vehicle with the generic tank cross-section as a function of tank geometry and liquid-fill depth. Two tank geometries were suggested by the study for tank vehicles involving large variations in liquid-fill depth and for the tank vehicles involving high liquid volumes 1.3. Similar optimal tank geometries for various fill levels were also suggested by Ziarani et al. [259] who developed a genetic algorithm for optimization of tank geometry based on the minimization of lateral and vertical load shifts in the liquid center of gravity. They also showed that elliptical containers are less stable than rectangular or modified rectangular containers with the same capacity. Three-dimensional

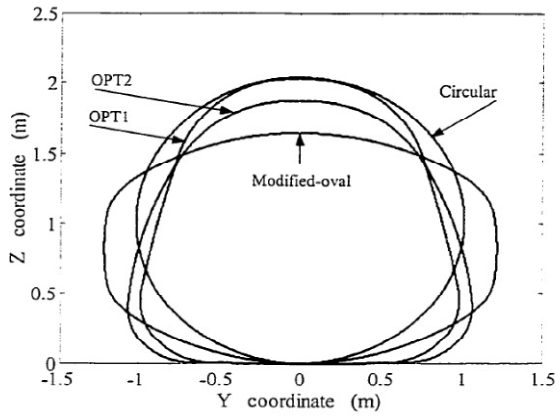

Figure 1.3: Two-optimal tank cross-sections proposed by Kang [108]

quasi-static method by considering simultaneous application of longitudinal and lateral acceleration is infrequently used in the literatures. Kang et al. [108] employed a three-dimensional steady-state fluid slosh model integrated to a three-dimensional articulated vehicle model with variable speed to study the effect of liquid cargo load shift on dynamics behavior of such vehicles subjected to braking-in-a-turn maneuver. The study neglected the effect of pitch motion on the position liquid free surface. The location of center of mass of

liquid was determined in both roll and pitch plane.

Although simulation of liquid sloshing in partly-filled tank trucks using quasi-static method makes it possible to accurately compute the steady-state position of liquid center of mass which contributes to computation of mean dynamic load shifts as well as mean directional responses, transitional behavior of liquid sloshing phenomenon is not taken into account by this analysis. Modaressi-Tehrani [143] and Yan et al. [255] confirmed that high magnitudes of transient fluid slosh results in a very limited application of this method for cases involving high fill volume and low amplitude excitation. In other words, this method is limited to the problems in which input frequency is below the fundamental sloshing frequency (Dai et al., [46] and Casasanta, [36]).

1.2 Dynamic Liquid Sloshing Method

In dynamic liquid sloshing method, the fluid motion within the tank is described by solving the Navier-Stokes equations. Studies on fluid slosh by this method can be performed by two approaches. First approach concerns small amplitude sloshing, assuming an ideal liquid having no viscosity as well as incompressible and irrotational flows in which Navier-Stokes equations reduce to potential flow equations with linear boundary conditions on the free surface (Abramson, [10]). This approach is called linear sloshing theory. In the second approach, high amplitude sloshing is simulated by solving the full Navier-Stokes equations using computational methods. In the following subsections, the authors aim to present a brief, but comprehensive, overview of these approaches by exploring the literatures regarding fluid sloshing in moving containers.

1.2.1 Linear Sloshing Approach

The general equations of motion for a fluid in rigid containers can be simplified by assuming an ideal liquid having no viscosity as well as incompressible and irrotational flow (Abramson, [10]). Under these conditions, Navier-Stokes equations reduce to Euler equations. Continuity and Euler

equations can be written in the vector form as:

$$\nabla.u = 0 \tag{1.11}$$

$$\frac{Du}{Dt} = -\frac{1}{\rho}\nabla p + g \tag{1.12}$$

Where u and g are the velocity and gravitational acceleration vectors. Based on the potential flow theory, for irrotational flow the velocity can be derived from a velocity potential, ϕ, so that the gradient of potential function gives the fluid velocity,

$$u = \nabla\phi \tag{1.13}$$

Substitution of equation (1.13) into continuity equation yields the Laplace equation,

$$\nabla^2\phi = 0 \tag{1.14}$$

Introducing equation (1.13) and irrotationality condition into Euler equation (1.12) gives

$$\nabla(\frac{p}{\rho} + \frac{|u|^2}{2} + gz + \frac{\partial\Phi}{\partial t}) \tag{1.15}$$

In which g is the effective gravity directed in the negative z direction. Equation (1.15) implies that the quantity within the parenthesis is not a function of spatial coordinates. Therefore, it can be a function of t only, say $C(t)$

$$\frac{p}{\rho} + \frac{|u|^2}{2} + gz + \frac{\partial\Phi}{\partial t} \tag{1.16}$$

The pressure at the free surface is equal to the ambient pressure (or it can be set to zero). This gives the dynamic boundary condition.

$$p_f = p_{atm} \tag{1.17}$$

Where p_f and p_{atm} refer to the free surface pressure and atmospheric pressure, respectively. Substituting equation (1.17) into equation (1.16) and absorbing the constant of integration, $C(t)$, into the definition of ϕ gives:

$$\frac{p_{atm}}{\rho} + \frac{|u|^2}{2} + g\eta + \frac{\partial\Phi}{\partial t} \tag{1.18}$$

Where η is the free surface displacement. The kinematic boundary condition at free surface is needed to relate the surface displacement, η, to the vertical

component of the liquid velocity at the surface.

$$\frac{D\eta}{Dt} = \frac{\partial \Phi}{\partial t} \tag{1.19}$$

Dynamic and kinematic boundary conditions at free surface, equations (1.18) and (1.19), are nonlinear. In order to linearize these equations, Abramson [10] discussed that the velocity magnitude in equation (1.18) is so small that squared of it can be neglected in comparison with linear terms; that is the equation (1.18) is linearized as follows:

$$\frac{p_{atm}}{\rho} + g\eta + \frac{\partial \Phi}{\partial t} = 0 \tag{1.20}$$

Furthermore, the linearized form of equation (1.19) can be written as (Abramson [10])

$$\frac{\partial \eta}{\partial t} = \frac{\partial \Phi}{\partial z} \tag{1.21}$$

By differentiating equation (1.20) with respect to t and eliminating η between this equation and equation (1.21), boundary conditions at free surface can be expressed by a single equation (Abramson, [10]).

$$\frac{\partial^2 \Phi}{\partial t^2} + g\frac{\partial \Phi}{\partial z} \tag{1.22}$$

The boundary condition at the tank wall is that the liquid velocity perpendicular to the plane of the wall has to be equal to the normal velocity of the wall. In case of free sloshing the potential solution can be assumed to be harmonic in time. Thus, the equation (1.22) becomes:

$$\frac{\partial \Phi}{\partial z} - \frac{\omega^2}{g}\Phi = 0 \tag{1.23}$$

Where ω is the sloshing frequency. Since the effects of viscosity and shear stress on the walls have been neglected, the usual no-slip condition cannot be imposed. Therefore, the free slip condition on the tank walls yields:

$$n.\nabla\phi = U_n \tag{1.24}$$

In which n is the unit vector normal to the wall and U_n is the normal velocity of the wall. The above linear boundary value problem, equations (1.14),

(1.22) and (1.24), is generally solved using method of separation of variables. However, analytical solution is limited to the regular tank geometry whose walls are straight such as rectangular and upright-cylindrical containers (Ibrahim, [97]). Fluid-free-surface natural frequencies and mode shapes for rectangular tanks in both two- and three-dimensional cases have been reported by Abramson [10] and Ibrahim [97]. They also reported the hydrodynamic force exerted on the walls of a rectangular tank along with the hydrodynamic pitching moment under sinusoidal lateral and pitching excitations, assuming two-dimensional flow where the length of the container is very long compared to its width. Furthermore, hydrodynamic yaw moment due to sinusoidal yaw excitation by considering three-dimensional flow in a rectangular container has been documented in Abramson [10] and Ibrahim [97]. In addition to the method of separation of variables, several other methods were employed to analyze the linear sloshing dynamics, particularly when employing the classical method of separation of variables for simulation of linear sloshing in the most practical tank geometries such as horizontal cylinder encounters difficulties. Conformal mapping is the most frequent and effective method which has been employed by several researchers to evaluate the dynamics of fluid sloshing. In this method, the original tank geometry has been transformed into a regular geometry in which the Laplace equation along with the wall and free surface boundary conditions can be solved explicitly. Budiansky [34] calculated the first three modes and frequencies of liquid sloshing in two-dimensional cylindrical and spherical containers as a function of liquid fill-depth based on an integral-equation approach. The wetted surface of the container in addition to its reflection about the axis through the free surface were transformed into an entire plane by a number of successive conformal mapping. The fundamental frequency is minimum for the nearly empty tank and increases monotonically with increasing the liquid fill-depth. He showed that the fundamental natural frequency for hall-filled circular tank with radius of R can be calculated by the following formula

$$\omega = 1.169\sqrt{gR} \tag{1.25}$$

The same formula was obtained by Lamb [122]. As the full condition is approached the natural frequency tends to infinity. The results of the study were confirmed by the experimental data presented by McCarty and Stephens [137]. Moreover, natural frequencies of liquid sloshing in two-dimensional cylindrical tanks with variable liquid depth were estimated by Kuttler and Sigillito [121] using a method which gives lower and upper bounds of eigenvalues. McIver [138] also solved the potential flow equation along with the wall and free surface boundary conditions in a transformed two-dimensional bipolar and three-dimensional toroidal coordinates and reported the first four natural frequencies of cylindrical and spherical containers in terms of liquid fill level (Figure 1.4). The results are in a very good agreement with those reported by Budiansky [34]. Papaspyrou et al. [164] investigated the liquid sloshing in two-dimensional circular cylindrical vessels subjected to transverse excitations using a semi-analytical approach. The proposed method is only limited to the half-filled tanks. The velocity potential was expressed in terms of a series of spatial and time functions which reduces the partial differential equations into a system of linear ordinary differential equations. Furthermore, the effect of suppression of liquid sloshing due to viscosity was considered by a Rayleigh damping technique where the damping matrix was considered to be a combination of mass and stiffness matrices (Liu and Gorman, [130]). Patkas and Karamanos [167] developed a mathematical model for simulation of linearized liquid sloshing in two-dimensional horizontal circular cylindrical and spherical containers with arbitrary liquid height under lateral acceleration using a variational formulation. In this approach, the linear boundary value problem was reduced a system of ordinary differential equations through expressing velocity potential by a series of non-orthogonal spatial functions.

Natural sloshing frequencies in addition to hydrodynamics forces were calculated and confirmed with those computed by McIver [138] and Evans and Linton [57]. Analytical studies on natural frequencies of liquid sloshing in spherical tanks using linear theory was also conducted by Barnyak et al. [19] where spherical domain was transformed to a half-space. Faltinsen and Timokha [62] developed a linear multimodal method to study the two-dimensional

liquid sloshing in a horizontal circular cylindrical tank. Multimodal approach was extensively discussed by Faltinsen and Timokha [61]. Based on the linear multimodal approach, the free-surface elevation and velocity potential were expressed by a series of the natural sloshing modes. This reduces the associated linear boundary value problem to a set of ordinary differential equations. Faltinsen and Timokha [62] compared the results obtained by the linear multimodal method with those obtained by fully nonlinear computational fluid dynamics simulations as well as laboratory-measured data. They concluded that the linear theory can predict the liquid sloshing for non-resonate condition and small liquid fill level effectively, while for large liquid fill level nonlinearity in free surface caused deviation from nonlinear CFD results (Figure 1.5).

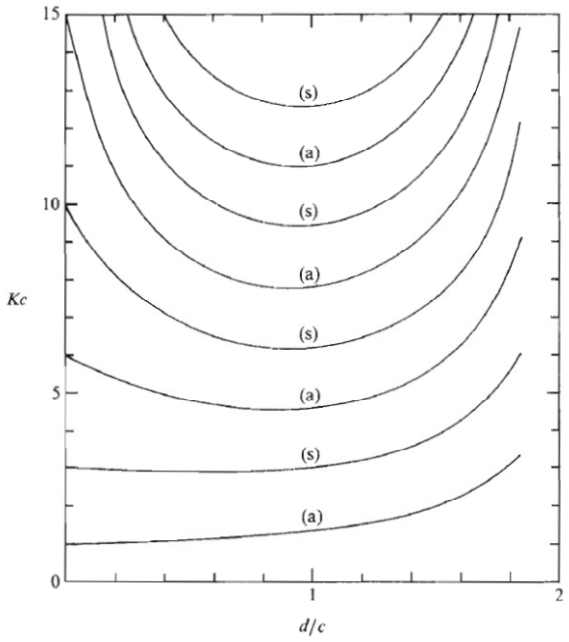

Figure 1.4: Non-dimensional natural frequencies for cylindrical tanks versus non-dimensional liquid depth. (Kc=2cg, in which c is the tank radius, and d is the liquid depth, McIver, [138])

Apart from the circular cross-section, linear analysis was applied for simulation of liquid sloshing in other tank geometries. Fox and Kuttler [70] suggested a method for modal analysis and evaluation of sloshing frequencies for

some general shaped containers based on conformal transformation of rectangles into two families of two-dimensional regions. The proposed technique was employed by Fox and Kuttler [71] to calculate the sloshing frequencies of a wide range of two-dimensional containers with various cross-sections including half-filled ellipse with lip, half-filled ellipse with bottom-mounted vertical baffle, half-filled ellipse without baffle and half-filled circle. Hasheminejad and Aghabeigi [86] computed the sloshing frequencies in half-filled two-dimensional elliptical container with and without horizontal side baffles mounted at the level of the free liquid surface. The original cross-section was transformed into the infinite rectangle in unbaffled case and finite rectangle in baffled case. Afterwards, transformed potential equations and boundary conditions were solved using the method of separation of variables. They showed that the natural sloshing frequencies for half-filled elliptical tanks increase with decreasing tank aspect ratio regardless of the liquid capacity and tank dimensions. Also, the study discussed that the used side baffles are more effective for nearly circular containers compared to the elliptical containers with high aspect ratio. The analytical modal analysis of linear liquid sloshing for different container geometries were also carried out by Henriei et al. [90], Fox and Sigillito [70], and McIver and McIver [139].

Evaluation of natural sloshing frequencies as well as sloshing forces and moments for three-dimensional horizontal cylindrical containers using analytical and semi-analytical linear sloshing approaches is extremely limited to a few studies, due to difficulties associated with the solving of hree-dimensional potential equations and implementation of the free surface boundary condition. Moiseev [146] and Moiseev and Petrov [149] developed a variational method for calculation of sloshing natural frequencies in various tank geometries including circular cylindrical container with horizontal axis. Evans and Linton [57] derived an expression for the potential as a series of bounded harmonic functions to evaluate the sloshing frequencies in half-filled two- and three-dimensional circular cylinder and half-filled spherical containers. The results for the case of three-dimensional cylinder were expressed in terms of the first four transverse modes for the first two longitudinal modes. In the similar way, the first four natural frequencies for the first three azimuthal

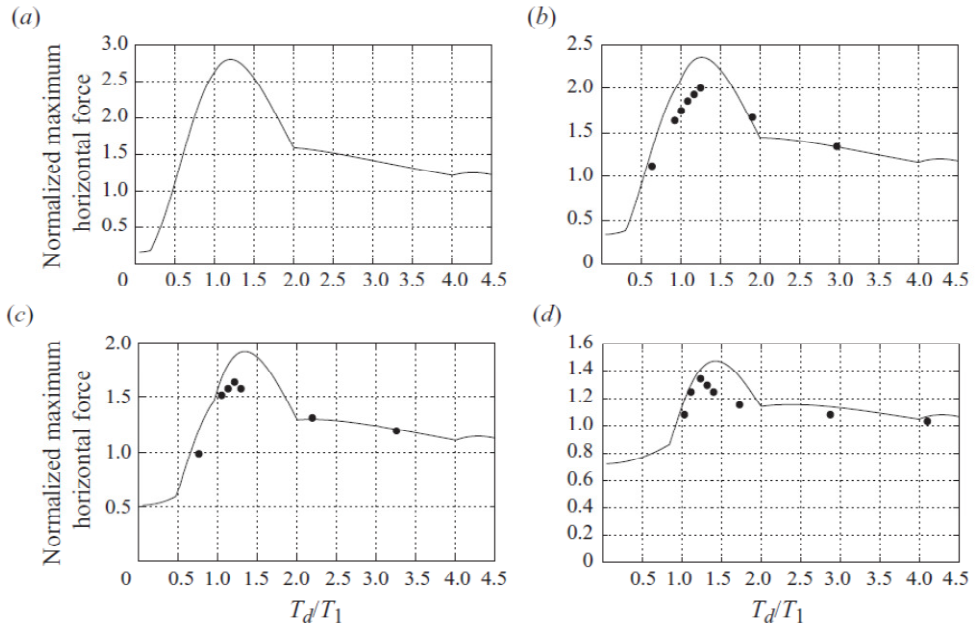

Figure 1.5: Non-dimensional maximum horizontal force for the lane change of a tanker vehicle with the lateral acceleration of 0.2g. The circles correspond to fully nonlinear viscous CFD simulation and the solid lines are predictions by the linear multimodal method. (a)hR0=0.4, (b) hR0=0.8, (c) hR0=1.2, (d) hR0=1.6 (Faltinsen and Timokha, [62]).

modes were computed for the spherical tank. The results for two-dimensional cylinder and sphere are consistent with those obtained by McIver [138]. Papaspyrou et al. [165] also extended the work of Evans and Linton [57] by introducing a Rayleigh viscous damping matrix to the system of governing ordinary differential equations and computed natural frequencies for three-dimensional horizontal cylindrical and spherical vessels. Hydrodynamic pressures and horizontal forces on the container walls under longitudinal excitation were also calculated. The studies were restricted to half-full vessels.

In addition to analytical and semi-analytical methods, numerical methods were adopted for solution of linear boundary value problem of liquid sloshing. Ru-De [200] presented a finite element analysis of linear liquid sloshing in upright circular cylinder under lateral excitation. Cho et al. [42] and Arafa [16] developed a finite element formulation for linear liquid sloshing in two-dimensional baffled rectangular tanks. Mitra et al. [142] employed the finite element method to study the motion of the liquid free surface in two-dimensional horizontal circular cylindrical, rectangular, trapezoidal and vertical annular cylindrical tanks due to lateral excitation, based on the linear theory . The results were presented in terms of hydrodynamic pressure distribution on the tank walls as well as transient free surface elevation. Teng et al. [228] employed the boundary element method based on finite elements to analyze the linear liquid sloshing in two-dimensional rectangular tanks. Boundary element method is a numerical method for solving integral equations in which only the boundary of the body was discretized (Katsikadelis, [110]). Dutta and Laha [55], and Firouz-Abadi et al. [65] developed a boundary element method founded on linear theory for calculation of natural frequencies as well as sloshing forces due to liquid sloshing in arbitrary three-dimensional tanks including rectangular, upright circular cylindrical and spherical tanks. Firouz-Abadi et al. [65] and Sygulski [226] also employed a similar approach and calculate the natural frequencies and mode shapes of liquid sloshing in three-dimensional baffled tanks with arbitrary geometry. The major contribution of these works was significant reduction of computational cost compared to the other numerical methods such finite element method.

In order to predict natural frequencies, the linear sloshing method is adequate [97]. Besides, within the frame work of linear theory, sloshing forces and moments can be predicted appropriately for small oscillations. However, by increasing excitation amplitude, complex surface phenomena contribute to increasing nonlinearities in the sloshing flow. This fact can be highlighted when these phenomena occur near resonance. In other words, as excitation frequency approaches to resonant frequencies, liquid free surface experiences nonlinear phenomena which cannot be predicted by linear equivalent mechanical model (Bauer, [24]; Funakoshi and Inoue, [76]). In addition, vertical displacement of the center of gravity of the liquid for large amplitudes of free-surface motion is not considered by linear theory [97]. Furthermore, using the linear theory for shallow filled tanks, complex tank geometries and containers equipped with baffles is extremely unreliable (Chen et al., [39]). Thus, linear sloshing models are only valid for small amplitude oscillation with excitation frequency far from the natural frequencies.

1.2.2 Nonlinear Sloshing Approach

Analytical and semi-analytical methods for simulation of nonlinear liquid sloshing utilize the potential flow theory along with nonlinear free surface boundary conditions (equaitons (1.20) and (1.21)). Earlier attempts concerning nonlinear phenomena in the sloshing flow were documented by Abramson [10] who discussed three different theories for solving the oscillation of nonlinear liquid free surface in rectangular and upright cylindrical tanks due to lateral excitation. Those theories were suggested by Moiseev [145], Penny and Price [168] and Hutton [94]. Analytical analysis of nonlinear liquid sloshing in two-dimensional rectangular containers were further developed by Bauer [24], Lepelletier and Raichlen [126], Faltinsen et al. [64], Faltinsen and Timokha [60, 59], Shankar and Kidambi [213]. It was claimed that in nonlinear analysis, sloshing forces and moments due to translational excitation are caused by a combination of odd and even modes, while fluid forces and moments are induced only by odd modes in linear theory. Three-dimensional analytical and experimental study of liquid sloshing in rectangular containers subjected

to combinations of longitudinal, lateral, pitch and roll excitations was also conducted by Faltinsen et al. [60, 60, 63]. Moreover, Yin et al. [257] analyzed the nonlinear liquid sloshing within a vertical circular cylinder under pitching motion analytically. Miles [140] studied the nonlinear resonantly liquid motion in vertical circular cylinder under lateral excitation. Komatsu [120] suggested a method for simulation of nonlinear liquid motion in three-dimensional rectangular and upright circular cylinder subjected to lateral excitation.

Inherent limitations of analytical methods as well as recent advances in computer technology and numerical analysis have been drawn great attention of many researchers and engineers to computational methods for addressing nonlinear fluid sloshing problems. A comparative review of recent numerical studies on fluid-structure interaction problems have been performed by Rebouillat and Liksonov [194]. Numerical methods for solving such problems can be classified into four categories:

- Lagrangian methods;
- Eulerian methods;
- Smoothed Arbitrary Lagrangian-Eulerian methods (ALE);
- Particle Hydrodynamics methods (SPH) (Koli and Kulkarni, [119]).

In Lagrangian methods, mesh moves with the fluid velocity in the entire domain. For discretization purpose, finite element method has been widely used (e.g. Hayashi et al., [89]; Radovitzky and Ortiz, [181]; Cremonesi et al., [44]). Although Lagrangian methods are computationally faster than Eulerian methods and movement of gird nodes with the fluid material results in an automatically tracking of free surface, large deformation of free surface can lead to a highly distorted mesh which causes an unstable and inaccurate solution. In order to resolve this issue, re-meshing or re-zoning techniques, which are basically tedious and very time-consuming, needs to be performed. Besides, material histories may be lost due to re-zoning (Liu and Liu, [129]). These numerical difficulties associated with Lagrangian methods have contributed to an extremely limited implementation of these methods

in analysis of liquid sloshing dynamics. Ramaswamy et al. [187] solved the incompressible inviscid/viscous Navier-Stokes equations based on a suggested numerical algorithm for Lagrangian finite element method to investigate the liquid sloshing in a two-dimensional rectangular container subjected to harmonic rolling motion. Okamoto and Kawahara [157] investigated large amplitude sloshing waves in a partly-filled two-dimensional rectangular container with four chamfers under harmonic lateral oscillation. Dogangun et al. [54] adopted Lagrangian finite element method to study liquid sloshing in a three-dimensional rectangular tank assuming inviscid flow under seismic excitation. Tang et al. [227] developed a Lagrangian method, called least square particle finite element method (LSPFEM), for simulation of laminar liquid sloshing in a two-dimensional rectangular tank with semicircular base under horizontal excitation.

In contrast with Lagrangian methods, Eulerian methods assume that the mesh is fixed on the domain. Therefore, deformation of free surface does not cause the change in the shape of the mesh cells. However, free surface of fluid needs to be modeled by an additional technique. The volume-of-fluid method (VOF) is the most frequent method in tracking the free surface for problems involving two or more fluids (or phases), which are not interpenetrating. Most researchers employed this method in their studies on fluid sloshing in moving containers to model the free-surface (e.g. [202, 203, 252, 249, 253, 254, 143]. The volume-of-fluid method (VOF) originally proposed by Hirt and Nichols [236] and further developed by several researchers such as Rudman [201], Harvie and Fletcher [85], Kim and Lee [114] on the basis of fractional volumes of liquid in a cell, which can be used to identify the position of the free-surface. Thus, if the *ith* fluid's volume fraction in the cell, f_i, takes the zero value, the *ith* fluid cell is empty; if the *ith* fluid's volume fraction in the cell takes the unit value, the cell is full of the *ith* fluid; and finally if it takes a value between zero and one, the cell contains the interface between the *ith* fluid and one or more other fluids. The ith fluid's volume fraction in the cell, f_i, is obtained from (Hirt and Nichols, [236]);

$$\frac{\partial f}{\partial t} + u.\nabla f = 0 \tag{1.26}$$

The above equation is solved in conjunction with Navier-Stokes and continuity equations to not only obtain properties of fluids at the free surface, but also identify the free surface position.

Instead of VOF method, Godderidge [83] suggested an inhomogeneous multiphase method, which was computationally very expensive, to simulate the free surface for liquid sloshing within a rectangular tank. In inhomogeneous multiphase method, each fluid has a separate flow flied which interact to the other fluid through mass and momentum transfer models (Ishii and Hibiki, [100]. By comparing the sloshing pressure results obtained by both inhomogeneous and volume of fluid method to the experimental results, Godderidge [83] concluded that pressure histories of inhomogeneous method were in a good agreement with experimental data, while VOF method underestimated the sloshing pressure peaks by up to $50,0\%$ for near-resonant sloshing flow.

Basic discretization approaches associated with Eulerian methods have been used for simulation of nonlinear liquid sloshing are finite difference method (FDM), finite element method (FEM), finite volume method (FVM) and boundary element method (BEM). Popov et al. [175] applied two-dimensional laminar incompressible Navier-Stokes equations to investigate the transient liquid response in partly-filled rectangular containers undergoing a braking/acceleration or a steady cornering manoeuvres using finite difference methodology. Kim [116] and Kim et al. [115] simulated sloshing flow in two- and three-dimensional rectangular and prismatic tanks with and without internal members using finite difference method. Liu and Lin [127] developed a numerical method to investigate three-dimensional violent liquid sloshing with broken free surfaces in a rectangular tank under arbitrary six degree-of-freedom (DOF) excitations using finite difference methods. Wu and Chen [245] also adopted finite difference method for simulation of three-dimensional liquid sloshing in rectangular tanks under coupled longitudinal and transverse excitations.

Modaressi-Tehrani et al. [143] used FLUENT software, which is based on finite volume discretization, to numerically study two- dimensional transient fluid motion within a partially filled circular tank for various fill volumes

and subject to different magnitudes of steady and harmonic lateral accelerations. Ming and Duan [141] used an in-house code based on the finite volume scheme to simulate liquid sloshing in two- and three-dimensional rectangular tanks under longitudinal excitation. Aslam [17] presented a finite element analysis for investigation of nonlinear liquid sloshing in two-dimensional containers assuming inviscid fluid flow. Karamanos et al. [109] developed a three-dimensional finite element method for calculation of natural frequencies in addition to sloshing forces as a function of liquid-fill depth for horizontal cylindrical and spherical vessels under lateral excitation. Nakayama and Washizu [150], Wang and Khoo [237] studied two-dimensional nonlinear liquid sloshing in rectangular tanks using finite element method assuming inviscid fluid flow. A similar technique was employed by Wu et al. [246] to perform a three-dimensional study.

Owing to the long computational time as well as high data storage requirements for FE, FV and FD simulation of liquid sloshing in moving containers, boundary element method was found very convenient for this purpose. Nakayama and Washizu [150] compared both boundary element and finite element methods for simulation of nonlinear inviscid liquid sloshing in a two-dimensional rectangular tank. The study confirmed the practical capabilities of BEM for solving such problems with significantly less computational resources. Romero and Ingber [198] employed the boundary element method for nonlinear sloshing analysis of a viscous fluid in a two-dimensional rectangular tank. Ortiz and Barhorst [159] also employed the boundary element method based on the potential flow theory for simulation of two-dimensional nonlinear liquid sloshing in an oscillating circular container. Chen et al. [40] performed three-dimensional analysis of nonlinear liquid sloshing in upright cylindrical and rectangular tanks using boundary element method assuming inviscid flow.

Arbitrary Lagrangian-Eulerian methods combine the advantages of Lagrangian and Eulerian methods. The concept of coupled Lagrangian and Eulerian methods was initially suggested by Noh [152] and Franck and Lazarus [72]. These methods were further developed by several researchers such as Hirt et al. [91] and Hughes et al. [93]. In the ALE description, grid nodes

may follow the fluid material (Lagrangian description), or be fixed on the domain (Eulerian description), or move arbitrary to give a more advantageous re-zoned mesh. This freedom in moving the computational mesh gives the opportunity to simulate significant deformation of free surface effectively. Studies on liquid sloshing dynamics by ALE methods have been performed by several researchers. Among those, Liu and Huang 1citeliu1994 developed a boundary element method based on the ALE description for nonlinear high amplitude liquid sloshing assuming inviscid flow. The suggested method was employed to study the liquid sloshing in a two-dimensional rectangular tank under harmonic excitation. They also discussed the critical amplitude recommended by Huerta and Liu [92], which was approximately $1,0\%$ of the liquid depth of container, for the small amplitude assumption. Instead of that criterion, Liu and Huang [131] derived the following formula for small amplitude assumption:

$$\eta_c <= 0,2\omega_0 2 \tag{1.27}$$

In which η_c is the critical amplitude of liquid wave, g is gravitational acceleration and ω_0 is the natural sloshing frequencies. Therefore, critical amplitude not only depends on the tank geometry, but also on the slosh modes. They suggested that for liquid sloshing whose amplitude is higher than the above critical amplitude, nonlinear analysis should be taken into account. Okamoto and Kawahara [158] presented a new Arbitrary Lagrangian-Eulerian finite element method for simulation of three-dimensional high-amplitude liquid sloshing. The suggested method was validated against the experimental data in the form of comparison of recorded free surface in a three-dimensional vertical rectangular container due to harmonic lateral/longitudinal excitation by experimental methods and free surface obtained by computational method. The method was also used for analysis of three-dimensional liquid sloshing in vertical rectangular and cylindrical tanks with obstacle and vertical rectangular containers with four chamfers due to harmonic lateral/longitudinal excitation. Ushijima [232, 233] developed an ALE method for prediction of nonlinear free surface oscillation and studied fluid sloshing in a three-dimensional vertical cylinder caused by horizontal and vertical excitations. Braess and Wriggers [31] used the ALE method to solve the sloshing problem

in a simple two-dimensional square tank under sinusoidal excitations. Souli and Zolesio [219], and Zhou et al. [258] investigated large amplitude sloshing in two-dimensional rectangular and circular containers using the finite element method of arbitrary Lagrangian-Eulerian formulation. Aquelet and Souli [15] obtained the sloshing frequency of a simple two-dimensional tank with and without baffles using Arbitrary Lagrangian Eulerian finite element method based on the potential flow theory. BaoZeng [18] studied three-dimensional liquid sloshing in rectangular and upright cylindrical containers subjected to pitching motion using ALE finite element method.

As an alternative to conventional grid-based methods, Smoothed Particle Hydrodynamics, (SPH), has been used in fluid sloshing problems by a few researchers. The basic idea of SPH is interpolation theory. Mass and momentum conservation laws are transformed into particle form using integral interpolant formula and smoothing functions (Kernel functions). Since fluid properties are only known at particles, integrals are estimated by sums over neighboring particles. Indeed, the Lagrangian nature of SPH gives it an opportunity to tackle problems involving free surface and moving interface, which are challenging problems in grid-based methods, so that tracking of free surface is performed automatically by tracking the particles in the fluid domain and no free-surface boundary condition is needed (Liu and Liu, [129]). Delorme et al. [48] employed the SPH method presented by Monaghan [147] to study two-dimensional sloshing flows in a rectangular tank. Liquid sloshing in two-dimensional tanks were also studied by Colagrossi et al. [43] using SPH method. This method was also adopted by Rafiee, et al. [182] to numerically model three-dimensional viscous liquid sloshing in rectangular tanks. Comparison between results obtained by SPH method and those obtained by experimental method proved a successful numerical simulation, however small discrepancies were attributed to neglecting the air phase in the SPH model (Figure 1.6). In addition to SPH method, several particle methods were developed for simulation of liquid sloshing. For instance, Pan et al. [162] employed a Moving-Particle Semi-implicit Method (MPS) for numerical modeling of liquid sloshing in partially-filled rectangular tanks assuming laminar two-dimensional flow. As indicated earlier,

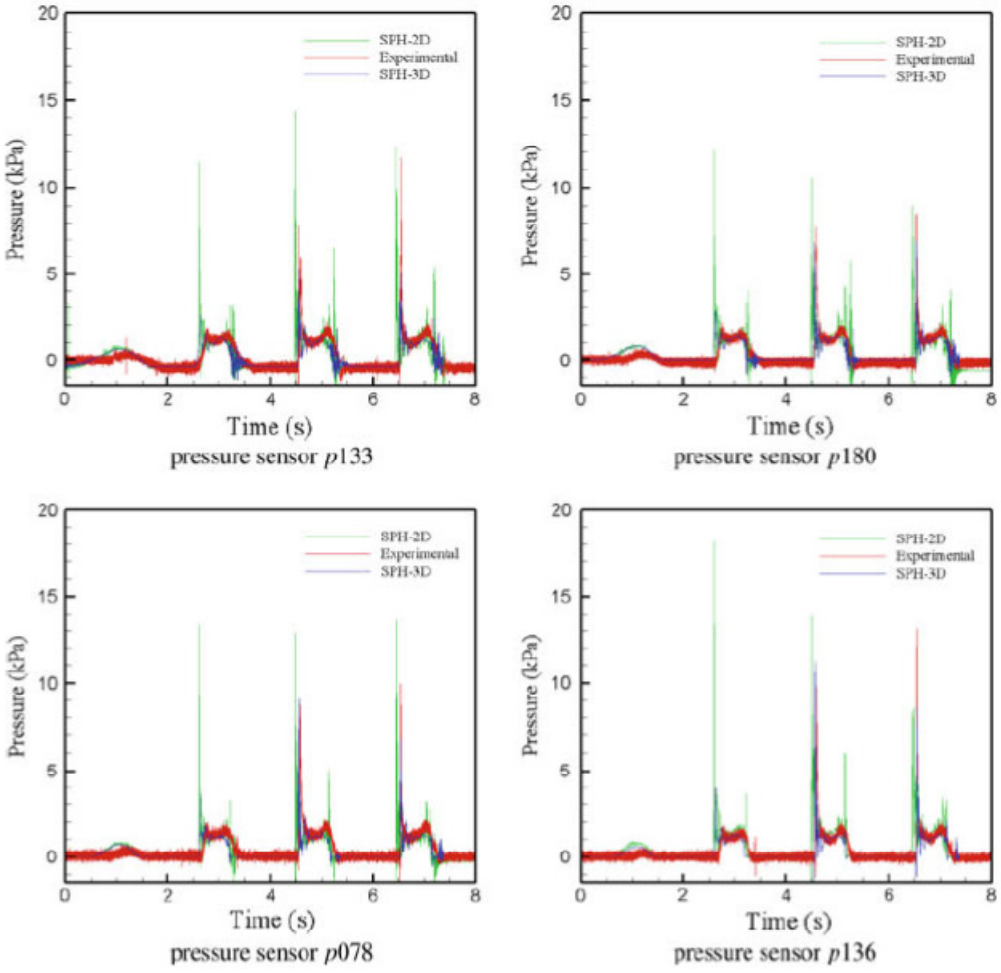

Figure 1.6: Comparison of variation of impact pressure between experimental, SPH-2D and SPH-3D at some pressure sensor due to lateral excitation (Rafiee, et al., [182]).

studies on nonlinear liquid sloshing in rectangular as well as vertical cylindrical containers have been attracted great attentions. However, simulation of nonlinear slosh in tank geometries, such as horizontal circular, elliptical and oval tanks, which are usually used for carrying liquid cargo by heavy vehicles, have not been received such attentions. Popov, et al. [174] studied the steady-state and transient solutions for liquid sloshing in two-dimensional horizontal cylindrical road containers under steady turn manoeuvres by finite difference method assuming laminar flow. Yan, et al. [255] simulated two-dimensional nonlinear liquid sloshing in circular and conical containers under ramp-step lateral acceleration using CFD commercial software FLUENT. Coordinates of center of gravity as well as horizontal and vertical components of hydrodynamic force were expressed as second-order polynomial regression functions in terms of lateral acceleration for different liquid-fill depths. These functions were integrated into the roll moment equilibrium of an articulated vehicle to calculate the rollover- threshold acceleration. The study confirmed that although tank trucks with lower fill volume have lower center of gravity, they may exhibit lower rollover threshold for constant cargo load (Table 1.1). This conclusion cannot be drawn by quasi-static analysis. Dai and Xu [45] investigated the transient response of nonlinear liquid sloshing in two-dimensional horizontal circular cylindrical tank under turning, lane-change and double-lane-change manoeuvres, based on the potential flow. In order to avoid dealing with complicated free surface boundary condition, the liquid domain was transformed to a rectangle in which the curved free surface became a line in the mapped domain. Then, finite deference method was employed for discretization of transformed governing equations in the mapped domain. A similar approach was followed by Frandsen and Borthwick [74], Frandsen [73]. Dai and Xu [45] also applied the suggested approach for three-dimensional cylindrical containers under both lateral and longitudinal excitation to demonstrate the capability of this approach for investigation of nonlinear three-dimensional liquid sloshing in arbitrary tank geometries. For an assessment of advantages and drawbacks of different numerical approaches for analysis of liquid sloshing, Brizzolara, et al. [32] conducted a series of simulations of liquid sloshing in a rectangular tank under sinusoidal

Table 1.1: Rollover-threshold accelerations of the 6-axle tractor-semi-trailer tank vehicle with circular and conical tanks carrying different liquid cargos with different fill volumes (Yan, et al., [255]).

Cargo	Density (Kg/m^3)	Fill volume (%)	Cargo load (kN)	Tank Shape	Rollover Threshold acceleration		
					Rigid Load	Mean/QS	Transient
Sulphuric acid	1826	44	323	Conical	0,44	0.35	0,24
				Circular	0,40	0,32	0,35
Water	998	50	202	Conical	0,46	0,39	0,29
				Circular	0,43	0,37	0,27
		80	323	Conical	0,37	0,35	0,29
				Circular	0,34	0,31	0,25

rolling motion with different periods for various liquid fill-depths using two commercial solvers (FLOW-3D and LS-DYNA), and two academic software (SPH developed by University of Genoa, and RANS developed by University of Southampton) with the assumption of incompressible laminar flow. Only the simulation by FLOW-3D was three-dimensional, while the others were two-dimensional. The RANS code employed the level- set method proposed by Price and Chen [178] for simulation of free-surface, while LS-DYNA as well as FLOW-3D, which are Eulerian finite element and finite volume codes, respectively, used VOF method. Brizzolara, et al. [32] compared the results obtained by those numerical methods with experimental data reported by Souto-Iglesias [221] and concluded that, in general, commercial software FLOW-3D and LS-DYNA can predict the sloshing pressure more successfully. Also, results obtained by those software codes appeared to be more robust, while ones obtained by SPH and RANS codes revealed high oscillations, particularly for near-resonant conditions (Figure 1.7). In terms of global torque predictions, FLOW-3D and SPH codes provided more accurate results (Figure 1.8). Moreover, the employed SPH method required extremely high computational time in addition to a series of difficult settings for a range of different parameters which were regarded as main drawbacks of this method. Cariou and Casella [35] also conduct a comparative study for numerical simulation of liquid sloshing in two- and three-dimensional ship tanks using 11 computational codes. The study confirmed that more investigate is required for accurate prediction of pressure peaks and impacts.

Although nonlinear fluid sloshing within the tank has widely been studied

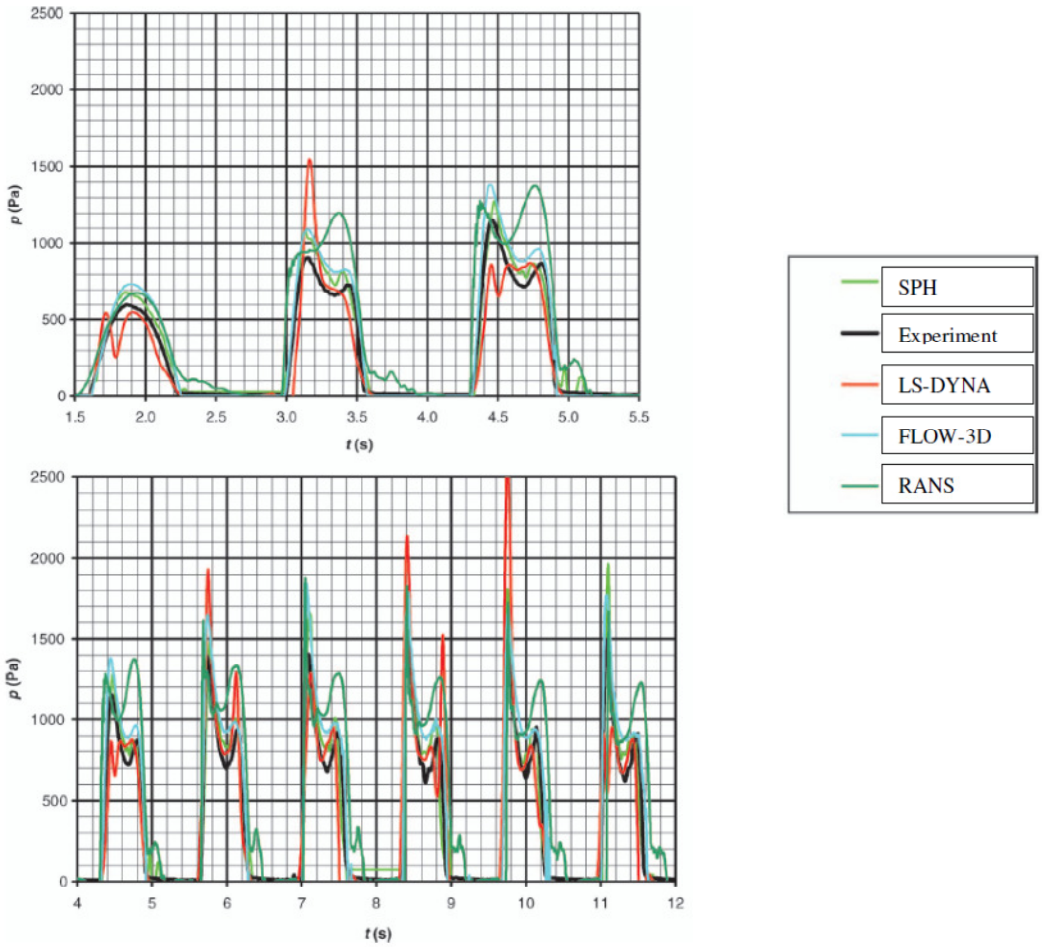

Figure 1.7: Comparison of variation of impact pressure between experimental, SPH-2D and SPH-3D at some pressure sensor due to lateral excitation (Rafiee, et al., [182]).

using computational fluid dynamics codes, interactions between nonlinear liquid sloshing and the vehicle system dynamics have been addressed in only a few recent studies. In addition, in order to achieve a real-time simulation and investigate the effects of transient liquid sloshing forces and moments on the directional dynamic performance of tank trucks, liquid sloshing and vehicle dynamics needs to be coupled. As an earlier attempt to address the coupled nonlinear fluid sloshing and vehicle dynamics, Sankar, et al. [207] performed a coupled simulation of fluid sloshing and vehicle dynamics to investigate the directional response of tank vehicles for steady and transient steer input. A

nonlinear fluid sloshing model, which was suggested by Popov et al. [174] for two-dimensional horizontal cylindrical containers based on finite difference scheme, was coupled with a three-dimensional vehicle model developed by Ranganathan [188] for a five-axle tractor-semitrailer consisting two sprung masses and five unsprung masses. Sprung masses, including mass of tractor

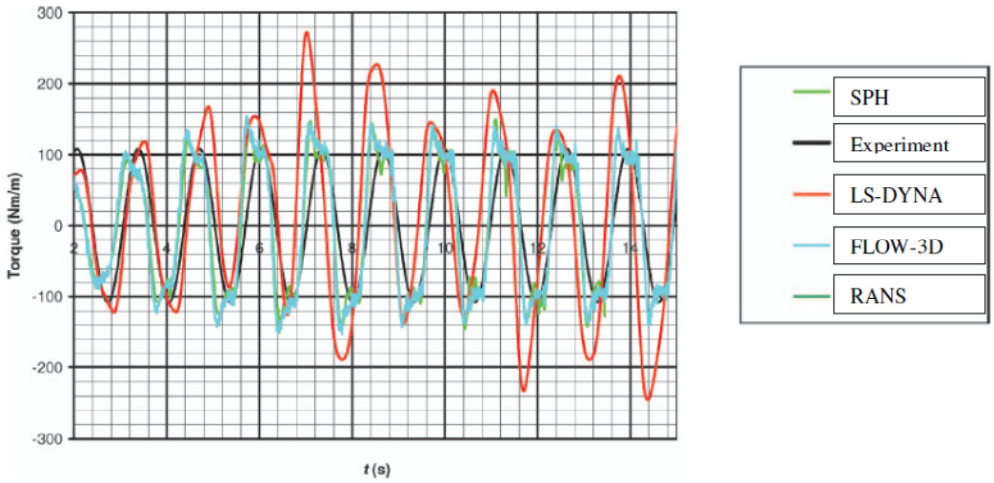

Figure 1.8: Torque with respect to the tank rolling center for the tank with 43, 7% of fill level at resonance (Brizzolara, et al., [32]).

and tare mass of semitrailer, were modeled as rigid bodies with five degrees of freedom; lateral, vertical, yaw, roll and pitch, while unsprung masses had two degrees of freedom; roll and bounce with respect to associated sprung mass. In order to carry out a real-time co-simulation, differential equations of vehicle dynamics model were solved at a small time step to calculate lateral and vertical acceleration of the semitrailer sprung mass. Then, these acceleration components were transformed to the non-dimensional accelerations along the tank axes to compute the acceleration components of each fluid cell. By solving the fluid governing equations at the same time step, sloshing forces and moments at the end of that time step were computed and incorporated to the vehicle dynamics model to proceed the calculation of the subsequent time step. The dynamic response of vehicle for constant steer input revealed an oscillating behavior about the steady state value obtained from the quasi-static model (Figure 1.9). However, dynamic response under

typical highway manoeuvres, including lane change and evasive, exhibited a good agreement between quasi-static and coupled CFD-vehicle simulation.

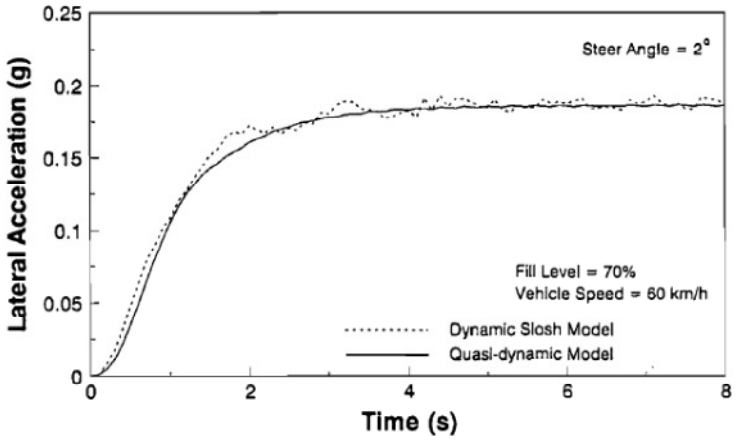

Figure 1.9: Comparison of lateral acceleration response of the tank vehicles using coupled CFD-vehicle and quasi-static model for constant steer input (Sankar, et al. [207]).

Rumold [202] also developed a coupled fluid-multibody dynamics model to investigate the braking characteristics of a partially filled square cross-section tank vehicle based on two-dimensional analysis. For this purpose, a modular approach was proposed to simulate the coupled liquid sloshing model based on the Navier-stokes equations and the multi-body vehicle model. The entire tank vehicle was modeled as a multi-body system comprising two subsystems; the tank vehicle without the fluid cargo and the fluid cargo within the tank. The two components were represented by a rigid body vehicle model and a fluid sloshing model, which was implemented in the software code UG (Bastian et al., [21]) using multi-grid method (Wesseling, [241]; Caughey and Hafez, [37]). The coupled system responses were obtained through data exchange between the two subsystem models at specific time steps. Rumold [202] formulated the Navier-Stokes equations in a reference frame fixed to the container assuming no-slip boundary condition on the tank walls and derived an equation for the external force acting on the fluid. The similar equation for external force, including translational and rotational forces as well as gravitational force, was derived by Batchelor [22]. The equations of motion of the fluid within the tank had also been expressed in the moving

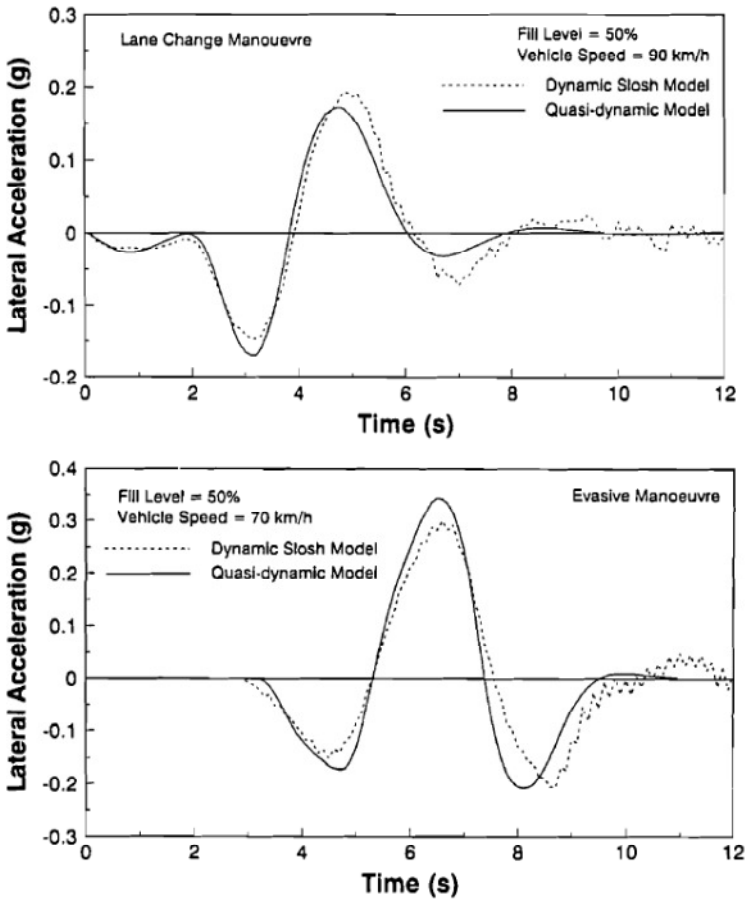

Figure 1.10: Comparison of lateral acceleration response of the tank vehicles using coupled CFD-vehicle and quasi-static model for lane change and evasive maneuver (Sankar, et al. [207]

frame of reference using the fictitious body forces acting upon the fluid by Batchelor [22]. Adoption of the non-inertial reference frame gives the opportunity to avoid the treatment of complicated boundary conditions on moving walls.

Rumold [202] used a simple vehicle model with three degrees-of-freedom (DOF) including translation of the car body and rotations of the front and rear axles to simulate the longitudinal dynamics of a small straight truck subjected to constant braking torque. Dynamics of suspension system was not considered and tangential tire forces were related to normal forces by the magic tire formula suggested by Pacejka and Bakker [160]. Based on the modular simulation of the two subsystems, Rumold [202] considered the sloshing forces and moments as the input to the rigid body subsystems and output of fluid subsystem. In the similar manner, the translational and rotational acceleration along with rotational velocity responses were considered as the output of rigid body subsystem and input to the fluid subsystem. The vehicle model revealed that an increase in the brake torque resulted in lower mean and amplitude of the oscillatory vehicle acceleration but higher mean and amplitude of the sloshing force (Figure 1.11). Furthermore, by comparing the transient rear tire normal loads for the liquid and equivalent rigid cargo vehicles, Rumold [202] concluded that liquid sloshing contributes to decrease in the tire normal loads, which can result in a rear tire lock-up and a loss of vehicle controllability (Figure 1.12). Such results were also reported by Kang [108] on the basis of quasi-static fluid slosh model. Thomassy et al. [229] developed a methodology for coupled simulation of vehicle dynamics and fluid slosh. For this purpose, they developed a master program, called Glue Code, that managed data transfer between two separate codes, FLOW-3D and MSC.ADAMS, which simulated independently liquid sloshing and vehicle dynamics. In order to verify the suggested methodology, they simulated a small-scale tank mounted on a rigid frame supported by three multi-axis load cells in MSC.ADAMS software. CFD simulation of fluid motion within the tank due to simulated maneuvers, including lane change and going over symmetric/asymmetric bumps, was performed in FLOW-3D software. Resulted obtained by this coupled simulation were compared with experimental re-

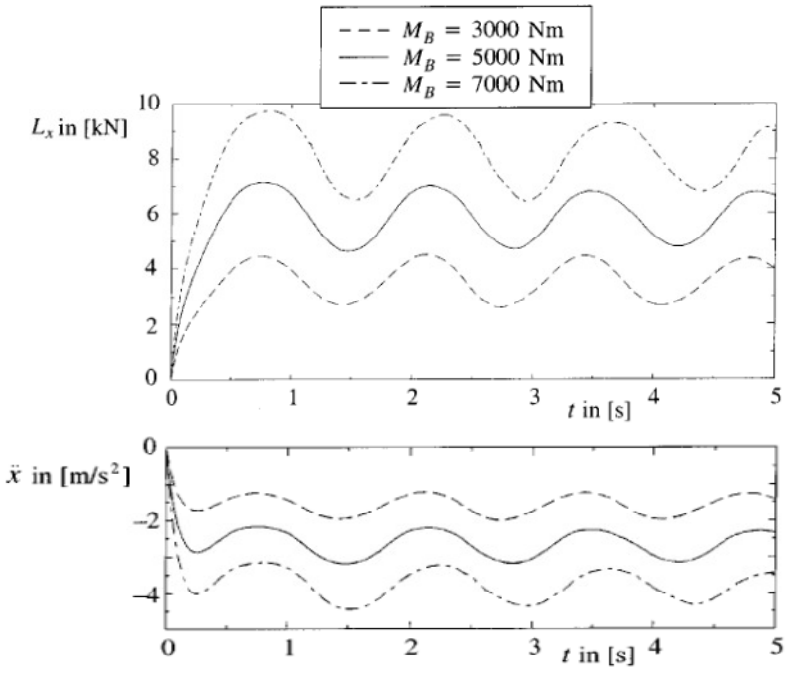

Figure 1.11: Horizontal liquid force and the vehicle acceleration during braking maneuver (Rumold,[202]).

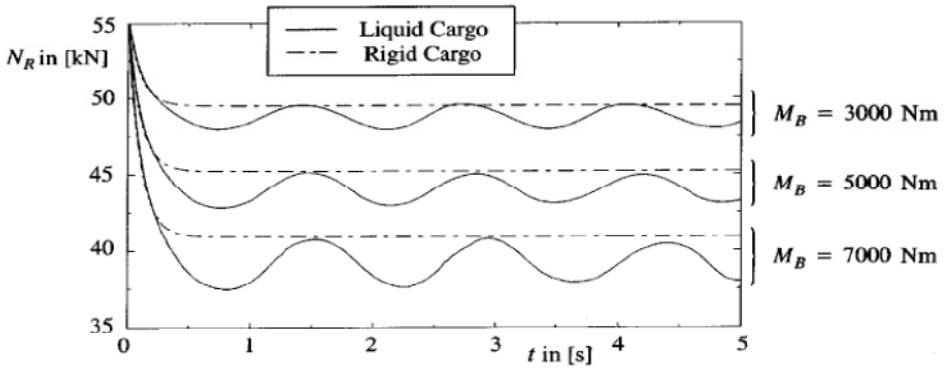

Figure 1.12: Rear tire normal force during braking maneuver (Rumold, [202]).

sults. Although resulted obtained by this coupled simulation were validated by experimental data, in their point of view, further development is required for simulation of a full scale tank vehicle by this methodology.

Biglarbegian and Zu [27] solved the coupled fluid and vehicle model for a tractor-semitrailer carrying liquid cargo under constant braking torques. Similar to the simulation performed by Rumold [202], vehicle model is used to obtain the kinematic parameters (angular velocity and acceleration, linear acceleration, and transformation matrices) at each instant. These response parameters at each instant serve as the input parameters to the liquid sloshing model to obtain the sloshing forces and moments at a successive instant. Biglarbegian and Zu [27] also developed a three-DOF (translational, roll, and pitch motion) tractor-semitrailer model with linear suspension to study the liquid sloshing under constant braking torques. They used the magic tyre formula to obtain the longitudinal forces applied from the ground to the tires. The study revealed that vehicles carrying liquid cargo need considerably greater braking torque compared to the equivalent rigid cargo vehicles to stop at the same distance from the beginning of braking action (Figure 1.13). Wasfy, et al. [239] used commercial finite element code DIS developed

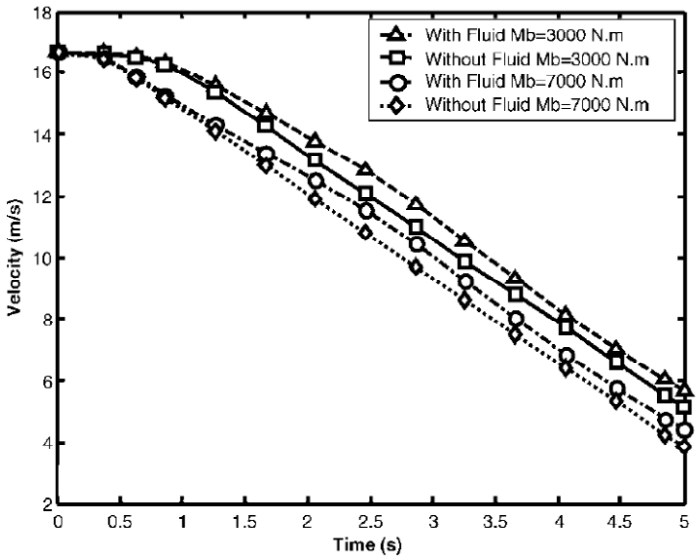

Figure 1.13: Velocity profile for different braking moments for rigid and liquid cargo (Biglarbegian and Zu, [27]).

by Advanced Science and Automation Corp. (2007) to numerically simulate transient response of a heavy vehicle carrying an oval tank with a single orifice baffle under typical manoeuvres including traversing a bumpy terrain, going over symmetric or asymmetric bumps, turning and lane-change in the presence of coupled nonlinear fluid sloshing and vehicle dynamics. They modeled the fluid motion in the partially-filled container using the Arbitrary Lagrangian-Eulerian (ALE) description of the full Navier-Stokes equations assuming turbulent flow, which was modeled by Large eddy simulation (LES) approach, and free-slip boundary condition at the walls. Apart from the fluid modeling, they employed multi-body dynamics methods to model a heavy tank truck whose components are simulated using rigid bodies, flexible bodies, joints and actuators. The tires were modeled using a one-node tire model in which tire is discretized into a grid of rectangles with a contact point at each rectangle. The frictional contact force at each point was assumed to be the sum of normal and tangential friction forces. The method proposed by Leamy and Wasfy [238] was used to account for the normal and tangential friction forces. The computational model was validated by laboratory experiments in the form of the displacements at rear axle of the trailer. A similar approach had been conducted by Wasfy, et al. [238] to perform a coupled simulation of a partially-filled small scale tank with oval cross section and equipped with a pair of partial longitudinal and transverse baffles.

Yan and Rakheja [249] used a coupled fluid-multibody dynamics method to investigate the straight-line braking performance of a partially filled tank truck with and without the baffles. The entire tank vehicle was modeled by the multi-body system (MBS) approach. Similar to Rumold [202], Yan and Rakheja [249] used the modular simulation of the two subsystems; the tank vehicle without the fluid cargo and the fluid cargo within the tank. They suggested a three-dimensional liquid sloshing model for a tank geometry, referred to as Reuleaux triangle ([108], assuming laminar incompressible flow and no-slip boundary condition on the tank walls which was implemented into the FLUENT software, while the vehicle model was a two-dimensional pitch-plane model of the vehicle in the presence of a straight-line braking manoeuvre. A seven-DOF model (longitudinal, vertical and pitch motions of

the sprung mass, vertical motions of two unsprung masses, and angular motions of the wheels) assuming linear stiffness and damping for the suspension system in addition to a tire model referred to as magic tyre formula (Pacejka and Bakker, [160]) was applied. Similar to the previously mentioned methods, fluid sloshing model was solved by considering the instantaneous vehicle response as the external acceleration imposed on the fluid. Consequently, the resulting transient sloshing forces and moments were applied to the vehicle model at the subsequent instant (Figure 1.14). The process was continued until the vehicle forward velocity diminished. Yan and Rakheja [249] used a tank shell with two configurations; a clean bore tank and a tank with four equally-spaced curved large single orifice baffles. The baffles included a circular orifice at the center of the tank and a semi-circular equalizer at the bottom. The study evaluated responses to time-varying braking torque by using a ramp-step change in the brake treadle pressure, such that wheel lock-up does not occur. The validity of the model was examined by comparison of the sloshing natural frequency as well as the sloshing forces and moments predicted by the model with those measured from the experiments performing on a scaled tank with different fill levels ($30,0\%$, $50,0\%$ and $70,0\%$), and with and without baffles under different excitations (yan [252]). The results by Yan [252] showed small deviations ($< 8,0\%$) between the experimental and computational results in the sloshing natural frequencies in both the lateral and longitudinal modes, irrespective of the tank fill level. Also, the transient and steady-state sloshing forces and moments obtained by computational method exhibited good agreements with the experimental data. Fleissner et al. [66, 67] coupled three-dimensional liquid/granulates sloshing model by a transport vehicle model with 17 degrees of freedom. The motion of fluid within the container was simulated by SPH method, which was applied through PASIMODO code developed at University of Stuttgar, while the tank truck was modeled using classical multibody system through SIMPAC software. Co-simulation between these two codes was performed by MATLAB/SIMULINK. They investigated the stability of tank trucks under different driving manoeuvres including full braking and double lane change. The study considered a cubic tank with one and two compartments as well

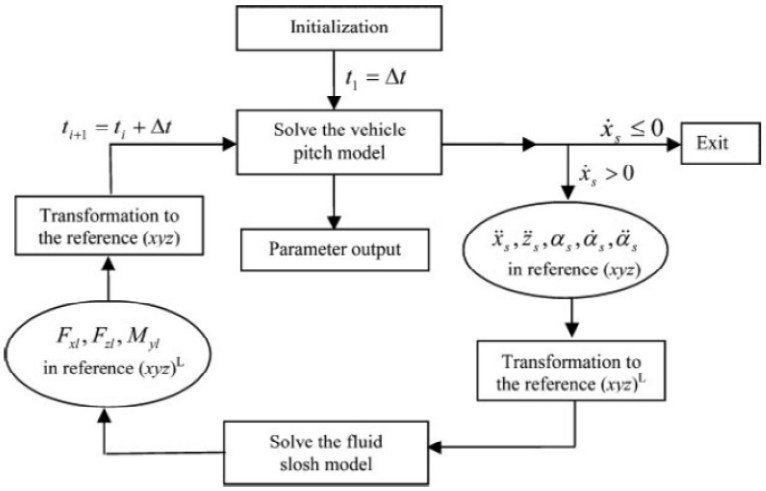

Figure 1.14: Procedure of the coupled fluid slosh and vehicle models (Yan and Rakheja, [249]).

as a cylindrical tank with three compartments to demonstrate the positive effect of dividing the tank into compartments on the braking stability.

1.3 Experimental Studies

Fluid sloshing within tank trucks is a complicated phenomenon particularly under multiple excitations as observed in the practice for the heavy vehicles. Laboratory experiments under controlled conditions not only can provide a deep insight into this phenomenon, but also set the stage for developing more reliable and efficient analytical and computational methods. Experimental investigation of liquid sloshing in spherical and vertical cylindrical containers was extensively performed by several researchers (Stephens, et al., [223]; Sumner, et al., [224], 1966; Abramson, et al., [10]; Kana, [102]; Dalzell, [47]; Barron and Chng, [20]; Royon-Lebeaud, [199]). Also, experimental study of liquid sloshing in rectangular tanks has received a great attention. Pal [161] investigated the liquid sloshing in a partially filled prismatic tank model of size 0.50 m in width, $0,35m$ in length and $0,40m$ in height. The slosh amplitudes were measured by the wave height measuring probes for different fill conditions and excitation amplitudes. Disimile, et al.[52] employed a high-speed imaging system for flow visualization of liquid sloshing in a baf-

fled rectangular model tank, which resembled an aircraft wing fuel tank, to measure the hydrodynamic jumps due to rolling motion at the resonance frequency. Khezzar, et al. [113] also used a flow visualization system to study the liquid sloshing in an accelerating rectangular container subjected to an impact excitation. The model tank had a dimension of $175x175x550$ which initially accelerated on a trolley by placing pre-defined weights in a weight carrier and suddenly stopped when it hit with a stopper. Effect of impact acceleration along the longitudinal axis on the liquid pressures in partially filled horizontal cylindrical containers was also experimentally studied by Ye and Birk [256]. The earlier attempt for measuring the natural sloshing fre-

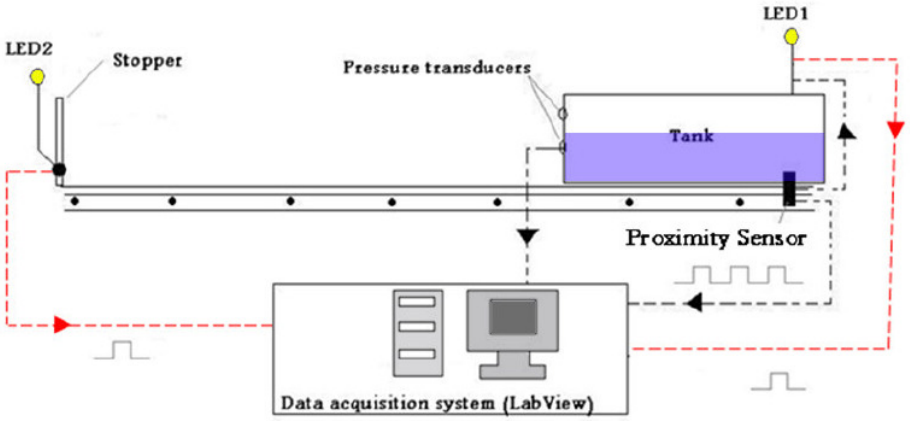

Figure 1.15: Experimental setup (Khezzar, et al. [113]).

quencies in horizontal cylindrical containers during lateral and longitudinal motions was performed by McCarty and Stephens [137]. Non-dimensional transverse and longitudinal natural frequencies versus liquid fill level were presented. Wasfy, et al. [239] used a full-scale army heavy class tactical trailer (with three axles and six wheels) carrying a water tank to experimentally validate the computational method. They placed the trailer on an n-post motion base simulator which was used to generate harmonic/ramp pitch, roll and stir excitations identical to those used in computational model (Figure 1.16). The n-post motion simulator consisted of six linear hydraulic actuators. The experiments were performed for a $65,0\%$-filled tank and an empty tank. The transient linear displacement responses were recording at

22 points using linear variable differential transformers (LVDTs) at a rate of 256 samples/s. The locations included the linear vertical inputs of the six actuators, vertical motion of each wheel center, the deflection of each tire, and longitudinal and lateral displacements of the trailer frame. In order to measure the motion of trailer tank, they used a camera with the frame rate of $30 frames/s$. It is of great importance to realize that this experiment was performed with a full scale tank which is a special case in study of liquid sloshing in heavy vehicles, since the reported experimental studies have explained only small-scale tanks. Rakheja, et al. [183] employed a test vehicle

Figure 1.16: Experimental setup (Wasfy, et al., [239]).

equipped with cylindrical tank of $1,22m$ in diameter and $1,73m$ in length to measure sloshing forces in three orthogonal axes, angular moments and dynamic load transfer in the roll and pitch planes. The field test was conducted for various fill conditions and maneuvers including constant radius turn, single and double lane change, braking in a straight line and braking in a turn. Also, the liquid free surface in the roll plane was recorded and compared with that obtained from the steady state analysis. In a similar way, Bottiglione, et al. [30] performed a field test using a steel tank of $1m^3$ capacity and $1,6m$ length mounted a trailer and equipped with an inertial platform for measuring lateral acceleration and yaw rate, laser projectors and a CCD camera (Figure 1.17). The reflected laser lights from the liquid free surface were recorded by the camera and used for the analysis of free surface oscillations under a steady turning maneuver. Romero, et al. [197]

used the experimental methods to study the effect of sloshing forces on the lateral stability of tank trucks when operating almost fully loaded (from 90 to 98 %). They employed three tanks with oval, modified oval and circular cross sections and scaled lateral dimension in the order of 1 : 5 of the actual tanks. The longitudinal dimensions were considered to be small to ensure minimum contribution of longitudinal slosh. Yan, et al. [249] experimentally investigate the fluid sloshing in three different small-scale model ($760l$) Reuleaux-triangle tanks; a clean-bore tank, tank with two equally spaced single-orifice baffles and tank with two equally spaced multiple-orifice baffle. The width of the tank was approximately 1/3 of a typical tank used on heavy vehicles. They placed the tank on a horizontal shake table subjected to lateral or longitudinal excitations. Three 3-axes dynamometers were used to measure the resulting sloshing forces and moments under various amplitudes and frequencies of acceleration excitation. The natural frequencies were estimated from the frequency response of measured lateral and longitudinal forces. Also, Wasfy, et al. [238] experimentally studied the liquid sloshing in a small-scale baffled oval tank with dimensions of $0,24m$ long, $0,428m$ wide, and $0,276m$ deep. The tank was mounted on three suspension spring-dampers which applied a wide range of roll and pitch excitation. A similar experiment was conducted by Wendel, et al. [240] concerning the liquid sloshing in a small-scale clean bore oval tank to validate a CFD code. Romero, et al. [197] conducted an experimental study to measure the nat-

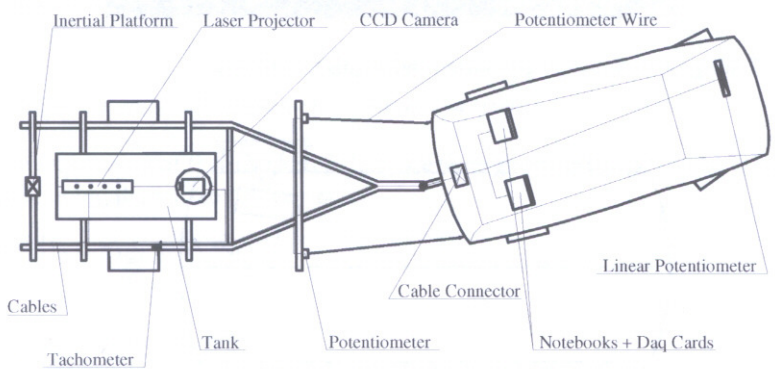

Figure 1.17: Experimental apparatus (Bottiglione, et al., [30]).

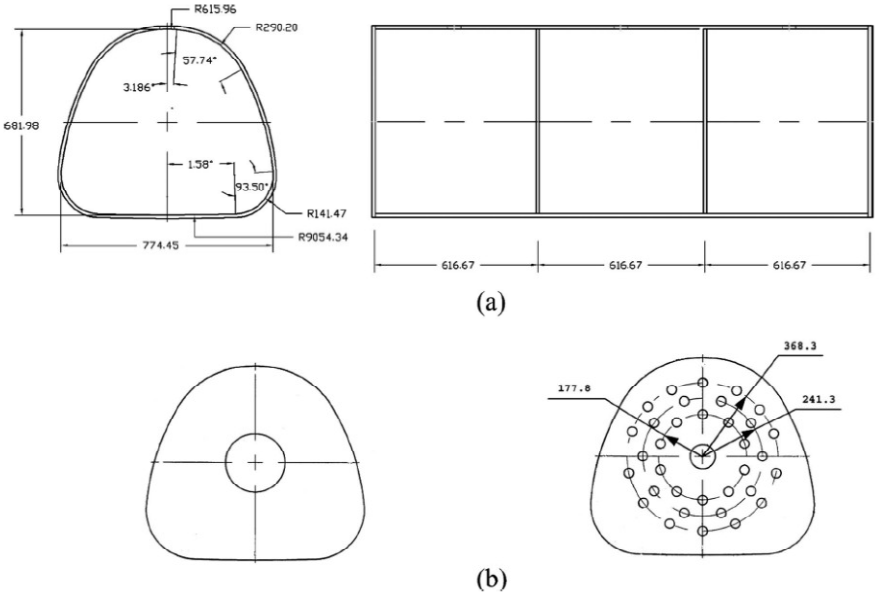

Figure 1.18: (a) Test tank, (b) single- and multiple-orifice baffles (Yan, et al., [251]).

ural sloshing frequencies in circular, elliptical and generic tank with almost the same capacities $(5,1 liter)$. The tank with different fill levels was excited by a lateral sinusoidal motion and the frequency of the peak sloshing force was attributed as the natural frequency. Experimental investigation of liquid sloshing in horizontal circular cylindrical containers was also performed by Kobayashi, et al. [118] where four model tanks with the same diameter of $470mm$ and four different lengths of $470mm$, $940mm$, $1410mm$ and $1880mm$ subjected to sinusoidal longitudinal/lateral and seismic excitation were employed to obtain natural frequencies as well as slosh-induced forces by measuring the displacement of the vessel legs.

1.4 Effect of viscosity and compressibility

Although the effect of liquid viscosity on sloshing natural frequencies and suppression of liquid free surface waves were demonstrated in the earlier studies on sloshing phenomena (see, e.g., Abramson, [10]; Demirbilek, [49, 51, 50]), inviscid flow assumption has widely been used for simulation of liquid sloshing, particularly for low-amplitude and non-resonance excitations (see, e.g.,

Nakayama and Washizu, [151]; Wang and Khoo, [237]; Karamanos et al., [109]). Lee, et al. [124] simulated several scenarios of liquid sloshing in a cubic LNG tank with the length and width of $1,0m$ and height of $0,6m$ under a roll excitation with the period of $85,0\%$ of the first natural period and 6° exciting amplitude around the center of the box using the commercial code FLOW3D. The study concluded that liquid turbulence and viscosity have insignificant effect on impact pressure (Figures 1.19 and 1.20). Wu, et al. [247] also discussed that effect of viscosity can be ignored for sloshing analysis of fluids which are not highly viscous. Furthermore, Modaressi-Tehrani, et al. [143] discussed that viscosity had a negligible effect on horizontal sloshing force and the roll moment for medium-viscosity fluids under typical road manoeuvres. However, it is recognized that viscosity may have a greater influence on effective damping of the sloshing waves. This was also confirmed by Popov [170]. Based on Modaressi-Tehrani, et al. [143], the decay rate of fluid sloshing increases sharply by increasing the liquid viscosity. Instead of inviscid flow, viscose laminar flow assumption was employed

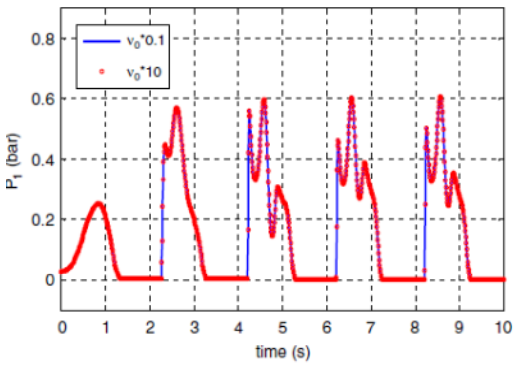

Figure 1.19: Pressure time histories for different kinematic viscosity at the point of intersection of static free-surface and the vertical side wall and 25,0 % fill ratio (Lee, et al., [124]).

by a large number of authors in tanker trucks applications where the effect of turbulence was disregarded and low velocity fluid sloshing under typical directional manoeuvres assumed. For instance, Popov, et al. [176] applied two-dimensional laminar incompressible Navier-Stokes equations to investigate the transient liquid response in arbitrary shaped containers subjected to a step input lateral acceleration using finite difference methodology. Aliabadi,

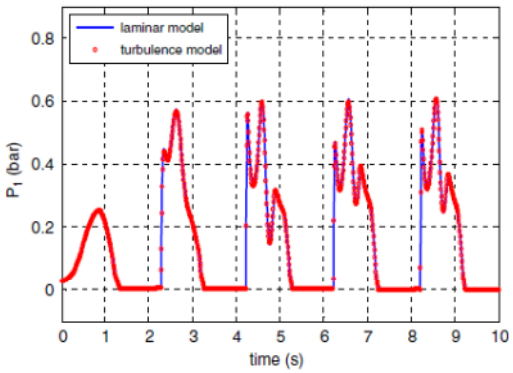

Figure 1.20: Pressure time histories for laminar and turbulent models at the point of intersection of static free-surface and the vertical side wall and 25,0 % fill ratio (Lee, et al., [124]).

et al. [13] employed a three-dimensional finite element sloshing model based on the laminar incompressible Navier-Stokes equations to obtain the transient sloshing force of a half-filled elliptical tank during constant braking and turning manoeuvres. Yan, et al. [255] obtained the transient slosh-induced forces and moments for partly filled circular and conical cross-section tanks under a time-varying lateral acceleration field using two-dimensional finite volume approach assuming laminar flows.

The requirement for inclusion of turbulence model in computational fluid dynamics simulation of liquid sloshing has not yet been established. While several researchers discussed that effect of turbulent flows should be taken into account for simulation of liquid sloshing, others found negligible effect of turbulence on simulation results. Rhee [195] suggested a computational fluid dynamics model based on the Navier-Stokes equations assuming turbulent flows to study liquid sloshing within a low-filled generic rectangular LNG tank with upper and lower chambers under harmonic roll, pitch and translational excitations. For turbulence modeling, the standard $k-\epsilon$ model was used. He showed that for low fill volume tanks, in which violent fluid sloshing contributes to generation of high turbulence fluid pockets, effect of turbulence should be considered in the computational model (Figure 1.21). Godderidge, et al. [83] also studied the effect of including a turbulence model versus assuming laminar flow for a rectangular LNG tank under transverse excitation near the slosh resonance. He suggested that the $k-\epsilon$ model for

such cases can predict liquid sloshing accurately, while the results obtained from the laminar flow model did not correlate well with the observed physical behavior. Effects of viscosity and turbulence have been considered in the computational fluid dynamics method suggested by Wasfy, et al. [238, 239] to model the violent free surface fluctuations due to high-amplitude excitations. Large eddy simulation (LES) approach was used for turbulence modeling, which creates additional unknown terms that must be modeled (Grinstein, et al., 2007). Unlike the Reynolds-averaged Navier-Stokes (RANS) equations, filtered Navier-Stokes equations are employed in the large eddy simulation (LES) approach. In fact, large eddies with sizes larger than the size of the filter, usually taken as the mesh size, are computed in a time-dependent simulation and small eddies are modeled by a subgrid model. This approach for turbulence modeling needs large computational resources in comparison with the common turbulence modeling based on Reynolds-averaged Navier-Stokes (RANS) approach such as the standard $k-\epsilon$ and $k-\omega$ methods. In agreement with Wasfy, et al. [238, 239], Liu and Lin [127, 128] employed the LES method to simulate the violent liquid sloshing in a baffled three-dimensional rectangular tank with distorted and broken free surface. On the other hand, Lee, et al. [125] implemented the Sub-Grid Scale (SGS) turbulence model into the CFD simulation of liquid sloshing in three-dimensional LNG carriers under high-amplitude excitations. The study concluded that turbulence has a negligible effect on pressure distribution and free surface profile. It is worth mentioning that laminar flow assumption for simulation of liquid sloshing in tank trucks under typical road manoeuvres leads to a satisfactorily results. In other words, implementation of a turbulence model for simulation of liquid sloshing in tank trucks is computationally ineffective, due to requirement for much more computational resources as well as insignificant influence on simulation results. Moreover, in order to calculate hydrodynamic pressures and forces, neglecting the effect of viscosity for medium-viscosity fluids in large tanks seems to be reasonable. The necessity for multiphase modeling (air-fluid), rather than one-phase modeling, in CFD simulation of liquid sloshing was established in the work by Godderidge, et al. [83], Lee, et al. [124]. However, effect of compressibility needs further ex-

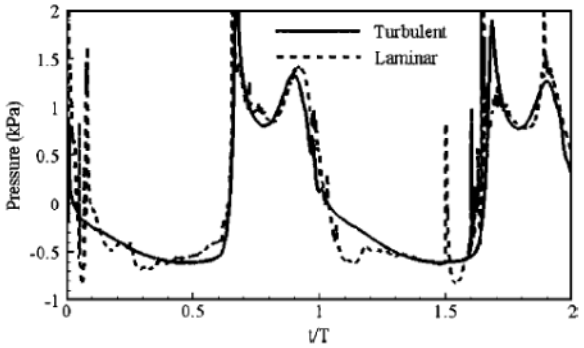

Figure 1.21: Comparison of pressure histories at a point at the bottom of the tank with and without turbulent model.

ploration since a few number of studies deal with it up to now. Godderidge, et al. [81] conducted a series of CFD simulation of water sloshing in a two-dimensional rectangular tank with $1,2m$ length and $0,6m$ height and filling level of $60,0\%$ subjected to a near resonance excitation. In order to investigate the compressibility effect, three different conditions were considered; incompressible water/compressible air, compressible water/incompressible air and incompressible water/incompressible air. Pressure histories at three different points on the tank walls in addition to free surface elevation and wall pressure forces were compared to those obtained by the experiment and a computational base model in which both air and water were modeled as compressible fluids. It was confirmed that an incompressible water/compressible air model provided a computationally cost effective approximation of the base model, while incompressible assumption for both water and air contributed to $pm60,0\%$ error in pressure histories. As it can be expected, assumption of compressible water/incompressible air resulted in significant errors.

1.5 Effect of baffles

Although baffles play a very significant role in damping the fluid sloshing in tank trucks, the effect of baffles has been investigated in a very few recent studies. However, effect of ring and radial baffles on suppressing of liquid sloshing within the missile tanks as well as storage tanks have been exten-

sively studied through experimental and computational analyses (Silveira, et al, [216]; Garza, [180]; Garza and Abramson, [180]; Gavrilyuk, et al., [77, 78]; Maleki and Ziyaeifar, [134, 134]). Significant advantages of flexible ring baffles in reducing the effect of liquid sloshing have also been demonstrated in several studies (Stephens and Scholl, [222]; Dodge, [53]). Furthermore, effect of different baffle designs on liquid sloshing in rectangular tanks has been studied in the literatures. Analytical steady state and numerical transient response of liquid sloshing within a compartmented and baffled rectangular tank under braking and steady cornering was discussed by Popov, et al. [171]. Panigrahy, et al. [163] conducted a series of experiments to study the effect of baffles on liquid sloshing in rectangular tanks. Three different configurations were used; horizontal side baffles, vertical baffles and ring baffle. Superior effect of ring baffle on horizontal and vertical baffles under lateral excitation was confirmed and attributed to the energy dissipation at all walls rather than on two walls normal to the excitation direction. Akyildiz and Unal [12] also performed laboratory experiments to investigate the effect of baffles in a rectangular tank under pitch oscillations where a combination of horizontal side baffles and vertical baffle were used. Effectiveness of baffles in reducing the amplitude of free surface response was also confirmed by Sheu and Lee [215], Celebi and Akyildiz [203], Cho and Lee [41], Biswal, et al. [29], Akyildiz and Unal [12] and Belakroum, et al. [26] through numerical simulation of nonlinear liquid sloshing in rectangular tanks.

Analytical modeling of anti-sloshing effect of baffles was limited to a very few studies in which linear sloshing assumption was applied. Goudarzi, et al. [84] developed an analytical model based on potential flow and linear sloshing to evaluate the damping effect of horizontal and vertical baffles in rectangular tanks. The damping ratio of baffles was estimated by energy-ratio formula including the damping coefficient of baffles which were expressed by the damping coefficient of free flat plates in oscillating fluids (Keulegan and Carpenter, [111]). The proposed analytical approach was supported by experimental measurements. Faltinsen, et al. [58] also performed an analytical simulation of linear liquid sloshing in rectangular tanks with a perforated plate mounted vertically in the tank middle under lateral excitation. The

pressure differential across the plate was estimated by steady state pressure differential and a pressure loss coefficient for perforated plates. Hasheminejad and Mohammadi [86] employed the conformal mapping technique to study the effect of surface-touching horizontal side baffles, bottom mounted vertical baffle and surface piercing vertical baffle in circular cylindrical containers under lateral excitation. As one can expect, a long pair of surface-touching horizontal side baffles have considerable effect on natural sloshing frequencies while bottom mounted vertical baffle was not recommended as anti-sloshing device. However, for high fill levels, surface-piercing vertical baffle was found to be an efficient means for controlling the liquid sloshing. The same conclusion was drawn by Hasheminejad and Aghabeigi [86, 87], and Hasheminejad and Aghabeigi [88] where an elliptical tank with the same baffle configurations were employed.

Computational fluid dynamic simulation of liquid sloshing in baffled tanks was performed by only a few number of researchers. Modaressi-Tehrani, et al. [143] developed a three-dimensional model of a partly-filled cylindrical tank equipped with three single-orifice lateral baffles to obtain the transient sloshing forces and moments under longitudinal and combined lateral/longitudinal accelerations using the finite volume approach (Figure 1.22). The study suggested that peak amplification of longitudinal force and pitch moment for the baffled tank at low fill level due to longitudinal acceleration of $0,6g$ was limited to $1,3$ and $0,7$, respectively, compared to $1,96$ and $1,24$ for an equivalent clean bore tank. Addition of baffles at combined lateral/longitudinal accelerations caused the roll moment amplification factor to limit to $1,47$ while this factor for clean bore tank was $1,85$. Yan, et al. [252] simulated three-dimensional liquid sloshing in a Reuleaux triangle cross- section tank through numerical and experimental methods with four different transverse baffles: single orifice full baffles; multiple-orifice full baffles; single semi-circular orifice full baffles; and partial baffles (Figure 1.23). The simulations were performed under excitations idealizing the straight-line braking manoeuvres. The results showed that the baffle design influences the natural frequency and the peak magnitudes of sloshing forces and moments in a significant manner, particularly under a higher liquid-fill depth. The study demonstrated that single-

and multiple-orifice baffles with the same porosity have the same anti-sloshing effect. Moreover, the single semi-circle orifice baffles as well as partial baffles decrease the transient peak and mean pitch moment in comparison with the conventional baffles very efficiently. Yan, et al. [253, 254] performed a similar simulation and concluded that baffle equaliser has negligible effect on longitudinal sloshing force and transient pitch moment. Kandasamy, et al. [106]

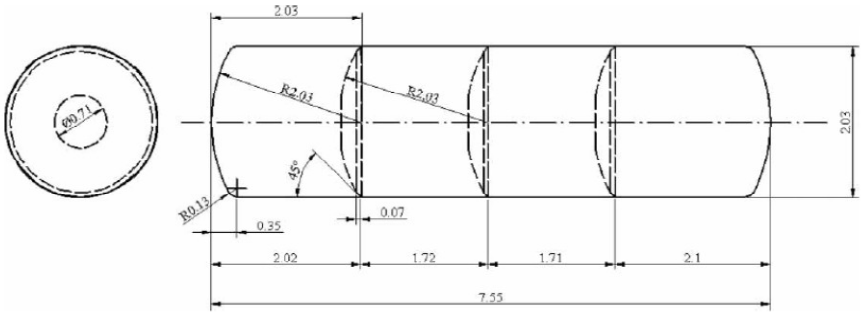

Figure 1.22: tank geometry with three single orifice baffles (Modaressi-Tehrani, et al., [143]).

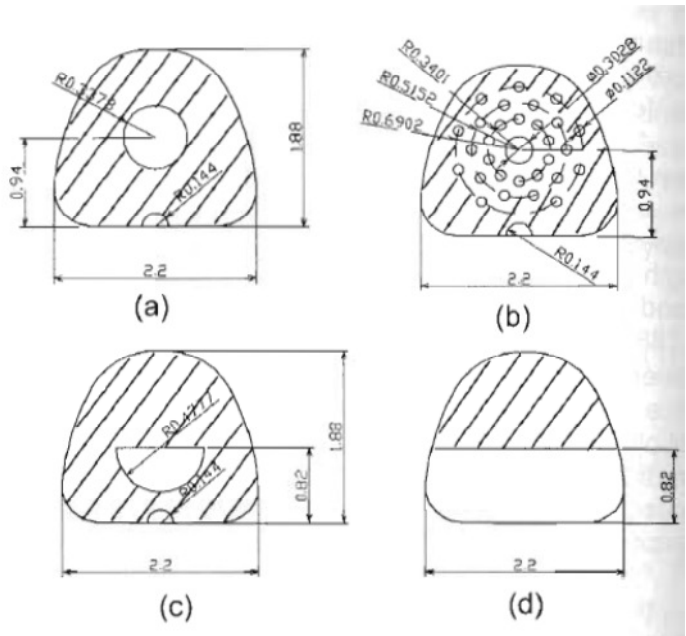

Figure 1.23: Cross-sections of baffles designs (a) Single orifice, (b) Multiple-orifice, (c) Single semi-circular orifice, (d) partial (Yan, et al., [252]).

developed a similar three-dimensional computational fluid dynamics model

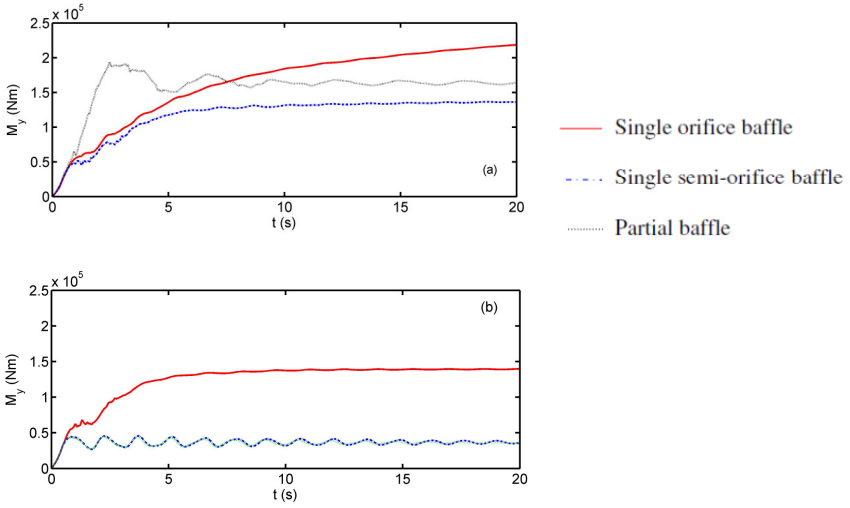

Figure 1.24: Comparison of transient sloshing pitch moment responses under 0.3g longitudinal ramp-step deceleration (a) 52,1 % fill ratio, (b) 69,5 % fill ratio (Yan, et al., [252]).

of a partly-filled circular cross-section tank under combined idealized longitudinal and lateral acceleration fields with four different transverse baffles; conventional baffles with a large central orifice, obliquely placed conventional baffles, partial baffles arranged in an alternating pattern and semi-circular orifice baffles. The results showed the effectiveness of conventional baffles in decreasing the fluid sloshing in the longitudinal direction and their negligible effect in the roll plane. The study indicated that obliquely placed conventional baffles offer considerably higher resistance to lateral liquid sloshing in the roll plane and longitudinal liquid sloshing in the pitch plane. Furthermore, partial baffles, like the conventional baffles but with lower structure weight and cost, have ineffective anti-sloshing performance in the roll plane and positive effect in the longitudinal direction. Besides, semi-circular orifice baffles not only yield lower magnitudes of steady-state roll and pitch moments under the intermediate fill levels, but also offer significant reductions in the longitudinal load transfer, which makes it possible for them to improve the braking performance and yaw stability limits. Kang and Liu [107] employed the commercial software FLUENT to simulate liquid sloshing in a three-dimensional compartmented cylindrical tank with constant fill level

of $85,0\%$ during the braking and turning. Each compartment had a partial transverse baffle at the middle of the compartment during the braking manoeuvre while this baffle was replaced by a partial longitudinal baffle during the turning manoeuvre. It was found that in order to minimize the longitudinal sloshing force during the braking manoeuvre and lateral sloshing force during the turning manoeuvre, the ratio of the unbaffled area over the baffle to the total tank cross sectional area should be between $0,2$ and $0,3$ while the ratio of baffled area to the total tank cross sectional area is $0,4$. In order to

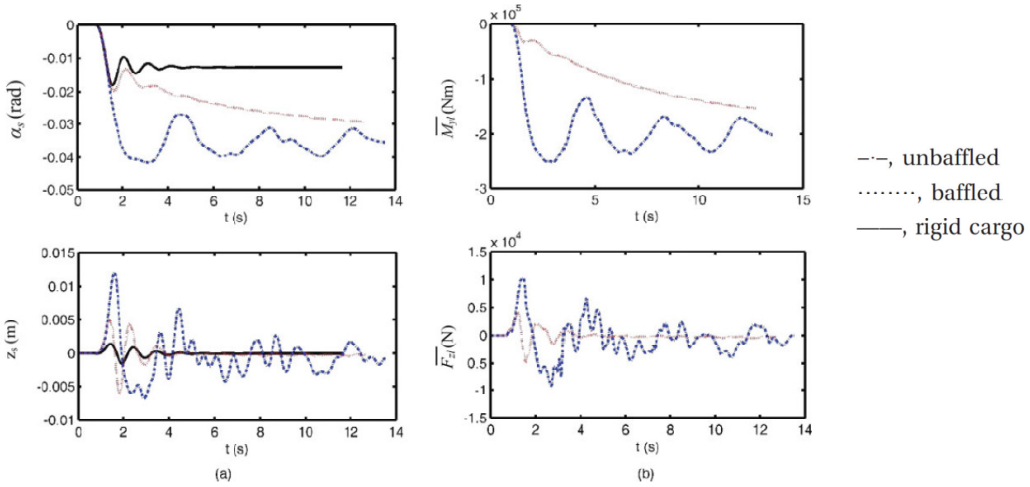

Figure 1.25: Transient response of the baffled and unbaffled tank truck (a) pitch angle and vertical displacement of the sprung mass, (b) slosh pitch moment and vertical force (Yan and Rakheja, [249]).

study the effect of baffles on the vehicle transient response under braking maneuver, Yan and Rakheja [249] presented the results in the form of transient vehicle vertical displacement and pitch angle, and transient sloshing vertical force and pitch moment for $52,1\%$ fill volume tanks with baffles and without baffles under a $395kPa$ treadle pressure on the dry road surface (Figure 1.25). The responses of the equivalent rigid cargo truck were also presented to illustrate the influence of fluid sloshing. The results showed a dynamic load transfer to the front axle due to the negative pitch angle of the sprung mass. Both the slosh pitch moment and the sprung mass pitch responses of the cleanbore tank revealed oscillations, while those responses for baffled

tank asymptotically approached the steady-state values. The magnitudes of the transient peaks in pitch moment and pitch angle for baffled tank were significantly smaller than those obtained for the unbaffled tank, which revealed anti-sloshing effectiveness of the baffles. Similar results were obtained from the longitudinal response of the vehicle. Furthermore, the dynamic load factor (DLF), defined as the ratio of the instantaneous axle load to the static axle load, response of vehicle under the same braking maneuver was discussed. The study concluded that the baffles can significantly limit the dynamic load transfer from the rear axle to the front axle. Effect of baffles on reducing longitudinal load transfer was also confirmed by Lloyd, et al. [133] where liquid sloshing in a one-sixth scale model of a cryogenic cylindrical tank with five different baffle designs (Figure 1.26), including solid dished, oblique, spiral, round, and perforated, was experimentally investigated. The perforated baffle was found to be the most effective design with the advantage of being lightweight.

1.6 Mechanical Analogy Method

An alternative approach for analyzing the liquid sloshing in moving containers can be represented by drawing an analogy between the liquid motion and mechanical systems. The key idea of this method is that the liquid within the container can be treated as consisting of two distinct parts; stationary part with respect to the container and the moving part which causes the liquid sloshing. In fact, this division is constructed on the basis of two distinct components of hydrodynamic pressure in the moving containers; a component of pressure which is proportional to the tank acceleration and convective pressure. The moving part of liquid is modeled by a series of mass-spring-dashpot systems or a set of simple pendulums assuming linear liquid motion. The parameters of the equivalent mechanical system can be evaluated by considering equivalent mass and moments of inertia, preservation of liquid center of gravity and equivalent oscillation frequencies, force and moment resultants. For this purpose, the difference between fluid total mass and the mass of stationary part of liquid can be equated with summation of a series

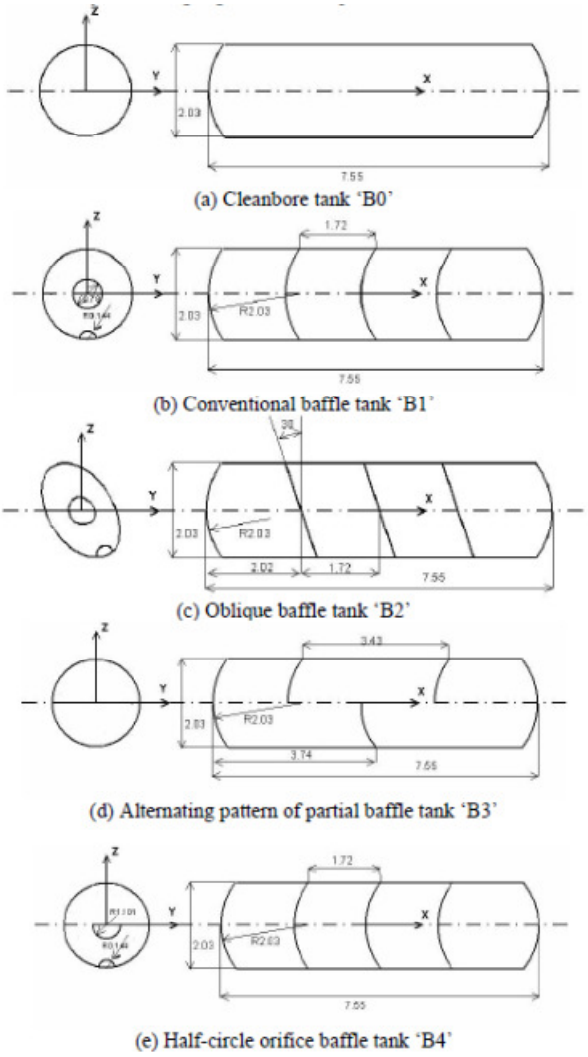

Figure 1.26: Tank and baffle configurations (Lloyd, et al. [133]).

of masses which represent the mass of each sloshing mode. In addition, the mass moment of inertia of such modal masses and rigid fluid mass through the fluid center of mass should be equivalent with the fluid mass moment of inertial. In case of mass-spring-dashpot system, the spring constants can be determined from the natural frequencies of liquid sloshing, while in case of pendulum system, length of pendulums are calculated from the natural frequencies. Finally, In order to obtain the sloshing forces and moments, the equation of motions of equivalent mechanical system along with the above constraints are developed. Comprehensive formulations of equivalent mechanical systems for a general-shaped container have been documented by Ibrahim [97].

Early attempts for simulation of liquid sloshing by equivalent mechanical model were reported by Abramson [10], where the parameters of equivalent mechanical system for upright cylindrical and rectangular tanks based on the simple mechanical model with one sloshing mass as well as complex mechanical model with more than one sloshing mass for both pendulum and mass-spring analogies were given. Furthermore, more extensive design formulae and graphs for parameters of equivalent mass-spring-dashpot and pendulum models in addition to sloshing forces and moments for different tank geometries under translational and pitching motion were presented by Roberts, et al. [196]. Besides, Ibrahim [97] developed the sloshing forces and moments for upright cylindrical and rectangular tanks under harmonic lateral and pitching excitations, based on both mass-spring and pendulum analogies. It is worth mentioning that parameters of equivalent mechanical model were usually obtained from the linear theory and experimental data (see, e.g., Sumner, [225]; Unruh, et al., [231]).

Since the equations of motion for point masses and rigid bodies are usually included readily in the overall equations of motion vehicles, the equivalent mechanical method has received a great attention in the field of vehicle engineering. Bauer [25] developed a mechanical model describing the liquid motion in rectangular and upright circular cylindrical containers by a mass-spring-dashpot model to obtain liquid natural frequencies as well as sloshing forces and moments exerted upon the various vehicles. Slibar and Troger

[217, 218] employed the similar mechanical model presented by Bauer [25] to investigate the effect of liquid sloshing on the lateral wheel-load transfer of a tractor-semitrailer-system under periodic steering. Khandelwal and Nigam [112] employed the pendulum analogy including one fixed mass and one pendulum mass representing the fundamental mode of sloshing to simulate the liquid sloshing in a rectangular railway wagon moving on a random uneven railway track with constant longitudinal acceleration. The dynamic response of vehicle-liquid system was determined by two models: a heave model and a heave-pitch model. The model parameters were calculated for harmonic vertical acceleration assuming small and stable displacement of free liquid surface. The effect of damping was also considered by a viscous damper attached to the pendulum.

Ranganathan et al. [192] integrated a pendulum model of liquid sloshing in two-dimensional circular tanks subjected to lateral excitation to a three-dimensional vehicle model to investigate the directional response of tank vehicle during steady state maneuver. Parameters of pendulum model were determined from the approach proposed by Budiansky [34]. The entire vehicle was simulated by considering five degrees of freedom for sprung mass and two degrees of freedom including roll and vertical motion for unsprung mass. Ranganathan et al. [193] developed an equivalent mass-spring system for liquid sloshing in a three-dimensional horizontal circular cylindrical tank by a summation technique to study straight-line braking performance of a tractor-semitrailer tank vehicle. By this technique, partially-filled tank divided into a number of rectangular elements and parameters of equivalent system were calculated for each individual element based on the linear theory. Afterwards, parameters of equivalent mass-spring system for entire cylindrical tank were computed by summation of parameters calculated for each rectangular element. The proposed model was validated in terms of fundamental frequency versus liquid fill level plot obtained from experimental study conducted by McCarty [137]. Aquaro et al. [14] conducted roll stability analysis of partially-filled tank trucks using mechanical analogy. A vehicle model in roll plane was implemented in ANSYS software based of finite element approach and integrated to a simple pendulum model.

Ibrahim [96] developed an equivalent pendulum-dashpot model of liquid sloshing in a cylindrical container having a longitudinal slotted partition and integrated it into a roll plane model of a truck with three axles. Damping ratio and damped natural frequency were measured experimentally using a small-scale model tank. Xu et al. [248] investigated the ride quality of partially-filled compartmented tank trucks in presence of liquid sloshing effect, which was modeled by a linear mass-spring-dashpot system. Acarman and Özgüner [11] suggested a controller to stabilize and attenuate the sloshing effect in heavy commercial vehicles. The study integrated a vehicle model with six degrees of freedom, lateral, longitudinal, vertical, yaw, pitch, and roll, to equivalent mechanical models of liquid sloshing in longitudinal and lateral directions proposed by Ranganathan et al. [192, 193]. Salem et al. [204] simulated the lateral fluid sloshing in two-dimensional partly-filled elliptical containers using equivalent trammel pendulums (Figure 1.27). The parameters of equivalent pendulum model including arms of trammel pendulum, fixed mass and pendulum mass, and the height of fixed mass with respect to the tank base were calculated by matching of pendulum natural frequency, horizontal force component and static moment around the tank base to those calculated from finite element simulation of fluid motion. The suggested trammel pendulum approach represented an approximation of nonlinear liquid sloshing dynamics and provided a computationally effective tool for coupled simulation of liquid sloshing and vehicle dynamics compared to CFD simulation of liquid sloshing. Mechanical analogy was also employed

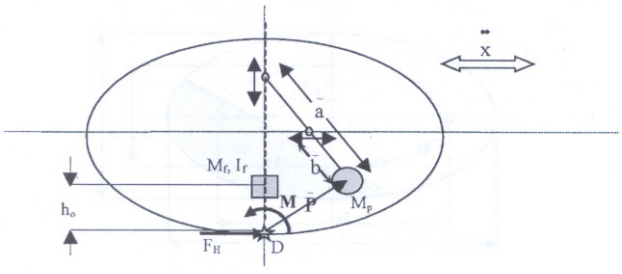

Figure 1.27: Trammel pendulum model (Salem et al., [204]).

to simulation the nonlinear characteristics of liquid sloshing problems. For

instance, Bauer et al. [23] developed an equivalent nonlinear mechanical model for simulation of liquid sloshing in a vertical circular cylinder under harmonic translational excitation. The model consist a rigid mass and a mass point attached to a nonlinear spring and constrained to move on a parabolic surface. The coefficient of spring constant was obtained from the experimental test results. Sayar and Baumgarten [208] added a cubic spring and a simple dashpot to a pendulum model proposed by Sumner [225] to account the effect of nonlinearity of liquid sloshing in spherical tanks. The coefficient of that cubic spring was obtained from laboratory-measured data. Dai et al. [46] presented a nonlinear mechanical model for simulation of liquid sloshing in horizontal cylindrical tank based on the summation technique proposed by Ranganathan et al. [193] and addition of a nonlinear term to the equation of motion of linear model. This nonlinear term was first suggested by Pilipchuk and Ibrahim [169] for simulation of nonlinear interaction of liquid hydrodynamic impact and elastic support structure. The proposed equivalent mechanical model was integrated into a pitch plane model of a partially-filled tank vehicle moving on a rough road. Also, Godderidge et al. [82] developed a nonlinear pendulum model based on the CFD simulation to study the liquid sloshing in rectangular containers. Furthermore, analogy between spherical pendulum model and nonlinear free surface phenomena were adopted by several researchers for simulation of nonlinear liquid sloshing within the context of aerospace applications which discussion about them is not in the scope of this literature review (see, e.g., Berlot, [179]; Kana, [103, 104]; Kana and Fox, [105]).

The simplicity of integration of mechanical equivalent models into the vehicle dynamics models allows convenient real time co-simulation. However, linear equivalent mechanical models are subjected to the same limitations as the linear sloshing analysis in terms of amplitude and frequency of excitation as well as tank geometries. In other words, parameters of linear equivalent models for tank configurations which are mostly used in the liquid-transporting vehicles should be determined experimentally, since these parameters can only be obtained for upright cylindrical and rectangular containers in closed forms. Furthermore, complications associated with

evaluation of nonlinear mechanical model parameters as well as accounting for damping require equivalent representation of nonlinear phenomena in the free surface through careful experimental measurements or analysis of CFD simulation results. These analyses and measurements should principally be conducted for each specific problem based on the researcher's experience and intuition. What is more, three-dimensional motion of liquid in moving containers, which can significantly affect the simulation results particularly for complex external loads such as simultaneous lateral and longitudinal excitations, cannot be model by mass-spring and pendulum systems.

Chapter 2

Review of North American and European tank trucks accidents surveys and standards design

2.1 Statistical surveys on accidents involving tank trucks

The risk assessment, represented by partly filled tank truck, is done by a review of the statistical survey of the reports in North America and European Union. In general, there isn‘t explicit relation between the tank trucks rollovers and the fluid sloshing, because no objective evidence exists. For instance, an un-tripped rollover in curve is commonly attributed only to the excessive speed, even if, the lateral load shift, in partly filled tank, gives a not negligible contribution to the load transfer [243, 255]. Nevertheless, the influence of the fluid sloshing on tank truck rollover can be find matching data coming from different databases, focusing on different aspects. For example, it has been found that the majority of rollovers in which the tank is partly filled refer to loss of control while the trucks were not travelling at excessive speed before the accident. This shows the influence of liquid surge on rollovers of partly filled tank truck [166]. Unfortunately, the databases‘ reliability is often too low, to inprouve which the quality of the collected data must be improved, to do so a team of experts must be established, which purpose is to investigate each accident in detail. The disadvantage of this

method is that a limited number of representative cases can be considered [166, 1].

Statistic survey on tank truck accidents focus on tank truck carrying hazmat, because of the hazardous related to the transport of such kind of goods. Hazmat transportation is regulated in similar way between Europe and North America (Canada and USA). Nevertheless, there are relevant differences on the vehicle design. Analyzing separately those two areas in terms of statistic accidents survey can help to address the problem. Historically more attention have been posed on the problem in North America, so more reports have been found, this may be due also to the higher frequency of the accidents in that area, which can be determined by different way of liquid distribution, in particular hazardous material, among those two areas.

In the first part the review of the North America accidents reports will be presented, than the European analysis will be reported. At the end, the analysis of the design standards used on the analyzed areas will presented.

2.1.1 North American statistical surveys

Many statistical survey of North American accidents have been consideredFor in this part, the most important are: [166, 243] for the USA and [186, 244] for the Canadian part. In [166] an extensive analysis of the four most important USA accidents' databases has been done. The considered databases are (refer to Appendix A):

- Motor Carrier Management Information System (MCMIS) [4];
- Large Truck Crash Causation Study (LTCCS) [3];
- Truck Involved in Fatal Accidents (TIFA) [6];
- General Estimates System (GES) [2].

A rough analysis of the data of MCMIS database is used in [166] to investigate the main cause factor, also known as Primary Reason of accidents. For this first analysis a sample of 1.260 accidents involving cargo tank in 2002 were selected from MCMIS database, among these, 264 or the 21% resulted in rollover (refer to Appendix A). Tank trucks rollovers are mainly single vehicle

accident, with 221 accidents about 84% of 264 rollovers sampled from MCMIS [166], refer to 2.1. Moreover, among driver factor, vehicle factor, highway factor and environment factor, the driver factor is identified as primary reason of accidents with 189 rollovers about the 85.5% of the 221 single vehicle rollover as reported in 2.1. In addition, driver error could be a decision error during an evasive maneuver, a performance error or a not-performance due to fall sick for instance, and a wrong recognition; among these the decision error during evasive maneuver accounts for about the 42% . These two finds are commonly recognized among all the literature, [166, 148]. This first analysis confirmed the low roll stability limits of the heavy vehicles, and in particular of tank trucks. In fact, because of the low roll stability limits, rollovers of heavy vehicles are mainly un-tripped which means that rollovers aren't caused by other vehicles, while the high frequency of diver error, in particular decision error during evasive maneuver, remarks the low controllability limits. A total of 482 trucks rollovers among the 1.837 tank trucks accident, collected

Table 2.1: Primary reason of rollover and relative frequency (MCMIS)

Primary Reason	**Single vehicle Rollovers**		**Multiple Vehicle Rollovers**	
	Number	**%**	**Number**	**%**
Driver Factor	189	85,50	11	25,60
Vehicle Factor	9	3,90	0	0,00
Highway Factor	8	3,70	0	0,00
Weather Factor	0	0,00	1	2,30
Other Vehicle Induced	12	5,30	31	72,10
Unknown	3	1,30	0	0,00
Total	221	100,00	43	100,00

from 1999 to 2003, and available in the TIFA database [6] (Appendix A), are used to investigate the driver errors [166]. In table 2.2 are reported a miscellaneous set of driver errors, with relative frequencies, that have been considered to contribute significantly to the rollover. It should be noted that each rollovers can have more than one diver factor coded in the database.

The first reason of rollover is run off road with almost the same frequency between straight truck and tractor semitrailer, respectively 31,6% and 34,0%. The second most frequent cause of rollover is the speed, in fact, the driver is travelling too fast in 13,2% of cases for straight truck and 17,1% for tractor semitrailer. Almost in another 14,0% of times it is not possible to define the causes of the rollovers, whereas the inattentive account for another 6,5% of the times. Furthermore, the drowsy and asleep accounts for the 5,2% of the times among driver driving tractor semitrailer, resulting in the fifth more frequently cause of rollover. In straight truck, the driver drowsy or asleep is really seldom, accounting for only the 1,6% of times. Resuming, in almost one third of cases the tucks ran off road before they roll over, while the trucks were not travelling too fast, furthermore, drowsy and asleep occurred really seldom. This scenario is coherent with the low controllability of tank trucks in fact the fluid sloshing may increase the difficult of keeping on road the vehicles during evasive manoeuvres. In [166] the frequency of tank trucks rollovers is compared with the frequency of vans rollovers (truck hauling rigid cargo). For this study the sample of 1.837 crashes involving tanker, collected in the TIFA [6] database from 1999 to 2003 (see Appendix A), is compared with a representative sample of 10.396 crashes involving vans, extracted from the original 25.704 crashes reported in TIFA for the same 5 five years. Tank trucks are most likely involved in rollover accidents respect to the vans trucks (trucks hauling rigid cargo). This is confirmed by the data reported in 2.3. In fact, the percentage of rollovers of tank trucks respect to the total numbers of accidents, involving tank trucks, is 26,2% with 482 rollovers in 5 years; this percentage is higher compared with the 10,3% of rollovers of vans. Moreover, in 2.3 is pointed out the high frequency with which the tractor semitrailers are involved in accidents, about 78,0%. Whereas, the straight truck are much prone to rollover when involved in accidents, with 31,2% of straight tank trucks compared with the 25,1% of tank truck tractor semitrailer. This study confirms how the tank truck exhibits lower stability characteristics compared with the trucks hauling rigid cargo, moreover, the overall lower stability limits of the tractor semitrailer is confirmed [243].

Table 2.2: Rollover crash driver error and distraction, relative frequency (TIFA)

Driver Factor	Straight truck		Tractor Semitrailer	
	Roll	Percent of All Rollovers %	Roll	Percent of All Rollovers%
None	26	13,70	87	14,60
Physical or Mental Condition				
Inattentive	13	6,80	39	6,50
Drowsy, Asleep	3	1,60	31	5,20
Other Physical	1	0,50	8	1,30
Miscellaneous Driver Errors				
Run Off Road	60	31,60	206	34,00
Driving too fast	25	13,20	102	17,10
Erratic/Reckless	8	4,20	29	4,80
Over Correcting	17	9,00	26	4,30
Failure to Yield or Obey	9	4,70	14	2,30
Other Driver Error	7	3,70	14	2,30
Other				
Avoiding, Swerving Sliding	11	5,80	15	2,50
Misc. Non-Driver Causes	2	1,00	9	1,50
Miscellaneous violation	4	2,00	7	1,10
Possible Distractions (inside the vehicle)	2	1,0	7	1,10
Vision Obscured	2	1,00	5	0,80
Total	111	100,00	171	100,00

Table 2.3: Rollovers of tank trucks versus van wiht relative frequencies (TIFA)

Configuration	Total Rollovers	Total Crashes	Percent Rollovers vs Crashes	Percent of all Crashes
VAN				
Straight Truck	215	1871	11,50	20,1
Tractor-Semi	856	8,525	10,00	79,9
Total	1071	10,396	10,30	100,00
TANK				
Straight Truck	111	356	31,20	23,00
Tractor-Semi	371	1481	25,10	77,00
Total	482	1837	26,20	100,00

In [166] the influence of the carried cargo is also investigated, as allowed by TIFA [6] database. From the sample of 1.837 accidents involving tank trucks, form 1999 to 2003, 1.129 were loaded with liquids or gases cargoes; 183 from the about 25.000 tankers accidents were carrying solid cargoes in bulks, and so added to the sample. The considered sample is of 1.312 tank trucks and is divided by type of cargo (Gases, Solids or Liquids) in table 2.4. Moreover, the crashes are divided in crashed resulted in rollover or not during the accidents. As reported in 2.4, tanker carrying liquids and gases, when involved in accidents, result in rollover at higher rate, about 38,8%, compared to tankers carrying solids cargoes, about 27,0%. Moreover, in the influence of the percentage of the load has been analyzed using the TIFA database (Appendix A) [166]. Table 2.5 provides the loadś percentage, as expected

Table 2.4: Rollover by type of loads vs all crashes whether roll or not (TIFA)

Tank type	No roll		roll		Total	
	Number	%	Number	%	Number	%
Gasses	67	69,9	43	39,1	110	100,0
Solids	134	73,2	49	26,8	183	100,0
Liquids	636	62,4	383	37,6	1.019	100,0
Total	837	63,8	475	36,2	1.312	100,00

the majority of the rollovers occurred among trucks that had partial to full loads, 291 accidents which corresponds to the 71,3% of 394 total accident for which those information are available. In addition, in [166] has been

Table 2.5: Tanks rollovers frequencies by percentage of load (TIFA)

Cargo percentage of GCW	**Total rollover**	**Percent of all rollovers**
0 to 10%	32	8,10
11 to 50%	81	20,6
> 50%	281	71,30
Total	394	100,00

reported that almost in 50% of cases the rollover occurs in curve, whereas in the other 50% of time rollover occurs in straight road, in both cases with road in dry condition and good visibility. Due to the high frequency of miles of straight road, it is possible to affirm that rollovers are more likely to occur in curve than in straight, while the dry condition means high friction and so high lateral acceleration. All the information collected allow to assume that partly filled tank truck carrying liquid cargo are much prone to roll over among the tank truck. Moreover, the driver error has been found to be the primary reason of rollover accident. Furthermore trucks are much prone to roll over in curve.

The tank truck employed in Canada transport of dangerous good are similar to the one employed in US market, furthermore road infrastructure have many similarity, therefore similar results are expected. In [244] 1.874 files of road accidents, from 1990 to 1998, involving dangerous goods have been analyzed (see Table 2.6). Among the 1.874 accidents 810 (43%) results in rollover, between these, 724 (89% of 810) were tank trucks and they were carrying cargoes of Class 2, 3, 5, and 8, respectively Gasses, Flammable liquids, Oxidizing substance and corrosive substances (refer to the appendix A for a detailed list). Table 2.6 shows that tank trucks carrying hazmat (hazardous material) of Class 3: Flammable liquids, like gasoline, are the most involved in accidents, with the 47% of 1.874 accidents. Hazmat Class

Table 2.6: Reported accidents involving vehicles carrying dangerous goods in Canada from 1990 to 1998

Commodity class	Accidents		Rollovers		
	Total No. Accidents	Accidents by class %	Total No. Accidents	Rollovers by class	Rollovers occurring per Accidents
1- Explosives	42	2,00	14	2	33
2- Gasses (Tankers)	276	15,00	162	20	59
3- Flammable Liquids (Tankers)	885	47,00	479	59	54
4- Flammable Solid	45	2,00	16	2	36
5- Oxidizing Substances (Tankers)	49	3,00	14	2	29
6- Poisonous substances	106	6,00	11	1	10
7- Radioactive material	43	2,00	16	2	37
8- Corrosive substances (Tankers)	342	18,00	69	9	20
9- Misc. products	52	3,00	18	2	35
Non Regulated	33	2,00	10	1	30
Unknown	1	0,00	1	0	
Total	1874	100,00	810	100	

8: Corrosive substance; and Class 2: Gasses; are involved respectively the 18% and 15% of time. The greater number of tank trucks hauling hazmat of Class 3 is one of the factors that leads to the greater involvement in accidents, in fact, hazmat of Class 2, which is involved only the 15% of time, is much more distributed via pipe line. Having a look at the percentage of rollover per Class type, the tank trucks hauling Class 3 hazmat type are involved in the 59% of rollovers, the tank trucks hauling Class 2 are involved in the 20% of rollover and trucks hauling Class 8 are involved in the 9% of rollovers, altogether they represent about the 90% of the rollover, so the first conclusion would be that tank truck are most likely prone to rollover. But the high frequencies with which those commodities are carried represent a bias in the data and so should be remarked. Moreover looking at the Rollovers per accident and Class type the most involved in rollovers are tank trucks carrying Class 2: Gasses, this is probably due to the common employed circular section that increase the high centre of gravity of those tanks. In table 2.10 is reported the yearly distribution of the accidents related to the vehicle type. The involved vehicle configuration type is the tank truck tractor semitrailer with an average of 31 rollovers per year, than the straight truck follows with an average of 15 rollovers per years. The scenario reported in Canada by [244] is similar to the one obtained by [166] for US. Even though, in [186] is emphasized the difficulty of having data with enough reliability. In fact, in [186] a total of 972 accident files involving tank vehicles during 1995 to 1999 were obtained from MTQ for the analysis. Of the total 972 reports, 609 contained the tank trucks, among these 219 were selected as showing probably instability. Analyzing the 219 reports, 22 referred to the rollover, 31 referred to tip over, 40 cited loss of control, 107 of the reports indicated overturning, fire and explosion, and 19 of these indicated the presence of a sudden braking or steering maneuver. Moreover, the reports provided very little information as to the type of vehicle, tank and the cargo. Thus the reports were considered inconsistent to generally conclude upon the rollovers and the contributing factors.

Table 2.7: Yearly reported accidents by dangerous goods vehicle type

Vehicle Type	Rollovers Accidents - Canada wide										Avg - year
	1990	1991	1992	1993	1994	1995	1996	1997	1998	Total	
Straight truck	17	15	19	21	20	17	17	5	4	135	15,0
Tractor Semitrailer	41	33	20	13	24	26	37	37	49	280	31,0
Doubles	16	30	15	9	11	20	36	34	29	200	22.2
Triples	1	0	1	2	0	0	0	0	0	4	0,4
Truck & Trailer	0	0	4	4	4	4	4	4	0	24	2,67
Total	75	78	59	49	59	67	94	80	82	643	71,4

2.1.2 European statistical surveys

In Europe only a few number of statistics on heavy vehicles accidents exist, and there are even less on tank truck accidents. Furthermore, it has been shown that tank truck accidents are even not reported in the main databases [9]. Moreover, the information contained is not adequate to allow specialists to draw any conclusion on the main tank trucks accidents causes. To fill the lack of studies the European Commission (EC) commissioned in past 10 years a lot of studies [1], for instance ETAC, TRACE, ASTERYX, APROSYS, CHILD, PEDANT etc. Unfortunately none of them deals with tank truck carrying dangerous good. Some of those studies are intended to build a methodology to develop a suitable database, other are intended to use data collected from those databases to draw the actual scenario on heavy vehicles accidents. The EC and the International Road Transport Union (IRU) commissioned the European Truck Accident Causation [1], which is the widest study on the European community dealing with accidents involving heavy vehicle. 8 teams of experts have been established, in 8 sampling area of the EU to investigate the main causes of the accidents on the accidents‘ spot. In this study both heavy vehicles carrying moving and rigid cargoes are involved. 624 truck accidents have been collected and investigated during 2 and half year, since April 2004 to September 2006. The study turned out that the main factor of the accident with a frequency of 85,2% is the human factor (truck driver, car driver, pedestrians etc.), out of this, only for 25% the accidents are caused by truck driver. Among the accident configuration type, the most frequent are

1. Accident at intersection 27,2 %;
2. Accident in queue 20.6 %;
3. Accident due to a lane departure 19.5 %;
4. Accident during an overtaking manoeuvres 11.3 %;
5. Single truck accidents: only one vehicle (a truck) is involved in the accident 7.9 %

In Single truck accidents, the driver lost the truck control 75,0 % of times, in 64,0 % of times was negotiating a bend or changing direction, in the 20,0 % of times the truck rolled over. Only 14 cases the truck were carrying hazardous material, 9 of them were truck and semitrailer and 5 straight truck, 50,0 % of them were carrying inflammable load, not better specified if liquid or solid, no more information exist about truck body and accident type. Even if the report doesn't have so much information about tankers, the low stability characteristics of the trucks are very well turned out.

Table 2.8: Accidents per vehicles type in Austria 2001

Austrian Calssification of Vehicles type	**IRTAD definition**	**Accidents 2001**	**CARE Calssification of Vehicles type**	**Accidents 2001**
Heavy goods Vehicles	Lorries > 3,5 t with and without Trailer Semitrailer trucks Tanker lorries with and without trailer	2.087(1)	Lorry, > 3,5 tonnes Road tractor	2.087(1)
Lorry < 3,5 ton	Lorries < 3,5 t with and without Trailer	2398(1)	Lorry, < 3,5 tonnes	2398(1)
Lorry > 3,5 ton	Lorries > 3,5 t with and without Trailer	1.519(1)	Lorry, > 3,5 tonnes	1.519(2)
Road tractor	Road tractor	578(1)	Road tractor	578(2)

ASTERYX is another project issued by European Commission [9], it is an investigation study of the CARE Database (CARE - Community database on Accidents on the Roads in Europe), for more info refer to the Appendix E. The Project's purpose was the identification of trend and characteristics of the lorries' accidents in Europe. Comparing the statistic's Austria and IRTAD with the CARE one, the authors found some discrepancy between

the databases. The 2.8 shows a difference of 41 accidents reports more, in the Austria national data respect to the CARE database. All the 41 accidents reports, that make the difference, involve tank trucks. The authors affirm that there are some differences on the definition between databases; moreover they could not understand where in the CARE database tankers are considered. However a number of 41 accidents involving tanker in 2001 are reported, unfortunately no more details are available.

A total number of 32 accidents and incidents are reported in [7], based on Hazardous Cargo Bulletin accident Log, related to the country in the Baltic Sea region. The DAGOB project was launched in 2000 by the European Commission with purpose of promote reliability and safety on dangerous good‘s transportation in the Baltic Sea Region. The authors assessed the lack of statistic data concerning accidents involving dangerous good. In the Appendix F are reported 22 accidents that could be attributed to truck or train instability, among those 18 (81,0 %) are attributed to road tanker, the 50,0 % of which resulted in overturning after the driver lost control, spill of dangerous good and in 10 cases (60,0 %) fire occurred. Moreover the statistics are related mainly to the Germany, which is the country in the Baltic Sea region in which the road mode of transport is the most used.

The lack of a common EU community‘s database of the roads accidents involving dangerous good is reported in [209]. Furthermore, the German Federal Statistics Office reported 52 road accidents in 2000, in which hazmat were released. Another study carried out by the Spanish University of Madrid [135] reports a total number of 88 road accidents involving hazardous material. The source is the Spanish Ministry of Foment. The authors found a lack of 54 accidents reports comparing this database with other database. Release of dangerous goods occurred on 43 of them, the most released hazmat types are flammables liquids, in special way gasoline and diesel. The greatest number of accidents occurred in road with one carriageway 15. The most involved tank trucks types are trucks semitrailers with 23 accidents. Furthermore the most frequent accident type are rollover and running out.

Another source of data, reported in [135], is the Spanish Ministry of Traffic. A total number of 2.059 road accidents from 1993 to 2005, involving at

least one tank truck carrying hazmat are reported in this database. Among these 1.259 are rigid cargos, and 800 are truck semitrailer. Furthermore, different collisions are the frequent type of accident whit a frequency of 65.5 % of time, whereas different forms of running out: with collision, or rollover or fall over, accounted for 23.4 %. Rollover is the third most frequent accident type with a frequency of 4.0 %.

The lack of a unique European database, collecting the road accidents involving dangerous good, make impossible to asset road safety concerned tank truck in EU by observing of statistical trends. Moreover, the European project ASTERYX [9] shows a lack of information on the CARE database (Appendix E) , concerning reports related to tank truck. On the basis of the afore mentionated statistical reports cannot be drown any conclusion regard the stability of the tank truck in the European Union‘s road.

The frequency of accidents involving tank truck is not so high compared with the overall number of accidents, almost 2,0 %. Nevertheless tank trucks are subject to roll especially if they are travelling partly filled, therefore the liquid sloshing is an important contributing factor, this is partly confirmed by an analysis of the statistics survey in North America. Whereas, in Europe a lack of information don‘t allow to drown conclusion. Furthermore, the difficult of using the available generic data collected in the databases is shown even in North America. Moreover the big efforts that have to be done to collect suitable data to produce reliable statistic survey are shown in other North American and European studies.

The driver error has been found to be the most relevant factor in 85,5 % of the overall accident, in both the North American and European continent. Moreover, the rollover of heavy vehicles has been found to be the most frequent single vehicle accident, which shows the low influence by others external factors such as other vehicles or weather conditions etc, and emphasize the low roll stability limits of heavy vehicles. In addition, some North American surveys have shown that in the majority of rollovers are involved tank trucks carrying liquid cargoes and travelling partly filled. Furthermore, heavy vehicles rollovers occur mainly while negotiating a curve and with high friction condition. In summary, it may be concluded that driver

input initiates to destabilize the truck by overcorrecting, for instance during an evasive maneuver or after tanking a curve too fast. This results is an hard and more often impossible task due to the low stability truck limits. Moreover, in partially filled tank the lateral acceleration due to the liquid surge increase the lateral acceleration due to the yaw motion and this may lead the over past of the static rollover threshold. In conclusion increasing the overall roll stability threshold, increasing the SRT, can improve the safety of all the heavy vehicles. Moreover, reducing the contributory factor due to the liquid surge increase the controllability limits of tank trucks which are extremely important during evasive maneuver.

2.2 European and North American tank truck standards design

The European and North American standards for tank design mainly deal with tank carrying hazardous materials; respectively there are two main regulations: the ADR (Agreement Dangerous Road) [69] for the European community; and the part 178 title 49 of the CFR (Code Federal Regulation) [155] for the United States which is adopted also in Canada where is known as $CAN/CAS\ B620$ to $B622$. It is worth to remark that for the tank carrying not dangerous goods there are not design rules or restriction.

In these regulations all aspects concerning the carriage of dangerous goods are regulated; like general provisions; dangerous goods classification; condition of carriage (loading, unloading and handling); packaging; etc. A complete documents review goes beyond the purpose of the present work, whereas the analysis of the regulations concerning the stability improvement of tank vehicles is the focus of this review. Prescriptions like the minimum static rollover threshold or the use of baffles for the limitation of the liquid surge, in a partly filled tank, will be analyzed.

ADR - Europe In the European Community the ADR agreement introduces from 2003 the standard 9.7.5 which is known as “Stability of tank vehicle”. This standard is divided in two parts & the 9.7.5.1 and the 9.7.5.2.

- The first one 9.7.5.1 regulates the tank vehicles' aspect ratio in the roll plan, it requires that the maximum width at ground level between the outermost contact points must be at least 90,0% of the center of gravity height of the laden vehicle;

- In addition, the second part 9.7.5.2 prescribes that all the tank vehicles with fixed tanks with a capacity of more than $3m^3$, intended for carriage of dangerous goods in the liquid or molten state tested with a pressure of less than $4bar$, shall comply with the technical requirements of ECE Regulation $No.111$ for lateral stability [68].

Regarding the requirements of verification and testing, the ECE Regulation $No.111$ provides that:

> the vehicle shall undergo a tilt table test in accordance with $annex3$ to the Regulation which simulates a non-vibratory steady-state turn, or as an alternative a calculation method in accordance with $annex4$ to the Regulation.

In case of tilt table test, the static rollover stability of the vehicle shall be such that the wheels on one side should not lost the contact with the tilt table surface when an angle of 23° has been reached, the test shall be repeated three times for each side. Furthermore the tilt table test shall be done in full load condition, not dangerous goods can be used and at least the $70,0\%$ of the volume should be filled. In case in which the maximum axle load is past, a fluid with less density shall be used. Moreover the tilt table angle should be increased slowly with an angular speed less than $0.3^{\circ}/s$.

Alternatively to the tilt table test the calculation method can be used. Using the calculation method the rollover stability of vehicle shall be such that the point at which overturning occurs would not be passed if a lateral acceleration of $4m/s^2$ has been reached. In annex 3 to the $ECE111$ all the details for the calculation are reported, all the main factors influencing the roll stability are considered, such as the centre of gravity height, the track width, the suspension and tire stiffness. The tires and suspensions stiffness is considered linear and the values can be provided from the manufacturer.

In partially filled tank truck the fluid sloshing can reduce seriously the truck stability, not only the pure lateral stability but also the yaw stability, leading to the jackknife phenomenon. The forces rising from fluid sloshing are proportional to the weaving mass and the acceleration rate, in order to prevent severe sloshing forces the ADR regulation 4.3.2.2.4 [69] provides that:

> Shells intended for the carriage of substances in the liquid state or liquefied gases or refrigerated liquefied gases, which are not divided by partitions or surge plates into sections of not more than 7.500 liters capacity, shall be filled to not less than $80,0\%$ or not more than $20,0\%$ of their capacity.

In other words if the capacity of the tank compartments is more than 7.500 liters, such tank cannot be filled in the range between $20,0\%$ and $80,0\%$ of fill level.

The surge-plates are not meant only for preventing the fluid sloshing; in fact the design of surge-plates (baffles) is regulated by the regulation 6.8.2.1.20 which provides some measures to quantify the protection against damage of the tank.

> In case of tank used for carriage of liquid goods, with a circular or elliptical cross section, with a maximum curvature radius of $2m$, the shell is equipped with strengthening members comprising partitions, surge plates or external or internal rings so placed that at least one of the following conditions is met:
>
> - Distance between two adjacent strengthening elements of not more than $1,75m$;
> - Volume contained between two partitions or surge plates of not more than $7.500liters$.

Moreover the regulation 6.8.2.1.22 provides that:

> Surge-plates and partitions shall be dished, with a depth of dish of not less than $10cm$, or shall be corrugated, profiled or otherwise reinforced to give equivalent strength. The area of the surge plate

> shall be at least $70,0\%$ of the cross-sectional area of the tank in which the surge-plate is fitted.

CFR 49 - North America The title 49 of the Federal Regulation Code (CFR) [155] is the code of the Department of Transportation (DOT) of USA which deals with carriage of dangerous goods. The $CFR49$ regulates mainly the transportation of goods and people by rail and road, moreover the $CFR49$ regulates the transportation of dangerous goods through part 100 to 199 (Pipeline and Hazardous Material Safety Administration Department of Transportation). The same regulation is adopted in Canada where is known as $CAN/CAS\ B620$ to $B622$.

The part 178 of the $CFR49$ regulates the design of the tanks used for carriage of dangerous goods; this regulation mainly regulates the thickness and the material of the shell and the bulkheads. The part $178.345-7$ refers to baffles as strengthening providing that

> a cargo tank with a shell thickness less than $3/8in$ must be circumferentially reinforced with bulkheads, baffles, ring stiffeners, or any combination thereof, in addition to the cargo tank heads; circumferential reinforcements must be located so that the maximum unreinforced portion of the shell does not exceed the $460in$ (about $1520mm$).

In the $CFR49$ as well as in $CAN/CSAB620$ to $B622$ there aren't any regulations concerning with the lateral stability limits like ECE Regulation 111 for the European Community. Recently, Canadian National regulatory authorities are analyzing the possibility of adopting $0,4g$ as minimum roll threshold for tank trucks. For this purpose the Transport Dangerous Goods Directorate (TDG) of Transport Canada commissioned to the Centre for Transportation for Technology of The National Research Council of Canada (NCR/CSTT) a comprehensive series of tilt tests to characterize the rollover threshold of tank trucks fleet that operate in Canada [28]. 17 vehicles were tested which included the principal configurations of tank truck in service across Canada and between Canada and US. 7 of 17 ($41,0\%$) distinct vehicles

Figure 2.1: Comparison between three different tank cross sections: from left to the right, a) low, b) medium and c) high cg heght.

tested would have a roll threshold under $0,35g$ when loaded to their allowable gross weight in Ontario, while 14 of 17 ($83,0\%$) would have a roll threshold under $0.40g$. More over the roll threshold of a vehicle with liftable axles drops by $0.01g$ to $0.03g$ when those axles are raised to turn. Table 2.9 resumes the experimental activity.

In [28] the authors clearly show that the $83,0\%$ of the considered tank trucks (14 tank trucks over 17), representing a significant part of the Canadian tankers fleet, have a low static rollover threshold (SRT) (under $0,4g$) and that 7 of them have a SRT even lower (under the $0,35g$). The main factors influencing SRT are the track width and the centre of gravity height which is influenced by the Gross Vehicle Weight (GVW). Figure 2.1 shows the cross sections of three vehicles among the 17 analyzed. From left to the right are shown the cross sections of vehicles 01, 03 and 12, refer to 2.9. All the three vehicles have the same trailer track width $2.54m$, whereas vehicle 01 is loaded with $61,603Kg$ of diesel fuel, vehicle 03 is loaded with $63,011Kg$ of gasoline and vehicle 12 is loaded with only $59,181Kg$ of liquid propane; In spite of its lower load condition, vehicle 12 has the lower SRT, only $0.333g$, compared with vehicle 01, $0.415g$.

Vehicle 01 is equipped with a TC 406 (also US-DOT 406) tank's spec-

Table 2.9: Summary of the experimental activity carried out by [28]

No	Vehicles Config.	Spec.	Year built	Axles/ Liftables	Cargo	GVW [Kg]	Avg RT [g]
16	B-Train	331	1996	8/0	Liquid propane	62,259	0.310
18	Tractor-Semitrailer	307	1974	6/1	Al2SO4	47,976	0.320
12	B-Train	331	1987	8/2	Liquid propane	59,181	0.333
05	Tractor-Semitrailer	331	1991	6/1	Liquid CO2	50,970	0.337
03	B-Train	306	1995	8/0	Gasoline	63,011	0.343
04	Tractor-Semitrailer	331	1982	5/0	Liquid CO2	37,695	0.346
17	Tractor-Semitrailer	341	1991	6/1	Liquid nitrogen	50,358	0.357
06	Tractor-Semitrailer	331	1991	6/1	Liquid CO2		0.359
13	Tractor-Semitrailer	341	1996	5/0	Liquid nitrogen	37,967	0.365
08	Straight truck	306	1995	2/0	Heating oil	16,366	0.365
15	Tractor-Semitrailer	341	1983	6/1	Liquid oxygen	52,038	0.367
07	Tractor-Semitrailer	331	2001	6/0	Liquid CO2	48,957	0.371
09	Straight truck	406	2001	3/0	Heating oil	25,637	0.383
11	Tractor-Semitrailer	341	1978	5/0	Liquid oxygen	39,414	0.385
10	Tractor-Semitrailer	None	2001	5/0	Water	33,006	0.408
01	Tractor-Semitrailer	406	2002	7/3	Diesel fuel	61,803	0.415
14	Straight truck	331	2001	3/0	Liquid propane	17,857	0.469
02	B-Train	306	1995	8/0	Diesel fuel	61,209	0.605

ification, which is designed to have a low cg height, whereas the vehicle 12 is equipped with a tank specification TC 331 designed for carriage of compressed gasses. It is evident that the 01 vehicle has a lower cg height compared with the other tanks (see Figure 2.1); the use of single wide tires instead of double tires allows to increase the frame width, this allows to design tank with section partly integrated into the frame and thus with a lower cg height; moreover enhancing the frame width increases the roll stiffness due to the suspension stiffness; these intervention can improve the SRT.

The two figures on the top of 2.2 show two B-train used to carry diesel fuel, the figure on the left shows a Canadian B-train with 8 axles with an allowable gross vehicle weight of $63,500Kg$, while the figure on the right shows an Australian B-train equipped with 9 axles and an allowable gross vehicle weight of $62,500Kg$, enhanced to $68,000Kg$ for route-specific permit. Both the tanks have the same capacity but it is evident that the top of the compartment of the Australian tank is lower compared with the Canadian one. In the bottom part of the 2.2 are shown two B-train tanks used for carriage of liquid propane, it is evident that the Australian one, on the right, slope severely down from front to the rear lowering in this way the cg height. From these considerations is clearly that the improvement of roll stability is not a priority for Canadian tank manufactures [28]. Reduction of capital cost seems to be of primary importance, similar consideration can be made for the USA tank manufactures; whereas the improvement of roll stability is a priority for the Australian tank manufactures. In Europe is much common the use of tractor semitrailer instead of B-train or other road train combination. The use of pneumatic suspension and wide single tires for trailer's axles allow the European manufactures to comply easily with the roll stability limits of $0.4g$ imposed from the authorities since 2003 for tank carrying dangerous goods.

Rollover accidents are usually initiated by severe steer inputs performed to avoid obstacle on a roadway or for lane keeping, to avoid to go off road. In such conditions, the stability limits determined with a static analysis (SRT) are reduced by the dynamical response of the system. The Dynamic Rollover Threshold (DRT), defined as the acceleration at which all the wheels on one

Figure 2.2: Comparison between Australian (right figures) and Canadian (left figures) B-train for carriage of liquid fuel (top figures) and liquid propane (bottom figures)

side of the vehicle are lifted in transient maneuver, has been estimated to be about $20,0\%$ lower compared to the SRT [243], [80]. In such scenario the liquid's response, within a partially filled vessel, further reduces the dynamic rollover threshold. The worst case sloshing conditions occurs when tank are filled in the range of $40,0\%$ to $70,0\%$ of the tank volume [243], [56]; Figure 2.3 shows the reduction of the dynamic rollover threshold as function of the sloshing volume. In such fluid loads condition the effective lateral acceleration during a rapid steering maneuver can be approximately double, thus half of the SRT acceleration can induces rollover. Generally steering wheel inputs having a frequency in the vicinity of $0,5Hz$ produces such a *resonant* response from the under filled liquid load.

In terms of standards to prevent such phenomenon only the European economic community has adopted one obvious approach, toward avoiding stability degradations due to the slosh, simply avoiding the under filled condition. The article 4.3.2.2.4 of the ADR agreement deals with this issue, this article has been already reported in the section dealing with the ADR regulation. This ADR Articles 4.3.2.2.4 states

> when tanks intended for carriage of liquids are not divided by partitions or surge plates into sections not more than $7,500liters$ in capacity, they shall be filled to not less than $80,0\%$ to their capacity unless they are practically empty.

Unfortunately in EU this article is applied only to dangerous loads, thus there

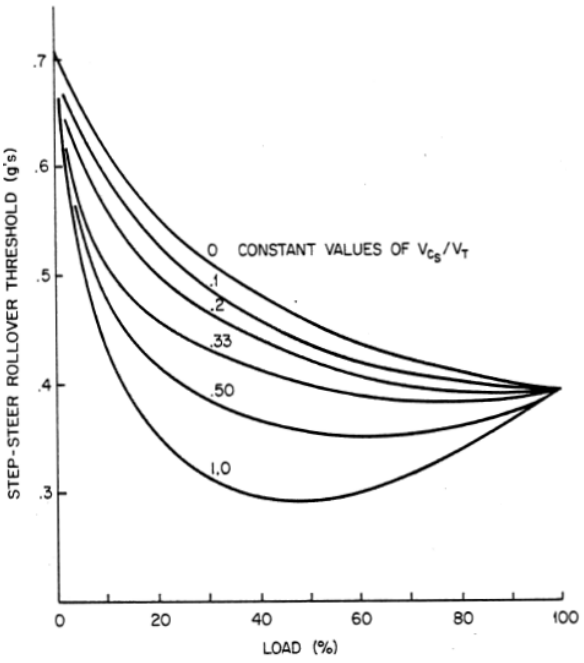

Figure 2.3: Dynamic Rollover Threshold as function of load percentage.

are half of the tank trucks fleet that can travel with whatever filling condition representing an hazard for road safety. Furthermore in North America there aren't any regulations dealing with this issue.

The standards scenario is deeply different between North America and European Community. In North America there is a consistent lack of regulations toward the improuvement of roll stability, moreover the use of design criterion based on a reduction of capital cost (use of double tires instead of single etc.), represent a hazard for road safety. The lack of a minimum Static Rollover Threshold (SRT) and the lack of minimum requirement about filling conditions, compared with European community are the main differences. In addition the use of different B-train combinations, (maximum GVW $65 ton$) which mean higher pay loads, further increase the hazard for road safety. It is worth to remark that some tank specifications, like US DOT 406 or the Canadian equivalent TC 406 (vehicle 01 see Fig. 2.1), has good quality in terms of SRT, even if not requirements about minimum SRT has been found on the official US Code of Federal Regulation title 49 [155].

In the European Community a minimum level of road safety is guaranteed

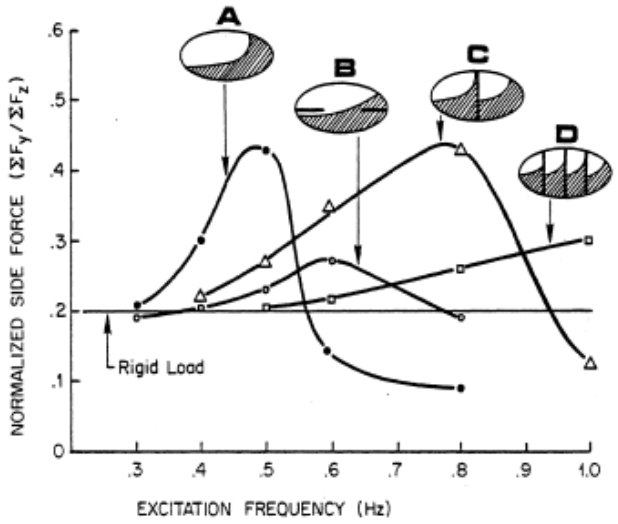

Figure 2.4: Influece of different baffles concepts on the normalized side force levels due to fluid sloshing in a 50,0 % - filled elliptical tank.

by the ADR agreement, through which a minimum SRT and a specified level of filling is required, in order to homologate and travel with tank-semitrailer. The habitual use of tractors in combination with tank-semitrailers (maximum GVW $44 ton$) designed with more stability criteria allows EU manufactures to easily copes with regulations requirements. Even though, a SRT of $0.4g$ imposed only for tank trucks carrying dangerous good (and busses), isn't enough in the authors opinion. In fact $0,4g$ is further reduced about $20,0\%$ in dynamic conditions which occurs during evasive maneuvers in full load conditions. The SRT is reduced more than $20,0\%$ when a tank truck is filled between $40,0\%$ and $70,0\%$ of volume, and this can easily occurs with tank carrying not dangerous goods.

A final observation should be made on the use of lateral baffles, neither in European nor in North American standards is considered the use of lateral baffles. Reason of capital cost reductions and the increase of complexty of tanks' cleaning are the main reasons that prevent the use of such kind of baffles. Even though, the use of lateral baffles can strongly prevent the hazard due to the liquid sloshing in partly filled tank. Figure 2.4is taken from [56], it clearly shows the effects of different baffles arrangements. In particular,

configuration B seems to be very efficient in terms of sloshing forces reductions. Furthermore, considering tanks for transportation of liquefied gasses, which SRT is the lowest of the whole tank trucks fleet, and for which sloshing effects can occurs even in full load condition, because the maximum liquid fill level is imposed to be the $80,0\%$ of the volume, the use of lateral baffles can improve the Dynamic Rollover Threshold.

Chapter 3

Experimental validation of CFD sloshing-model

3.1 Introduction

As has been discussed in the introduciton, aim of the CFD model is to run in co-simulation with a truck vehicle model in order to simulate the coupled vehicle-fluid dynamics. The coupling of the models is done through the forces and moments arising from the fluid sloshing, in a partly filled tank, acting on the wetted wall. So for this purpose, a CFD sloshing model validation should be done comparing experimental and numerical sloshing forces and moments. The use of full scale road tanker, to validate the CFD sloshing model, is inadequate because even if it gives precise information about vehicle performace subject to the sloshig, those tests are very expensive and they don't give insight about the behaviour of the fluid sloshing. For these reasons controlled laboratory tests are prefered to validate the CFD sloshing model.

As has been reported in the literature review (section 1.3) the majority of the experimental works used to validate sloshing model are based on very small-scaled model tanks, for instance, Abramson et al [10] used a cylindrical model tank wiht a cross-section area of no more than $0,03m^2$. The majority of the previous studies of slosh frequency, regardless of the methods employed, have been performed to analyze the 2D behavior. However, when the excitation is in the neighbourhood of resonance frequencies, the swirling

motion may be induced and superimposed on the normal slosh motion. Furthermore, the beating phenomenon could make the slosh motion even more complicated. In this case, the slosh becomes a 3D motion and the 2D analysis is inadequate, these limitations exist for the majority of reported experiment studies of slosh.

The present validation is done using the experimental work carried out by Gorong Yan in his phd thesis [251, 250] under the supervision of professor Subash Rakheja at the Concordia University of Montreal Department of Mechanical and Industial Engineering. The experimental setup used by Gourong in his phd work is probably the largest in scale. In view of the limitations of previous experimental slosh studies, the slosh experiment plan presented by Gourong aims to achieve the further understanding of liquid slosh phenomenon, especially in 3D aspect and within the model tanks of larger cross-section subjected to various excitations. Morever the experiment results will be also used for the extensive validation of slosh simulation (Gorong [251, 250]).

The CFD sloshing model developed in this work is a nonlinear model which has been developed using the FLUENT CFD code. FLUENT uses the Finite Volume Method to integrate the Navier Stokes equations, whereas the free surface motion is obtained using the Volume of Fluid method which is based on the assumption of immiscible fluid. The main difference between the model developed by Gourong and the model used in this work is about the method used to apply an external excitation. In this work the external excitations are applied to the fluid domain by mean of 'Mouving Mesh Method', whereas in the Gourong works [251, 250] the 'Body Forces Method' is used. Other than the afore mentionated settings other parameters have to be setted such like: the mesh density; the use or not of a viscous model (e.g. $k-\epsilon$); the minimum time step. To choose all of those parameters numerical-experimental comparison have to be done, in particular the validation will be done comparing sloshing forces shapes and fundamental frequencies.

In the follow a brief introduciton on the experimental setup and results obtained by Gourong [251, 250] will be given; then numerical and experimental validation will be discussed.

3.2 Experiment setup

The experiments were conducted in a downscaled conical model tank. The tank was placed on a shake test table. Figure 3.1 shows the schematic of shaking mechanism of the slosh experiment. The shake table is made of magnesium. It is connected to the hydraulic actuator and is placed on the granite support table. The surface of the support table is fully covered with oil during the experimental run to achieve the smooth motion of the shake table with very small friction. The oil film was maintained on the table surface through an oil circulation system. The hydraulic actuator is controlled by a servo controller (MTS 407). The servo-valve controls hydraulic flow to the actuator that moves the actuator piston rod. The actuator piston rod applies the force required to displace the shake table. The MTS 407 controller can generate excitation signals of sinusoidal, square, and triangle waveforms. The slosh experiments were performed using the model tank of the conical cross-section (Figure 3.2), which is the scaled model of an optimal tank proposed by Kang [108]. The model tank is assembled with three sections of identical length (Figure 3.2). The total length of tank is $1,85m$ and the cross-section area is $0,426m^2$. The geometrical details of the conical cross-section are presented in Figure 3.2. From the literature survey, this model tank is probably the largest experimental setup in the laboratory use. The width of the cross-section is approximately 1/3 of the real tank of road vehicles. The tank was made of transparent plexiglass with the thickness of $12,7mm$. The transparent wall allowed visualization of the flow behavior. The tank was mounted on an aluminum plate that was fixed on the shake table through three force dynamometers. The tank position could be rearranged such that the excitation is in either lateral or longitudinal direction, with respective to the tank orientation. Water is used as the test liquid within the tank and a colouring agent is added to visualize the flows.

The tank was designed in a way to allow installation of baffles inside the tank. In the present setup, two different baffle designs have been considered to study their effect on slosh damping. One is the baffle with a single-orifice of diameter $245,5mm$, located at the baffle centre (Figure 3.2). Another is

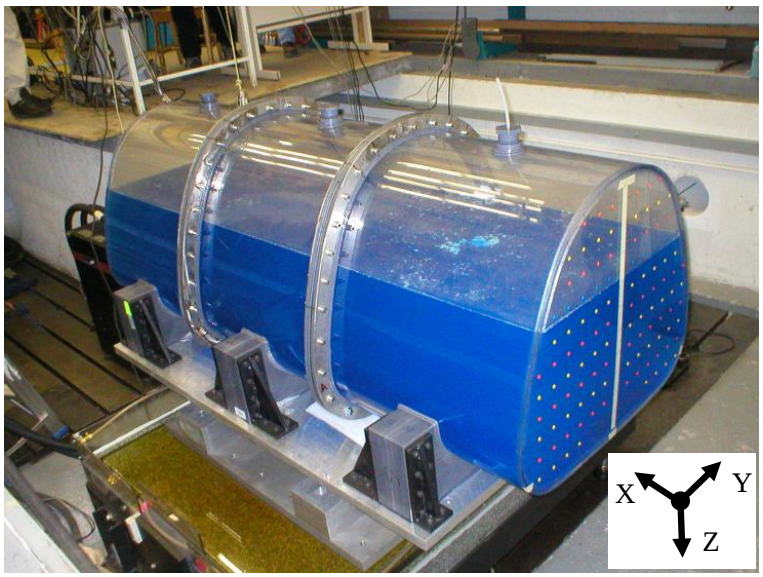

(a)

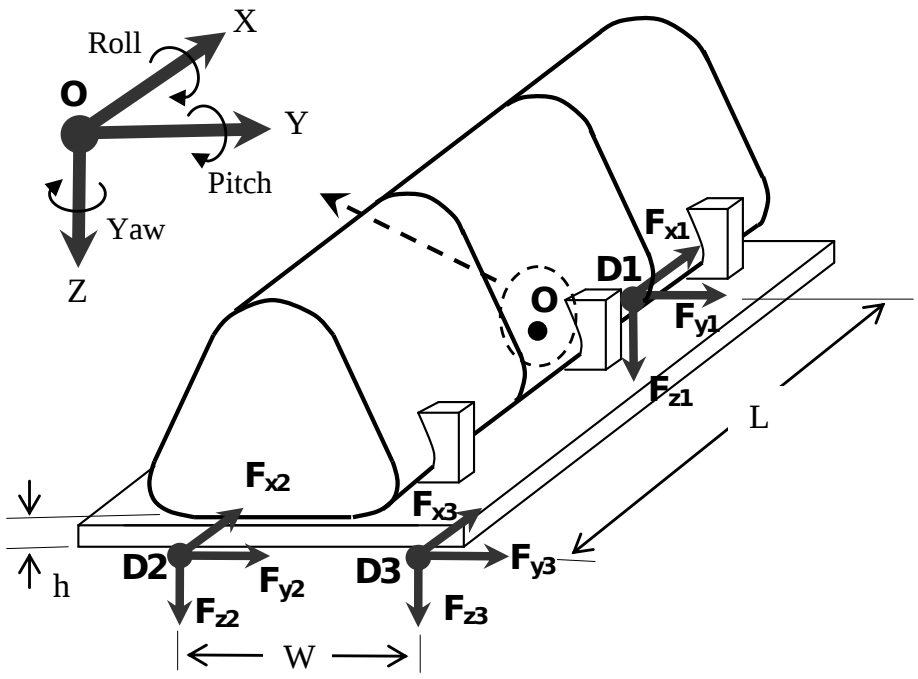

(b)

Figure 3.1: (a) pictorial view of the experimental setup; (b) schematic view of the tank illustrating the global and local coordinate systems and location of the three dynamometers (D1, D2 and D3)

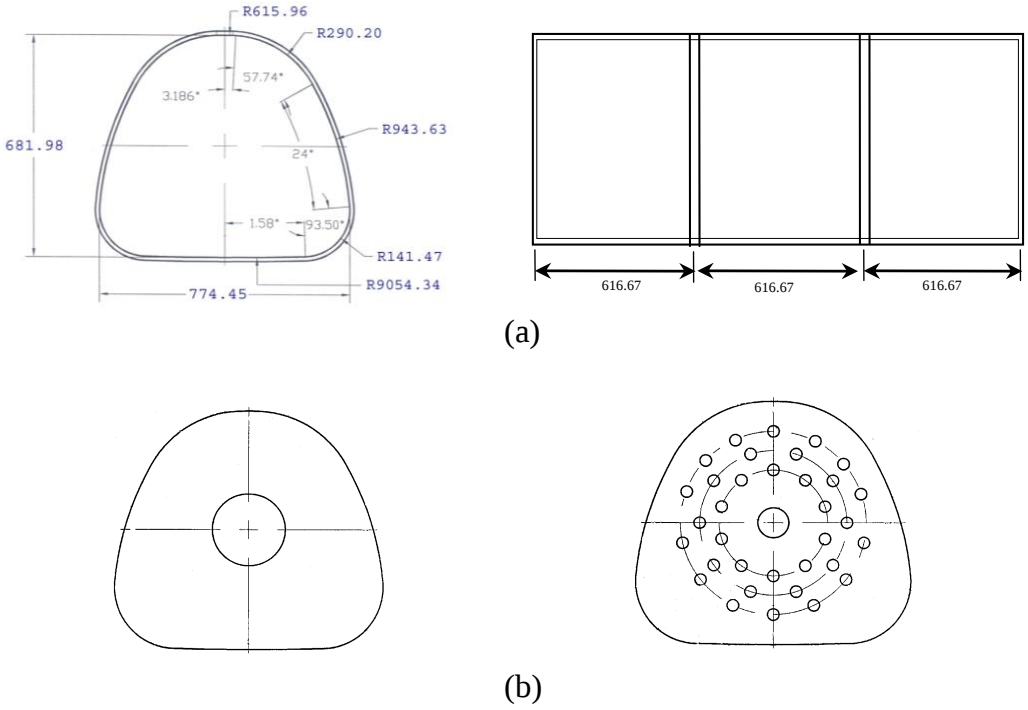

Figure 3.2: Schematic view of the tested tank (a); the single orifice ('T1'); and multiple orifice ('T2') balffles.

the perforated baffle with one big orifice of diameter $101,6mm$ at the baffle centre and 34 small orifices of diameter $38,1mm$ located around the center orifice. The opening area of the two baffles is approximately $11,0\%$ of the whole cross-section area. The baffles are made of transparent rigid PVC.

The forces arising from the liquid slosh were measured using three quartz dynamometers Kistler 9257BA with built-in charge amplifiers. The three dynamometers were mounted beneath the tank mounting plate, one located in the front and two in the rear of the plate (Figure 3.1). Each dynamometer consists of four 3-component force sensors thus can measure the 3-orthogonal component of a force. The sensitivities of force dynamometers are set at 1 N/mV for x- and y-components and 2 N/mV for z-component, which correspond to a working range of 5 and 10 kN respectively. The acceleration and displacement of the platform and tank were measured using an accelerometer and a linear variable differential transformer (LVDT). The operating range of the accelerometer is $4g$ with the sensitivity of $500mV/g$. The range of the LVDT is $254mm$ ($10inch$) with the sensitivity of $39,4mV/mm$ ($1V/inch$). The force, acceleration and displacement signals were acquired using National Instrument PCI-6036E DAQ board. A total of 11 channels were used for acquisition of the force component signals from three dynamometers as well as the signals of platform acceleration and displacement. The data was acquired at a rate of 256 Hz using the Labview 7.0 software, for more information about the instrumentation refer to [251].

3.3 Test conditions

The goal of the experiment is to investigate the slosh frequency response and the magnitude of slosh forces and moments under given test conditions. Table 3.1 shows the test conditions under which the experiments have been carried out for three tank configurations. The three configurations are the tank without any baffles, with two single-orifice baffles as well as with two perforated baffles. Experiments were conducted for $30,0\%$, $50,0\%$ and $70,0\%$ fill volumes. For the single-orifice baffle configuration, $30,0\%$ fill volume was not tested. It is because the static liquid surface, in $30,0\%$ fill volume, is

Table 3.1: Test conditions of slosh experiment for the tank with different baffles. X and Y indicate respectively the longitudinal and lateralexcitation directions.

Tank configuraiton	Fill volume (fill height, cm)			Type and direction of excitation		
	$30,0\%$ $(19,96)$	$50,0\%$ $(29,39)$	$70,0\%$ $(41,79)$	Harmonic	Step	Single-cycle sinusoidal
Cleanbore				X,Y	X,Y	Y
single-orifice baffle	no test			X,Y	X,Y	Y
Perfored baffle				X,Y	X,Y	Y

below the orifice bottom edge. The liquid longitudinal slosh motion may result in the different surface heights for different compartments because no equalizer was designed on the bottom of the baffles.

For each tank configuration at a selected fill condition, the tank is forced to shake under harmonic and idealized step excitations in terms of acceleration in both lateral and longitudinal directions. The purpose of harmonic excitation tests is to study the dependence of slosh on frequency and magnitude of external disturbance. Considering the natural frequency range and the space limitation of shake table motion, the harmonic excitations were generated at different combinations of frequency and magnitude. The frequency in lateral direction ranges from $0,5$ to $3Hz$, while the magnitude varies from $0,5$ to $3m/s^2$ in terms of acceleration. The longitudinal harmonic excitations were generated at various frequencies from $0,25$ to $1,5Hz$ in three acceleration magnitudes: $0,25$, $0,5$ and $1m/s^2$. The harmonic acceleration is converted into the corresponding displacement and then they are used to control the actuator for the tank motion through the servo controller. The single-cycle sinusoidal function and the step excitation, in terms of acceleration, are synthesized and fed to the servo-controller as the external functions of corresponding displacement via the Visual Designer software.

The sloshing forces are evaluated subtracting from the aquired dynamometric signals the inertial contribution due to the tank structure and mouint-

ing plates. To obtain the inertial mass of the system the empty tank was tested under different excitations condition, than using linear regression the overall mass of the tanker simulator has been determined. The value of the mass so obtained was compared with the static one yielded using a weighing machine, in this way the measurement system has been validated. Because the dynamometers do not have the output of moments, the calculation of moments is also validated. A frequency of 13 Hz has been found from the spectral analysis of the acquired signals which is attributed to the highen frequency of the piston rod and the mounting plate coupling system. This frequency is considered out from the frequency range of interests which is between $0,0$ and $3,0Hz$. To eliminate such frequency the acquired time series voltage signals were post-processed using low-pass filter. The 8th order Butterworth digital low-pass filter was used with the cutoff frequency of $6Hz$ for the cases with the lateral excitation and $3Hz$ for the cases with the longitudinal excitation. Since the big variations of signal magnitude are observed 96,0% confidence was applied for the calculation of force and moment magnitude in order to reduce the uncertainty.

For the validation purpose focus will be placed on the amplitudes and the frequencies of the sloshing forces in steady state conditions, thus from the experimental tests carried out by Gourong only the steady state harmonic excitation tests, in lateral and longitudinal direction, are considered, consequently only single harmonic excitations are numerically simulated. Furthermore, beign of main interest the non-linear sloshing behaviour only the tank without baffles will be numerically investigated. For a deep analysis of the fluid sloshing behaviour refer to Gourong [250].

3.4 Lateral and Longitudinal harmonic excitation

Purpose of lateral and longitudinal harmonic excitation is to study the steady state sloshing forces in terms of amplitude and frequency response. As reported in Figure 3.3 (a) and (b) the numerical and analitical natural frequencies of the fluid agree very well. As expected the natural frequencies increase monotonically with the filled volume, in both longitudinal and lateral direc-

tions (Figure 3.3 (a)). In Figure 3.3 (b) the baffles influence on the natural frequencies are reported, as expected the natual frequencies increase sharply in longitudinal direction with a negligible difference between the two baffles configurations (multiple 'T2' and single orifice 'T1'), whereas in lateral direction the influence on the natural frequency is negligible.

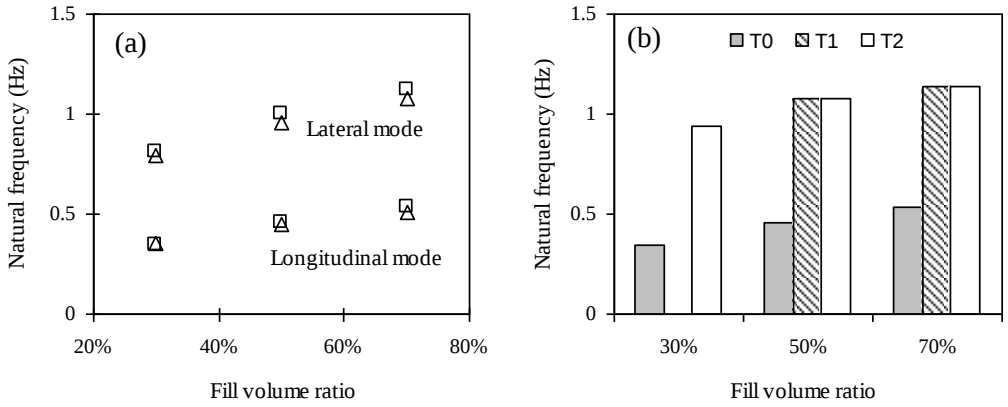

Figure 3.3: (a) Comparison of the measured and estimated natural frequencies of longitudinal and lateral fluid slosh in the clean bore tank; (□, measured; △, estimated). (b) comparisons of the fundamental longitudinal slosh frequencies in different tanks configurations.

In Figure 3.4 the time histories of the x-, y- and z-components of the fluid sloshing force are reported. The reported time hisrories are related to 50,0%-filled volume and $1,0m/s^2$ of excitation amplitude and at $1,0Hz$ of excitation frequency, in this condition the system is excitated in resonance. The amplitude of the x- and z-components indicates that the motion is a 3D motion thus only a 3D model can capture the right sloshing behavior. In Figure 3.5 has been investigated the sloshing amplification factor for the 50,0%-filled tank excitated in lateral direction at different excitations amplitudes and frequencies. The amplification factor has been calculated as the ratio between the average semi-amplitude of the sloshing force divided by the semi-amplitude of a equivalent rigid mass excitated with the same frequency and amplitude. The maximum amplification factor is as high as 4 times the inertial force produced by an equivalent rigid mass, for an excitation amplitude of $0,5m/s^2$ and an excitation frequency of $1,0Hz$, which is as expected

the natural frequency.

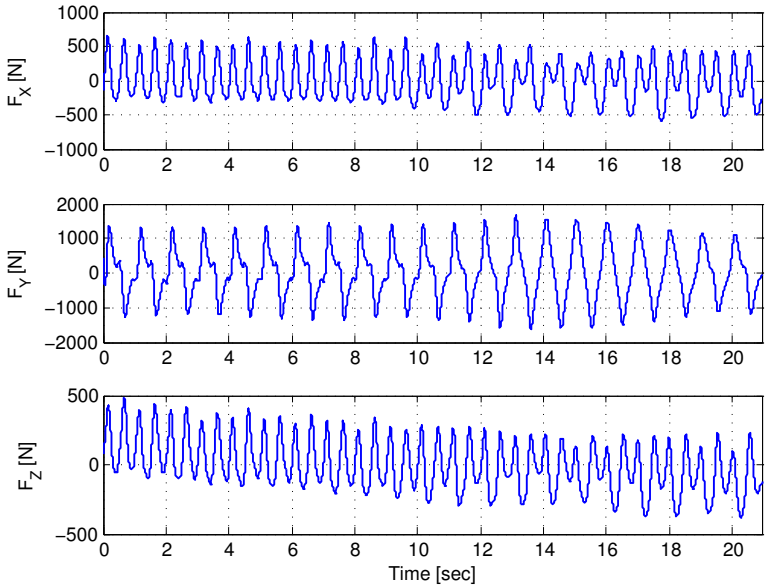

Figure 3.4: Time histories of longitudinal, lateral and vertical sloshing forces at 50,0%-filled tank under lateral excitation of $1,0m/s^2$ of amplitude and $1,0Hz$ of frequency.

Increasing the excitation amplitude the amplification factor decreases at about two time (Figure 3.5), for an excitation amplitude of $3,0m/s^2$, even excitating the system in resonance. Moreover a slight increase of the natural frequency can be observed. Excitating the system with frequency higher than the natural frequency the amplification factor decrease drastically, whereas excitating the system for frequencies smaller than the nautal one the amplification factor approaches to one. This behaviour is similar to a single mass spring damping system. The amplification factor of the roll moment (Figure 3.5 (b)) presents a similar behaviour, infact it reaches 8 times the equivalent inertial force of a rigid mass and decrease sharply for excitation frequencies higher than the natural frequency of $1,0Hz$. Furthermore also the longitudinal force and the pitch moment presents an amplification factor in the vicinity of the resonance for the lateral mode (Figure 3.5 (c) (d)). The vertical force and the yaw moment presents similar behavior (Figure 3.5 (e) (f)).

In Figure 3.7 (a) are reported the amplification factors for the longitudinal,

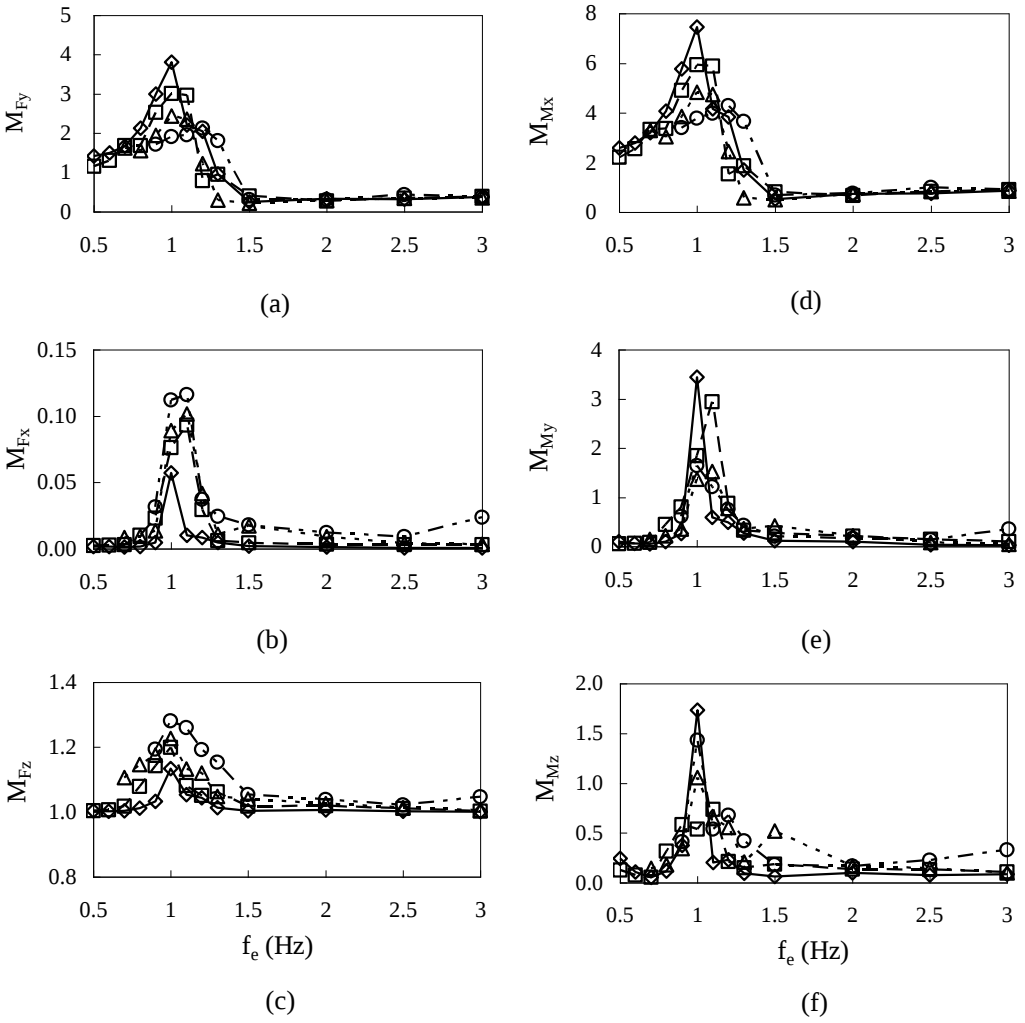

Figure 3.5: Variations in the normalized slosh forces and moment components with the excitation frequency for the 50,0%-fill clean bore tank underlateral excitations: (a) lateral force; (b) longitudinal force; (c) vertical force; (d) roll moment; (e) pitch moment; (f) yaw moment. ($\diamondsuit$, A=$0,5m/s^2$; $\square$, A=$1,0m/s^2$; $\triangle$, A=$2,0m/s^2$; $\circ$, A=$3,0m/s^2$;)

lateral sloshing forces and pitch moment for a 50,0% filled volume of the clean bore tank 'T0' under a longitudinal excitation at different amplitudes and frequencies. Also in longitudinal direction the amplification factors present similar behavior, the maximum amplification is observed on the longitudinal force for a frequency close to the natural frequency which is $0,5Hz$. Also for the longitudinal direction is confirmed a slight reduction of the amplification

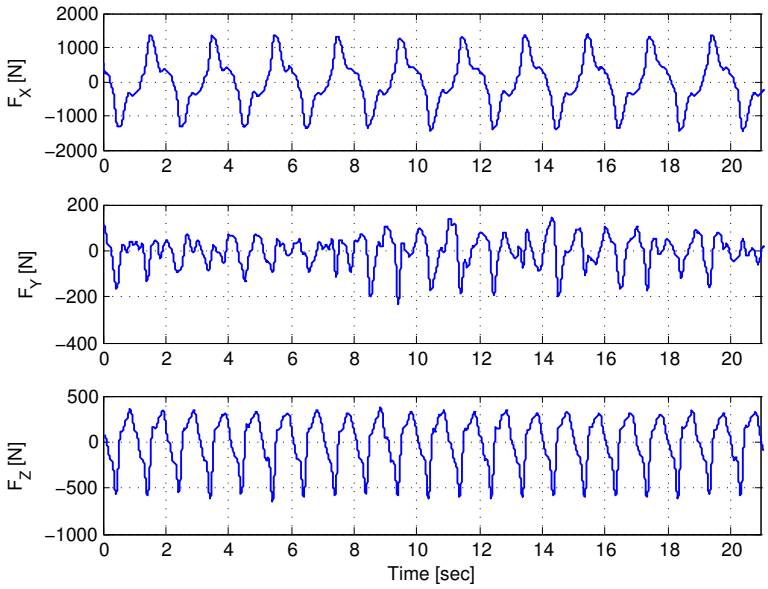

Figure 3.6: Time histories of longitudinal, lateral and vertical sloshing forces at 50,0%-filled tank under longitudinal excitation of $1,0 m/s^2$ of amplitude and $0,5 Hz$ of frequency.

factor with the increse of the excitation amplitude.

Furthermore also the increse of the natural frequency can be observed as increase the excitation amplitude. In Figure 3.7 (b) are reported the amplification factors for the longitudinal, lateral sloshing forces and pitch moment for a 50,0% filled volume of the mulitple orifices baffled tank, indicated with'T2' in Figure 3.2, under a longitudinal excitation at different amplitude and frequencies. A considereble reduction of the amplification factors can be observed in the vicinity of the resonance which indicates the effectiveness of the baffles in reducing the sloshing forces.

3.5 CFD model and validation

The CFD sloshing model has been developed with the software FLUENT. The purpose of this CFD model is to find the best set of parameters that gives the best match of the experimental resutls. The main parameters that has been setted is the mesh density. Three meshes densities have been tested indicated in table 3.2 as: low, medium and high mesh density. The use of the

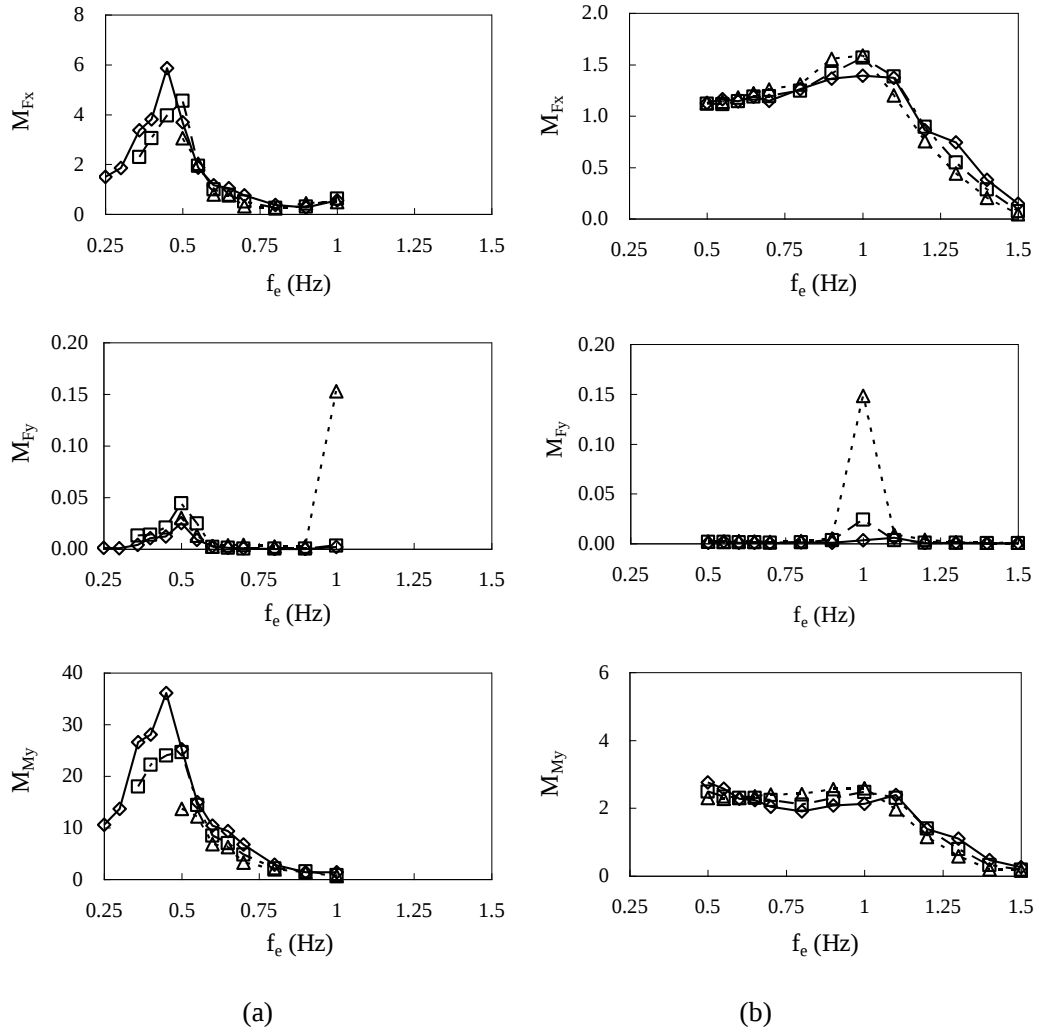

Figure 3.7: Variation of peack amplification factors of longitudinal and lateral forces, and pitch moment with the excitation frequency for the 50,0%-filled tanks (a) 'T0' tank, and (b) 'T2' tank ($\diamondsuit$, A=$0,25m/s^2$; $\square$, A=$0,5m/s^2$; $\triangle$, A=$1,0m/s^2$;).

mesh density allows to easily find the number of mesh's cells in case of scaling the volume of the geometry. As has been reported in the litterature review (section 1.4), the majority of the works doesn't use any viscous models, like $(k-\epsilon)$ or $(k-\omega)$, but the laminar flow condition is used. As will be presented later, even if the best match of experimental results has been found using the mesh with the highest mesh density in combination with the $(k-\epsilon)$ viscous model, the laminar flow condition allows the use of the medium mesh density

to have a very good match of the experimental results. The main drawback of using the laminar flow condition is the presence of numerical spike in the solution which can lead to the instability of the solution itself.

Table 3.2: List of mesh density used to built the CFD model.

	Low	**Medium**	**High**
Mesh Density $[cells/m^3]$	50.000	110.000	440.000
Cells Number	40.000	91.000	350.000

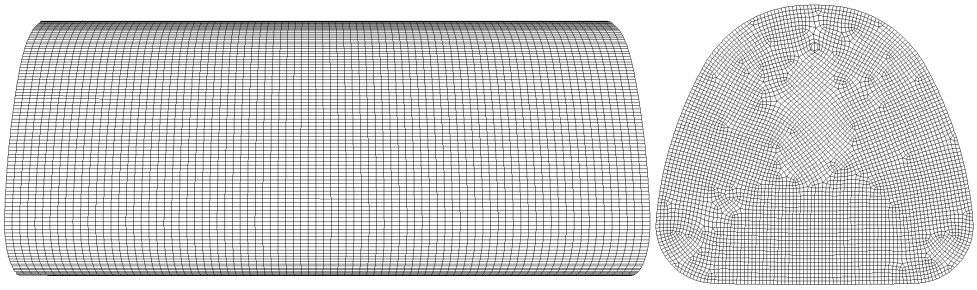

(a) Longitudinal view (b) Lateral view

Figure 3.8: Pictorial view of the meshed geometry: (a) longitudinal direction; (b) Transversal direction .

Another important setting is the method used to excitate the tank. The two possible methods that can be used to excitate the tank are: 'Dynamic Mesh' and 'Source Term'. The dynamic Mesh method is an ALE method [152, 72] whereas the Source Term is a Eulerian method [202, 203, 252, 249] (see subsection 1.2.2). The Eulerian method is easily implemented in FLUENT, because the method used in FLUENT to discretize the Navier Stokes equations is the Finite Volume which is a Eulerian method itself. Even though the Dynamic Mesh method presents better results and allows an easier post processing analysis from the vehicle dynamics point of view.

In the follow the comparison between numerical and experimental results, under longitudinal and lateral excitations, will be shown, the influence of viscous model insted of the laminar flow condition will be discussed.

Longitudinal excitation

In Figure 3.9 are reported the time histories of x-, y- and z-components of sloshing forces under a longitudinal excitation of $0,5m/s^2$ of amplitude and $0,4Hz$ of frequency, with tank volume filled up to 30,0%. The blue line represents the experimental results whereas the green and red lines represent the numerical results, respectively obtained with the medium and high mesh density (see table 3.2). Numerical and experimental results agree very well, the main differences in the longitudinal component of the sloshing force are attributed to some dynamic effects of the rigid structure which are very difficult to eliminate. Having a look at the longitudinal force, a medium mesh density is already able to capture the force shape, also the veritcal force variation is obtained very well with a medium mesh density. A further increase of mesh density allows to approximate better and better the behavior of the lateral force, as reported in the middle graphic of the Figure 3.9.

In Figure 3.10 are reported the spectra of the longitudinal , lateral and vertical sloshing force. The blue lines represents the spectra of the experimental results, whereas the green and the red represent the spectra of the numerical results. As it is possible to observe from Figure 3.10(a) the harmonic content of the numerical signal is the same as the experimental one, it is possible to observe the excitation frequency of $0,4mHz$, which is also the fundamental one for this fill level. Furthermore all the odds multiples frequencies of the fundamental one can be observed, for instance the first three are $1,2Hz$, $2,0Hz$ and $2,8Hz$ which are respectively 3 times, 5 times and 7 times the fundamental $0,4Hz$.

In Figure 3.10(b) are reported the spectra of the lateral sloshing forces. The blue line represents the spectrum of the experimental result, whereas the green and the red represent the spectra of the numerical results. From the experimental spectrum is possible to observe the presence of the natural sloshing frequency $0,8Hz$ of lateral mode which is also observed in both the numerical spectra. Instead the frequency of the longitudinal excitation $0,4Hz$, which is also the fundumental one of the longitudinal mode, it is not clearly observed within the numerical spectra. The slight improvement on the

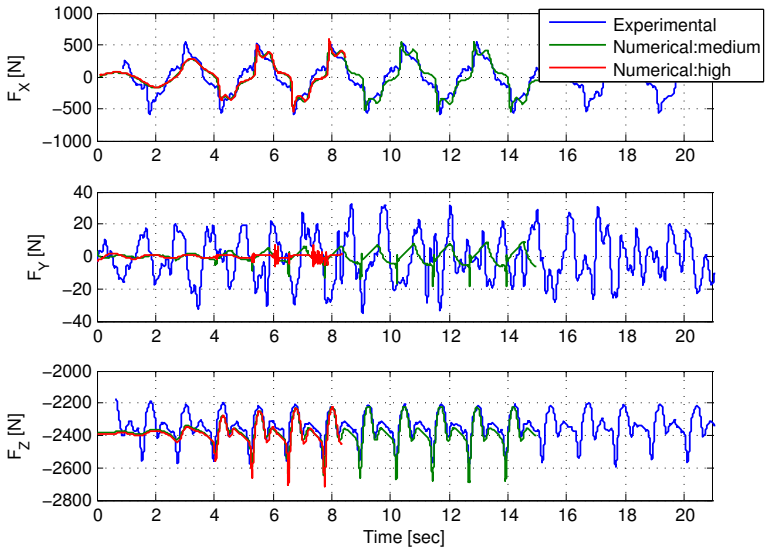

Figure 3.9: Numerical and experimental comparison of time histories of longitudinal, lateral and vertical sloshing forces at 30,0%-filled tank under longitudinal excitation of $0,5m/s^2$ of amplitude and $0,4Hz$ of frequency: High and medium are reffered to the mesh density.

lateral force increasing the mesh from the medium to the high mesh density suggests that a further increase of the mesh can improve the 3D effects. From the experimental spectrum, blue line, and the numerical one obtained with t he high mesh density are observed also the frequencies multiples of the fundamental.

Longitudinal excitation: influence of the viscosity

In Figure 3.11 are reported the time histories of the longitudinal, lateral and vertical sloshing forces, obtained for an excitation amplitude of $0,5m/s^2$, a frequency of $0,4Hz$ and 30,0%-filled volume. The blue lines represent the time histories of the experimental results, whereas the green and the red represent the time histories of the numerical results. The green are obtained using a medium mesh density under the condition of laminar flow, whereas the red are obtained using a high density mesh and the $k-\epsilon$ as viscous model. The use of laminar flow condition introduces a significant over estimation of the peack force, which are due to numerical error caused by the high value of

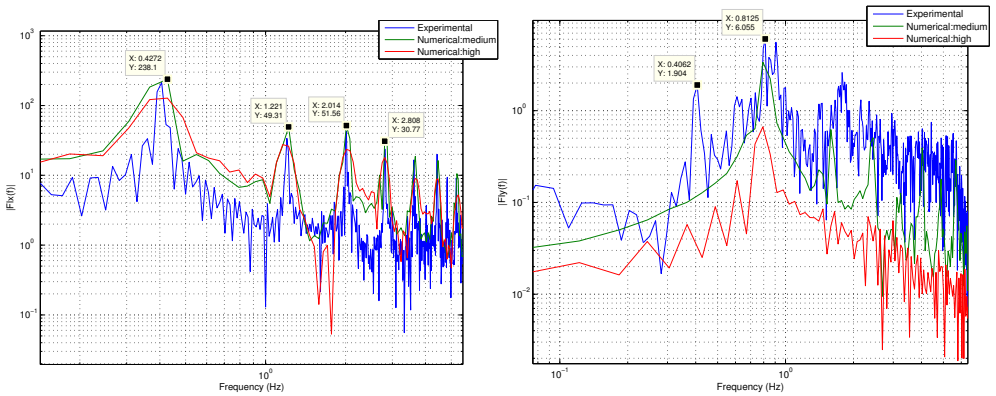

(a) Longitudinal sloshing force

(b) Lateral sloshing force

(c) Vertical sloshing force

Figure 3.10: Numerical and experimental comparison of the spectra of the longitudinal (a), lateral (b) and vertical (c) sloshing force at 30,0%-filled tank under longitudinal excitation of $0,5m/s^2$ of amplitude and $0,4Hz$ of frequency: High and medium are reffered to the mesh density.

the pressure locally (see Figure 3.11). Even though the advantage of using a mesh density up to 4 times smaller lets prefer the use of the laminare flow condition respect to the viscous model.

In Figure 3.12 are reported the spectra of the longitudinal, lateral and vertical sloshing force, obtained for an excitation amplitude of $0,5m/s^2$, a frequency of $0,4Hz$ and 30,0%-filled volume. The blue lines represents the spectra of the experimental results, whereas the green and the red represent the spectra of the numerical results. The green are obtained using a medium mesh density under the condition of laminar flow, whereas the red are ob-

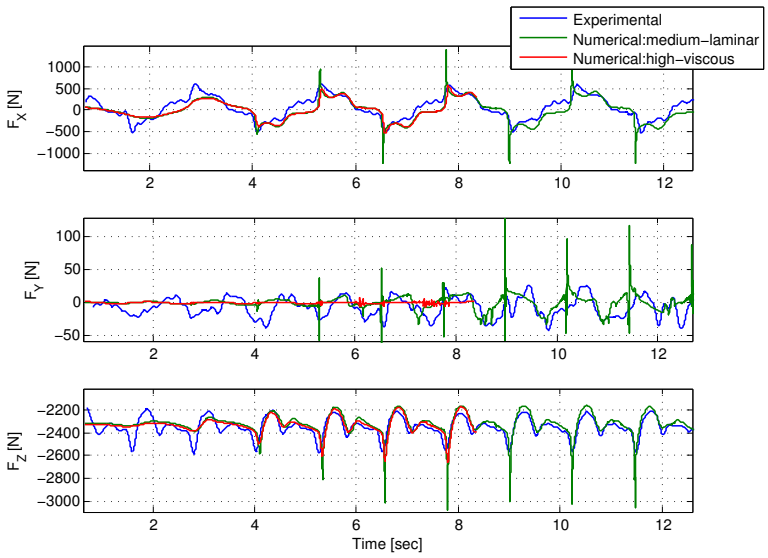

Figure 3.11: Numerical and experimental comparison of time histories of longitudinal, lateral and vertical sloshing forces at 30,0%-filled tank under longitudinal excitation of $0,5m/s^2$ of amplitude and $0,4Hz$ of frequency. Green line medium mesh density and laminar flow condition; Red line high mesh density and $k-\epsilon$ as viscous model.

tained using a high density mesh and the $k-\epsilon$ as viscous model. Also in terms of harmonic content can be drawn similar considerations as for the time histories shown in Figure 3.11. The spectra of the longitudinal sloshing force, Figure 3.12(a), indicates that the fundamental sloshing frequency and the odd multiples of the fundamental one are presents on the numerical signals. Also the spectra of the lateral and longitudinal forces, respectively Figure 3.12(b) and 3.12(c), agree well with the experimental one.

In Figure 3.17 are reported the pictorial views of the tank and the fluid free surface excitated in longitudinal direction. The arrows dimensions and directions indicate respectively the acceleration magnitude and direction at different simulation time. It is possible to observe an phase shift of $180deg$ between the acceleration and the fluid position, which further indicates that the system is ecitated in resonance.

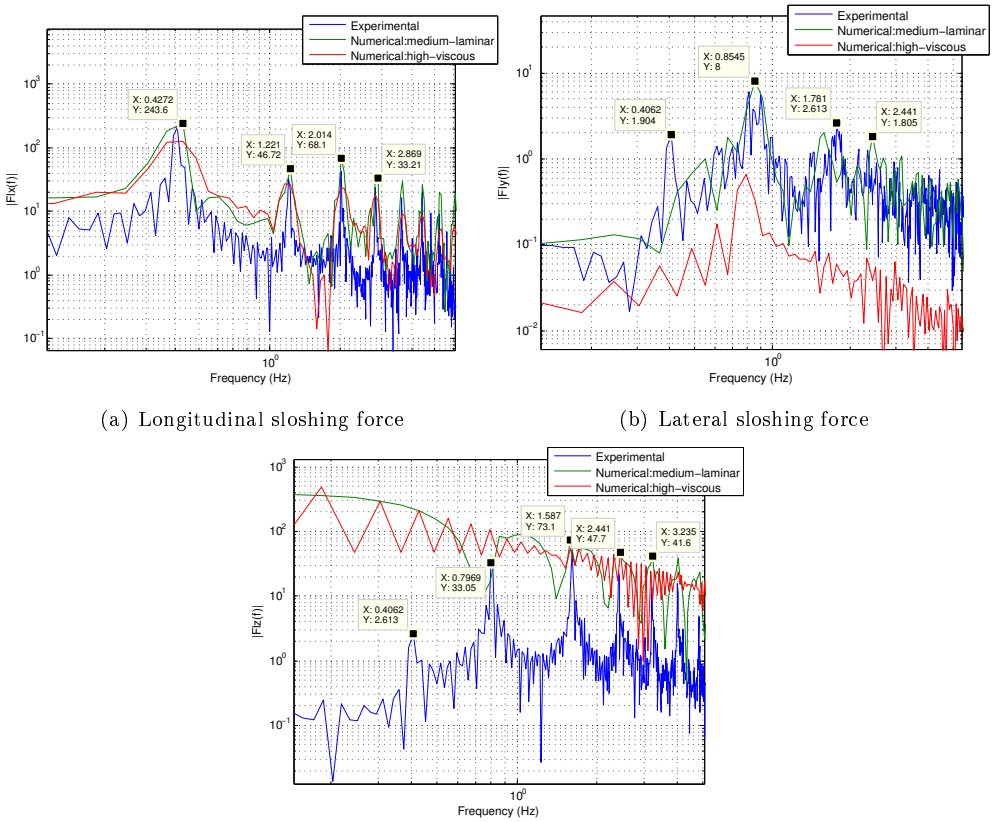

(a) Longitudinal sloshing force

(b) Lateral sloshing force

(c) Vertical sloshing force

Figure 3.12: Numerical and experimental comparison of the spectra of the longitudinal (a), lateral (b) and vertical (c) sloshing force at 30,0%-filled tankunder longitudinal excitation of $0,5m/s^2$ of amplitude and $0,4Hz$ of frequency. Green line medium mesh density and laminar flow condition; Red line high mesh density and $k-\epsilon$ as viscous model.

Lateral excitation

In Figure 3.13 are reported the time histories of x-, y- and z-components of sloshing forces under a lateral excitation of $0,5m/s^2$ of amplitude and $0,8Hz$ of frequency, with tank volume filled up to 30,0%. The blue lines represent the experimental results whereas the green and red lines represent the numerical results, obtained respectively with the medium and high mesh density see table 3.2. Numerical and experimental results agree but not very well. Between numerical and experimental time histories of the lateral force is observed a difference in terms of maximum amplitude, which is

considereble reduced increasing the mesh density. Moreover the amplitude of the longitudinal forces are completely missed. The behaviour of the veritcal and longitudinal components of the experimental forces let's suppose some problem on the experimental result. However, to improve results in lateral direction is suggested the use of a even higher mesh density, in contrast with the mesh density required to match experimental results in longitudinal direction (see Figure 3.9). This indicates that as the natural frequency increase, from longitudinal $0,4Hz$ to lateral $0,8Hz$ for the same fill volume (30,0%-), a finest spatial discretization is required to capture the modale shape and the natural frequency and thus the sloshing forces amplitude.

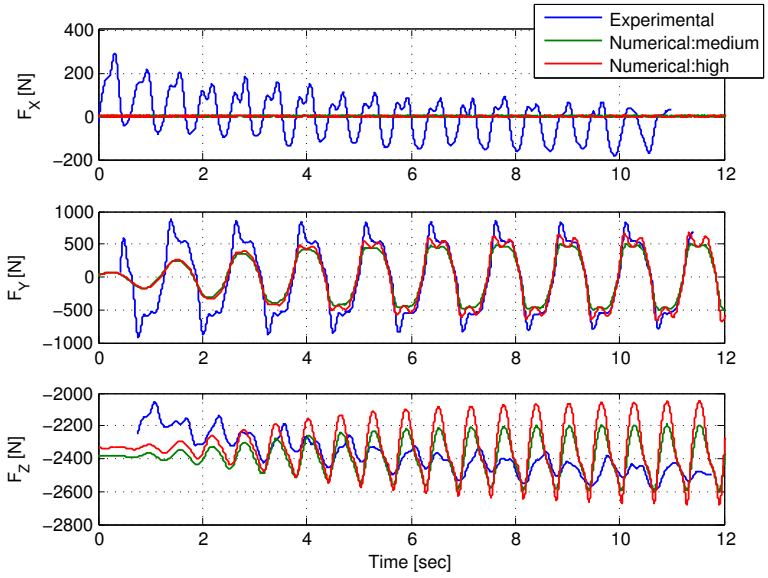

Figure 3.13: Numerical and experimental comparison of time histories of longitudinal, lateral and vertical sloshing forces at 30,0%-filledtank under lateral excitation of $0,5m/s^2$ of amplitude and $0,8Hz$ of frequency: High and medium are reffered to the mesh density.

In Figure 3.14 are reported the spectra of the longitudinal, lateral and vetical sloshing forces. The blue lines represent the spectra of the experimental results, whereas the green and the red represent the spectra of the numerical results. As the Figure 3.14(b) shows numerical and experimental spectra of the lateral sloshing forces have the same harmonic content, the fundamental frequency $0,8Hz$ and the odd multiples of the fundamental

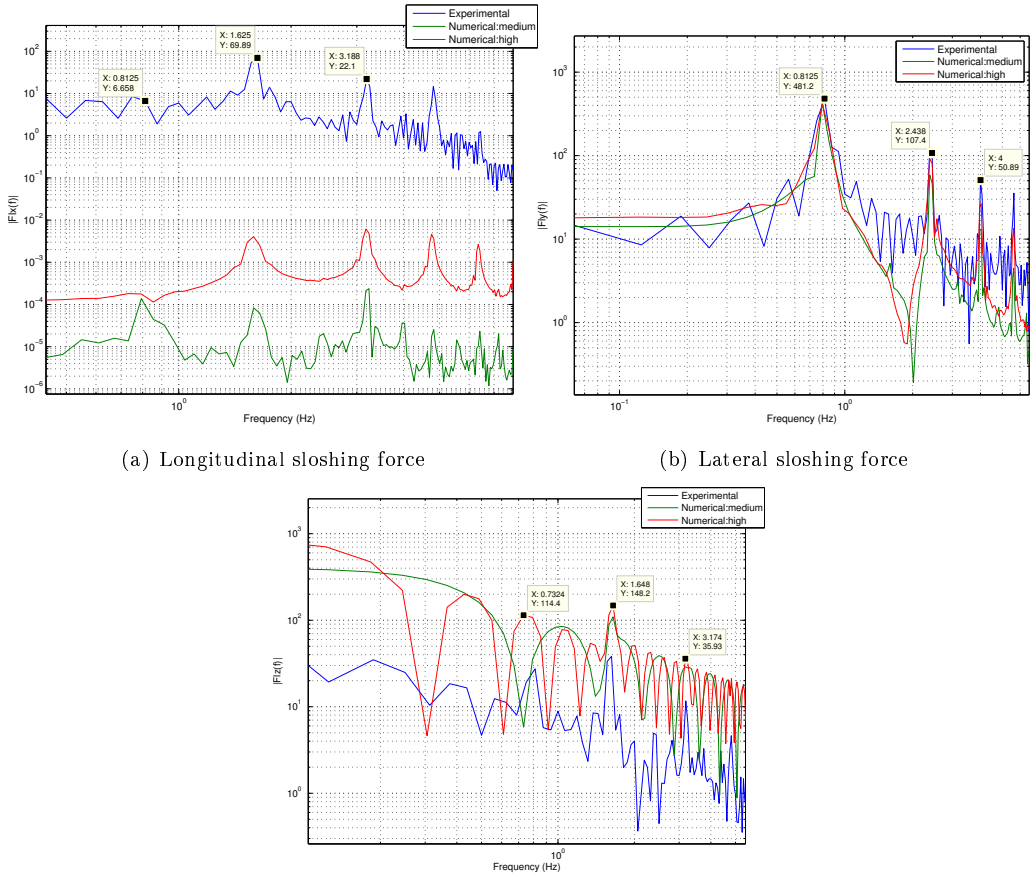

(a) Longitudinal sloshing force

(b) Lateral sloshing force

(c) Vertical sloshing force

Figure 3.14: Numerical and experimental comparison of the spectra of the longitudinal (a), lateral (b) and vertical (c) sloshing force at 30,0%-filled tankunder lateral excitation of $0,5m/s^2$ of amplitude and $0,8Hz$ of frequency. Green line medium mesh density and laminar flow condition; Red line high mesh density and $k-\epsilon$ as viscous model.

one, $2,4Hz$, $4,0Hz$ and $5,6Hz$, are observed. Figure 3.14(a) are reported the spectra of the longitudinal sloshing forces. Figure shows that numerical and experimental spectra have similar harmonic content, in terms of the odd multiples of the fundamental one, $1,6Hz$, $3,2Hz$ and $4,8Hz$, and the fundamental frequency $0,8Hz$ itself. Even if the harmonic content is obtained, the amplitude is wrong and this is confirmed also from the comparison of the time histories presented in Figure 3.13. Figure 3.14(c) shows the spectra of the vertical sloshing forces. The spectra present the same harmonic content whereas the difference in terms of amplitudes is due to the subtraction of the

constant inertial component of the vertical experimental force.

Lateral excitation: influence of the viscosity

In Figure 3.15 are reported the time histories of x-, y- and z-components of sloshing forces under a lateral excitation of $0,5m/s^2$ of amplitude and $0,8Hz$ of frequency, with tank volume filled up to 30,0%. The blue lines represent the experimental results, the green are obtained with a medium mesh density under laminar flow condition and the red lines are obtained with an high mesh density and the use of $k-\epsilon$ as viscous model. Also in this case the

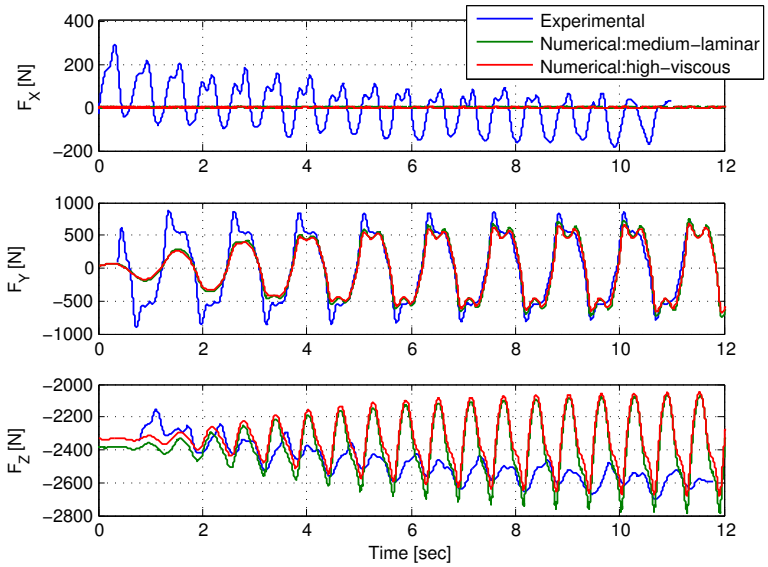

Figure 3.15: Numerical and experimental comparison of time histories of longitudinal, lateral and vertical sloshing forces at 30,0%-filled tank underlateral excitation of $0,5m/s^2$ of amplitude and $0,8Hz$ of frequency: Hihg and medium are reffered to the mesh density.

use of a medium mesh density in combinaiton with a laminar flow condition gives good results at least similar to the one obtained using high density mesh in combinaiton wiht a the $k-\epsilon$ as viscose model. Between numerical and experimental time histories of the lateral force is observed a difference in terms of maximum amplitude, which can be reduced increasing the mesh density. As in the previouse case the amplitude of the longitudinal forces are completely missed. However, to improve results in lateral direction is

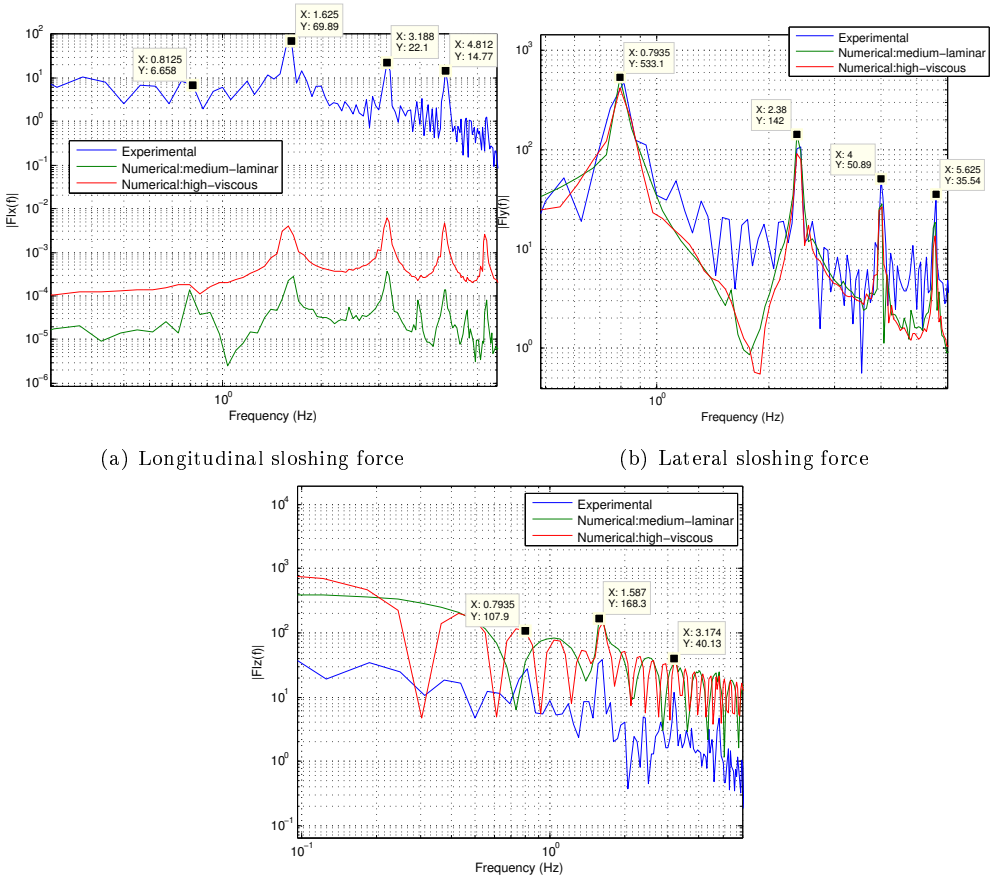

(a) Longitudinal sloshing force

(b) Lateral sloshing force

(c) Vertical sloshing force

Figure 3.16: Numerical and experimental comparison of the spectra of the longitudinal (a), lateral (b) and vertical (c) sloshing force at 30,0%-filled tankunder lateral excitation of $0,5m/s^2$ of amplitude and $0,8Hz$ of frequency. Green line medium mesh density and laminar flow condition; Red line high mesh density and $k-\epsilon$ as viscous model.

suggested the use of a even higher mesh density. In Figure 3.18 are reported the pictorial views of the tank and the fluid free surface excitated in lateral direction. The arrows dimensions and directions indicate respectively the acceleration magnitude and direction at different simulation time. It is possible to observe a phase shift of $180deg$ between the acceleration and the fluid position, which further indicates that the system is ecitated in resonance.

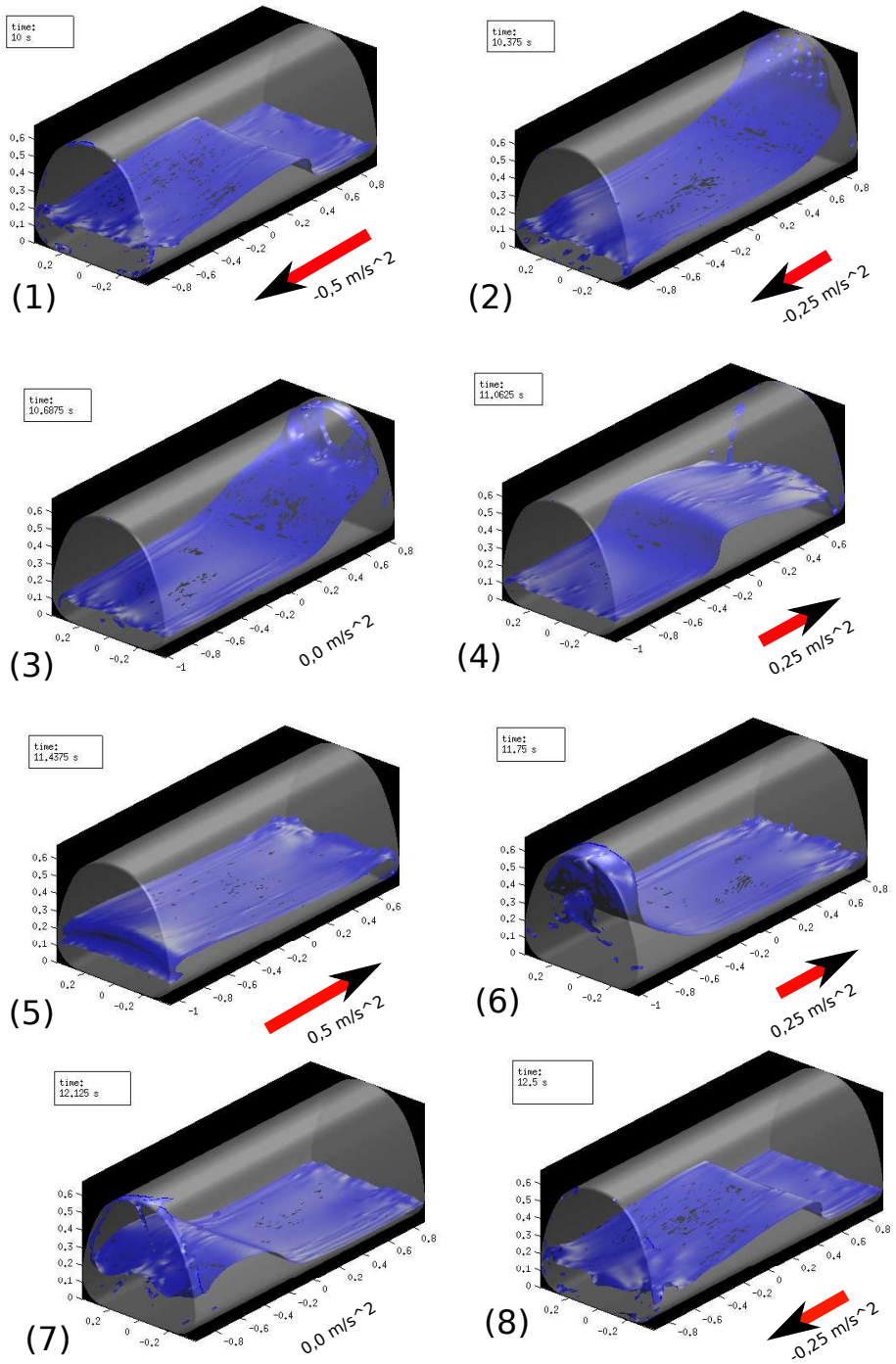

Figure 3.17: Pictorial view of the tank filled up to 30,0% of the volume excitated in longitudinal direction with $0,5m/s^2$ of amplitudeand $0,4Hz$ as excitation frequency. The arrows indicates the acceleration amgnitude and direction. The numbers indicates the frame order.

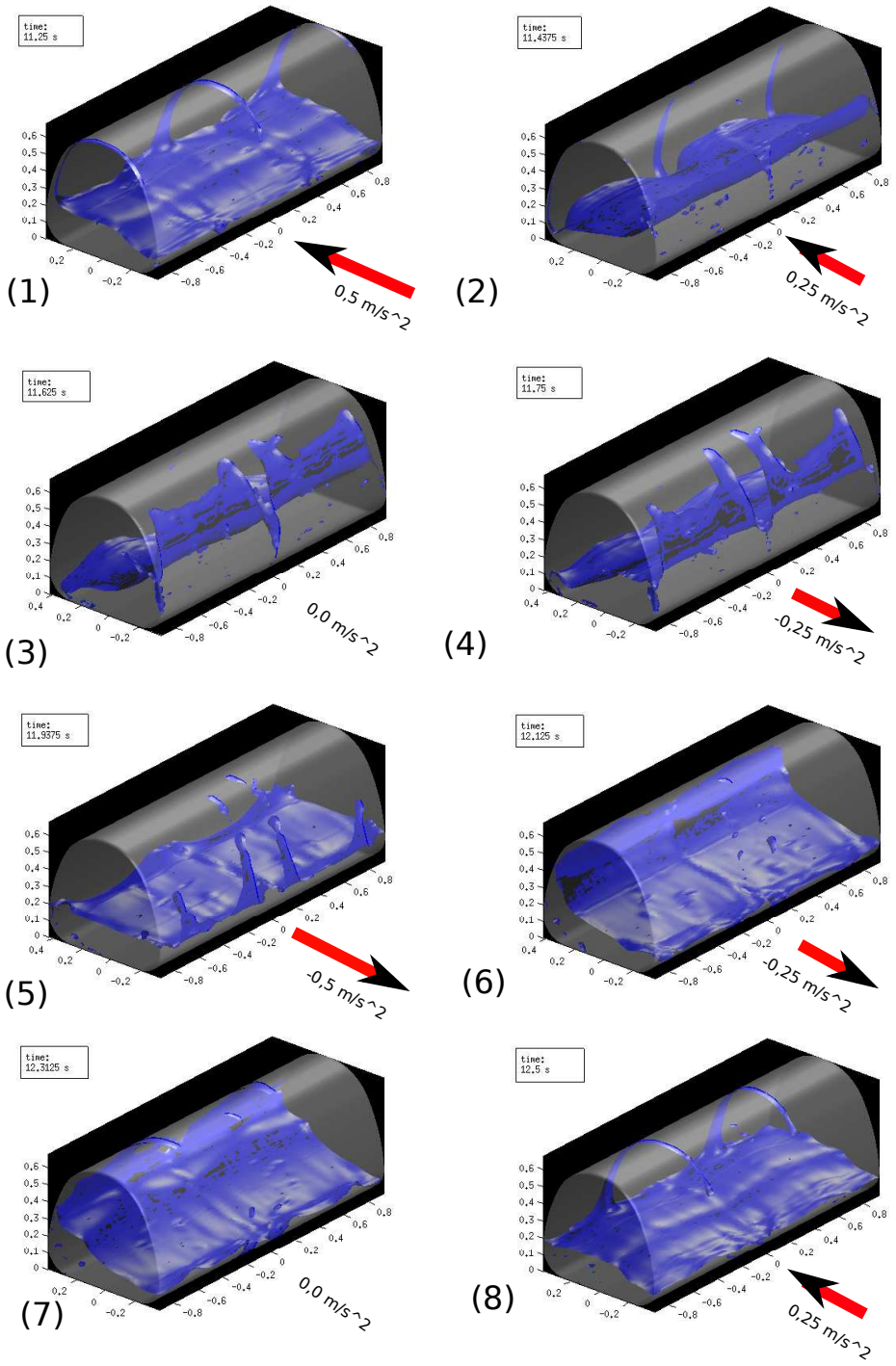

Figure 3.18: Pictorial view of the tank filled up to 30,0% of the volume excitated in lateral direction with $0,5m/s^2$ of amplitudeand $0,8Hz$ as excitation frequency. The arrows indicates the acceleration amgnitude and direction. The numbers indicates the frame order.

3.6 Sloshing cargo model

The tank geometry that has been considered is displayed in Figure 4.8. As proposed by Kang [108], it is based on the Reuleaux triangle principle. The significant tank dimensions are: the length $4,7m$, the width $2,3m$ and the sectional area $3,27m^2$, to yield a capacity of $14,5m^3$. In order to show the influence of the fluid sloshing on the vehicle's pitch dynamics, two different baffles arrangements and the clean bore condition has been simulated, the results are compared with an equivalent rigid cargo. The two considered

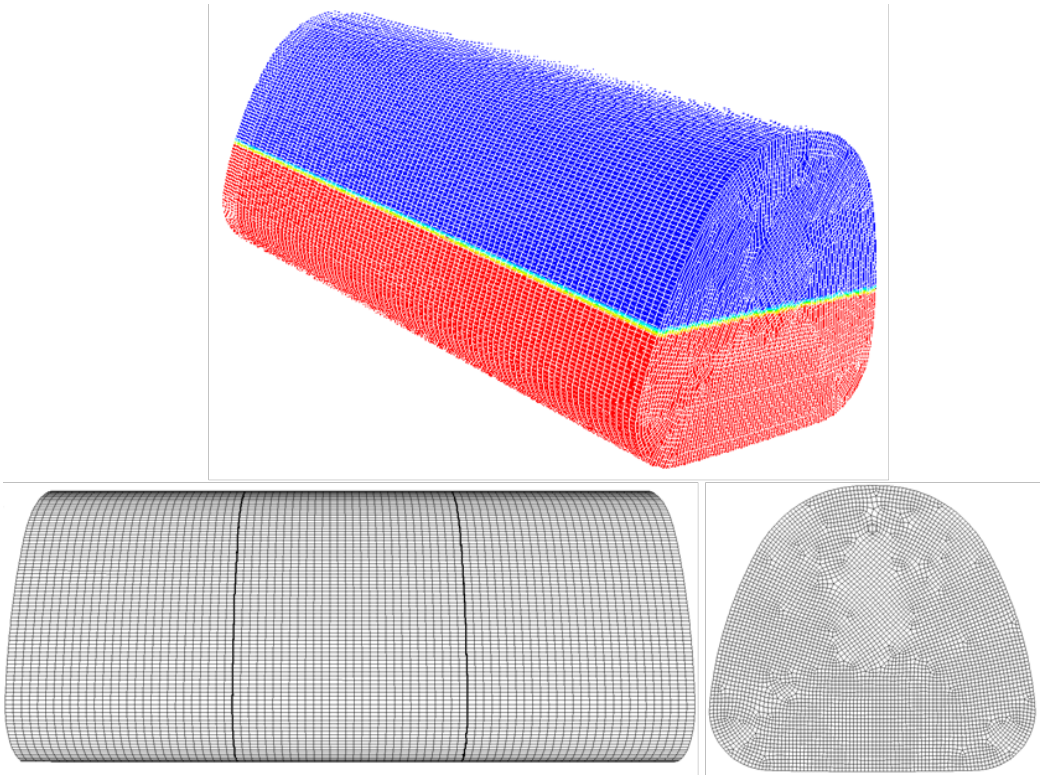

Figure 3.19: Mesh of the tank (upper), sketch of the 2 baffles arrangements and structured mesh along longitudinal direction (down left), sketch of thenon structured mesh on the transversal tank's direction (down right).

baffles arrangement consist in one baffle, indicated as B1, which divide the tank in two compartments of less than $7500litres$, and two baffles, identified as B2, which divide in three compartments the tank of about $4800litres$ each compartments. Different fill volumes are considered. The 50,0%-filler

volume, volume is allowed by the rule 4.3.2.2.3 of ADR (chapter 4.3 section 2 subsection 2.3 of European Agreement of Transportation of Dangerous by Road) and lane change results will be proposed for this fill volume to verify the validity of this rule. The mesh size is about 1.400.000 cells, for a mesh density of about 100.000 cells for m^3, under laminar flow condiitons, as has been discussed in the previouses secitons. The mesh is structured along the longitudinal direction whereas it is not structured along the transversal direction. The volume has been meshed using a Cooper method.

Chapter 4

Tank truck model

4.1 Introduction

In the state of arts, chapter 1, has been widely discussed the necessity of modelling the coupled vehicle-fluid dynamical interaction in order to develope a suitable model of road tanker. The main difficult on modelling tank trucks is represented by the interaction between the vehicle and the sloshing cargo. To solve such difficult have been proposed 'Quasi Static Methods' (see seciton 1.1), which neglects the transient fluid dynamics,whose influence on vehicle dynamics during evasive maneuver cannot be neglected. 'Mechanical Analogy Methods' have been proposed (see section 1.6) to model the transient sloshing dynamcs, wich are not able to model properly the fluid sloshing non-linearity. Recent advances in Computer Science allowed, since 2000, the use of 'Non-linear Dynamics Sloshing Methods' (see subsection 1.2.2) to model sloshing cargo in tank vehicles using co-simulation to model the interaction between the vehicle and the sloshing cargo. In this work, a Non-Linear dynamical model of the sloshing cargo in co-simulation with a non-linear vehicle model has been developed. The whole model has been developed in FLUENT [98], which is a non-lienar CFD code. The vehicle-fluid interaction has been modelled using the 'Dynamic Mesh' which is a feature of FLUENT, which allows to move rigidly the mesh according to a generic 3D motion. This motion applied to the mesh is calculated solving the vehicle equations of motion, which are integrated into the FLUENT solver using the

UDF FLUENT's features. In the follow a description of the two sub-systems and of the interaction between them is given.

4.2 Vehicle model

The vehicle model is a 3D model of a straight truck of 18 tons as maximum gross weight. The equations of motion are derived usign a MBS approach. The model has 14 degrees of freedom (dofs), which are listed in table 4.1, and is divide in three rigid bodies: chassis, front axle and rear axle. In the inertial properties of the chassis are included the cabin, the drive chain and the tank structure. The cabin dofs are neglected because the model is not meant for comfort analisys. As listed in the table the chassis has 6 dofs: longitudinal,

Table 4.1: List of the vehicle model degrees of freedom.

Symbol	Degrees of Freedom	Units
X_0	Longitudinal vehicle displacement	m
Y_0	Lateral vehicle displacement	m
Z_0	Vertical vehicle displacement	m
α	roll angle	rad
ψ	yaw angle	rad
γ	pitch angle	rad
Z_f	Vertical displacement of front axle	m
ρ_f	roll angle of front axle	rad
Z_r	Vertical displacement of rear axle	m
ρ_r	roll angle of rear axle	rad
ω_{fl}	angular velocity of the front left whell	$\frac{rad}{s}$
ω_{fr}	angular velocity of the front right whell	$\frac{rad}{s}$
ω_{rl}	angular velocity of the rear left whell	$\frac{rad}{s}$
ω_{rr}	angular velocity of the rear right whell	$\frac{rad}{s}$

lateral, and vertical displacement plus the rotations: roll, pitch and yaw angular rotation; all related at the absolute coordinate system. Suspensions are modelled as rigid axles with two dofs: the vertical displacement and the axle roll angle; also related to the absolute coordinate system. The stiffness and the damping are considered linear and are introduced into the model by

dashpot elements. In Figure 4.1 is presented a schematic view of the truck vehicle model showing the bodies, degrees of freedom and suspensions elemts.

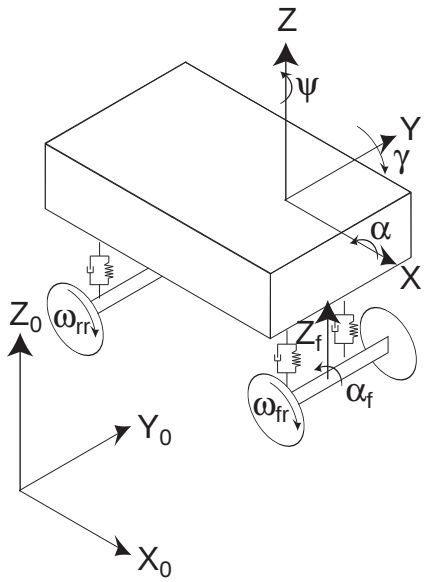

Figure 4.1: Schematic view of the bodies and dofs of vehicle model.

Contact forces

The contact forces are modelled using the 'Magic Formula' (MF) tyre model [160], which is the most used in vehicle dynamics simulations. The MF tyre model is an empirical model, it is based on a series of cofficients determined using experimental tests. The MF tyre model is based on the equation (4.1) which can be used for longitudinal F_x and lateral F_y forces under the pure longitudinal or lateral slip condition.

$$y(x) = D \cdot \sin\{C \cdot \arctan[B \cdot x - E \cdot (B \cdot x - \arctan(B \cdot x))]\} \tag{4.1}$$

$$\begin{cases} x = X + S_H \\ Y(x) = y(x) + S_V \end{cases} \tag{4.2}$$

The input variable, indicated with X, corresponds to the longitudinal slip σ or lateral slip α. The coefficients S_H and S_V are used to shift the curve along

the horizontal or veritcal axis and they allow to take in to acount effects of conicity and ply-steer. Playing with the coefficients B, C, D, E the curve shape can be manipulated to fit differents experimental data and thus to reproduce different tyres. As depicted in the Figure 4.2 at each coefficients can be associated a physical meaning: B is the stiffness factor, C shape factor, D peack value, while E curvature factor.

The dynamical change of the contact force is modelled using a first order differential equation (equation (4.3)) in which the most important parameter is λ noun as relaxation leght, whose meaning is the longitudinal lenght that the tyre must travel to develop a force.

$$\frac{L}{V} \cdot \dot{F} + F = \bar{F}(\alpha) \tag{4.3}$$

In equaiton 4.3 $\bar{F}$ (α) corresponds to the steady state value of the lateral force yield by the equaiton (4.1) F and $\dot{F}$ are respectively the instantaneous lateral force and its first-derivative.

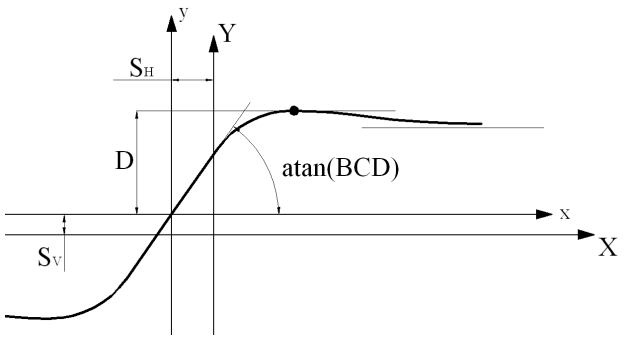

Figure 4.2: Sketch of the tyre force as function of the input X.

The inputs of the MF tyre model are the longitudinal and lateral slip, respectively σ and α defined as in the equation (4.4) and (4.5).

$$\sigma = \frac{V_{xr} - R_e \cdot \omega}{V_{xr}} \tag{4.4}$$

where $R_e = \frac{V_{xr}}{\omega_0}$ is the effective rolling radius.

$$\alpha = \arctan\left(-\frac{V_{yr}}{V_{xr}}\right) \tag{4.5}$$

The model inputs are: the steering angle, the braking and driving torques. The steering input is applied directly to the wheel plate. The steering angle is based on a feed forward model to simulate maneuver without the driver influence, whereas a feed back model is used to simulate the driver. The driver is simulated using a simple driver model proportional to the trajector error based on the equations (4.6):

$$\delta = -k_p(Y - Y_{rif}(X)); \tag{4.6}$$

where

$$\begin{cases} X = X_0 + Lcos(\Psi_0); \\ Y = Y_0 + Lsin(\Psi_0); \end{cases} \tag{4.7}$$

In equations (4.6) δ is the steering angle, K_p is the proportional gain, Y is

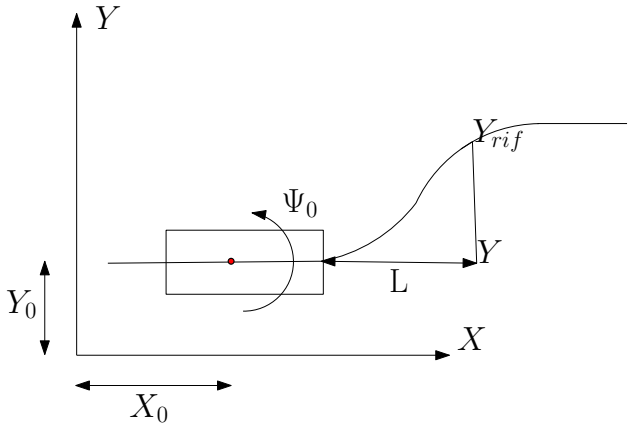

Figure 4.3: Sketch of the driver model.

the actual vehicle position, whereas $Y_{rif}(X)$ is the desired trajectory. Equations (4.7) is used to predict the future vehicle position (see Figure 4.3). In equations (4.7) L is the prediciton distance, X_0 and Y_0 indicate respectively the X and Y actual vehicle position, while Ψ_0 is the actual yaw angle.

4.3 Vehicle model with rigid load

The vehicle model presented in the previous section can be parameterized to study different load conditions, this model can be used to easily study the influence of the load condition on vehicle dynamics. The purpose of the rigid

load is to run simulations whose results will be compared to the results of the simulations carried out with vehicle-fluid model, in this way is clarely pointed out the influence of the liquid sloshing on the vehicle dynamcis.

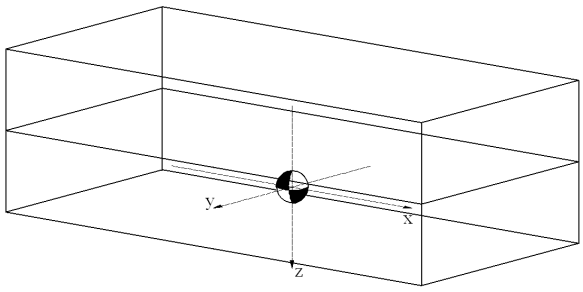

Figure 4.4: Skethc of a rigid load inertially equivalent to liquid model filling the same volume.

To compare simulations between rigid loads and sloshing loads the rigid ones are derived idealy freezing the fluid cargo in its quite position which yield a load with the same inertial properties (mass and moments of inertia) but rigidly fixed to the truck chassis (see Figure 4.4). Being the rigid cargo

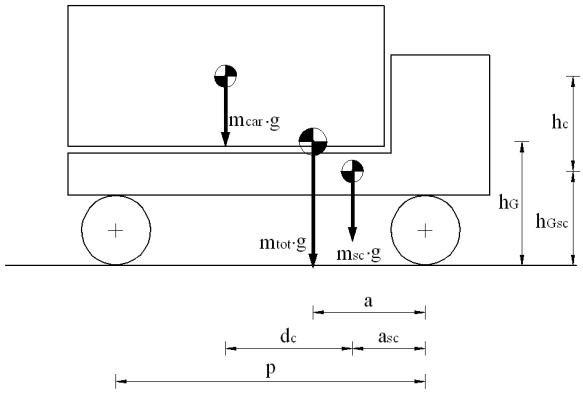

Figure 4.5: Skethc of the centre of gravity as funtion of the load mass.

homogeneously distributed within the tank, a change of the fill level results in an upright shift of the cargo centre of gravity and a backward and upward shift of the vehicle centre of gravity. In Figure 4.5 a_{sc} and h_{Gsc} represents respectively longitudinal and vertical centre of gravity (cg) position of the unload vehicle with mass m_{sc}. Adding the load mass m_{car} a new cg position

is observed, indicated in Figure with a and h_G for a new total mass m_{tot}.

An increase of the h_G increases the load transfer in longitudinal direction, during braking, as well as in lateral direction while cornering, leading to an increase of braking distance and a reduction of the rollover threshold.

Longitudinal braking

In Figure 5.4 is reported a comparison between two simulations performed with 50,0% and 100,0% of rigid load, respectively blue lines and green lines. Figure 4.6(a) shows the longitudinal vehicle accelerations; as the load increases the maximum acceleration decreases, infact the blue line (50,0% rigid load) shows a steady state value of $0,77g$, whereas the green line in steady state shows a value of $0,69g$. Moreover, less vertical contact load, with the same brake torques, determines an easier wheels lock up, as depicted in Figure 4.6(c) blue lines. The wheels lock up determines an higher jump value on longitudinal acceleration, because all the four wheels are in sliding.

In Figure 5.4(b) are depicted the vertical contact loads. The blue lines represent the 50,0% load condition, while the green lines represent the 100,0% load condition, the front wheels are depicted with solid lines, while in dashed lines are reported the rear wheels vertical contact loads. As Figure 5.4(b) shows an increase of the load determines an upward displacement of the cg position (h_G increse see Figure 4.5) thus a lower longitudinal acceleration yield however an higher load transfer as indicated by the arrows.

Rollover stability

The rollover stability of the heavy vehicles is mainly influenced by the aspect ratio defined with equation (4.8)

$$SSF = \frac{T}{2h}; \tag{4.8}$$

where T is the track width, h is the height of the centre of gravity. Equation (4.8) is easily derived from Figure 4.7, where ay is the lateral acceleration; F_i is the vertical tire loads with $i = 1, 2$; W is the weight of the vehicle and Δy is the lateral motion of the cg relative to the track. The influence of the cg height on the roll stability is clearly pointed out by the Static Stability

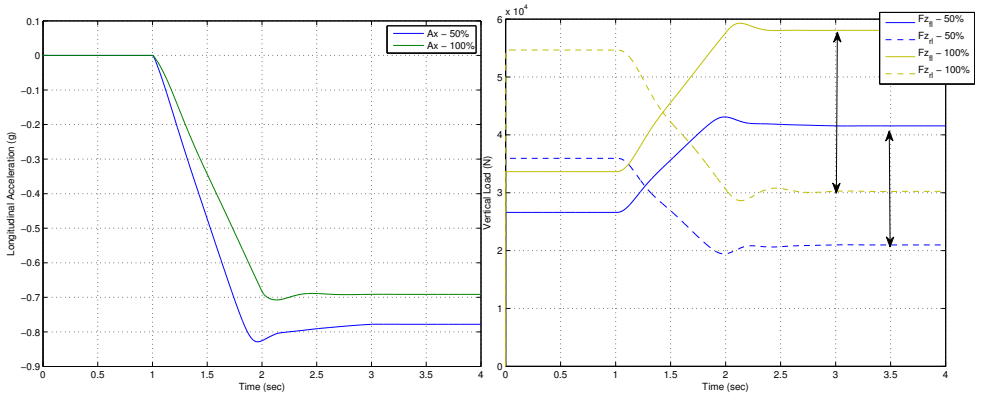

(a) Longitudinal accelerations

(b) Vertical contact loads

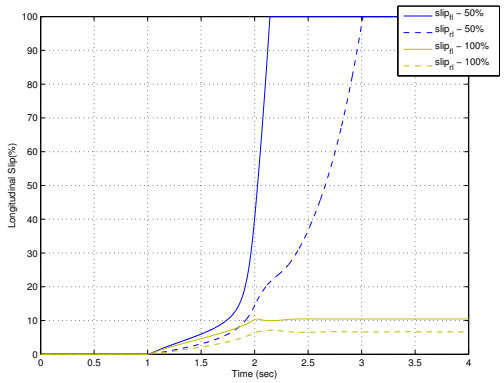

(c) Slip ratios

Figure 4.6: Comparison between longitudinal braking simulations in full load condition, (100%) green lines, and half load condition, (50%) blue lines,Simulations are performed with 10.000$[Nm]$ and 22.000$[Nm]$ of braking torques respectively at rear and front wheels..

Factor (SSF) (4.8); in fact increasing the h result in a reduction of the SSF. The SSF doesn't take into account the effects of the suspensions and tyres deformation on the rollover threshold, this is done through the SRT which is defined as the smallest lateral acceleration leading to the lift of all the wheels of one vehicle side. The SRT can be determined by mean of titl table test of by mean of simulations. In many study, [148, 186, 177] has been shown the relationship between rollover crash frequency and rollover stability limits evaluated through tilt table test. In order to investigate the rollover stabilty of the vehicle model with rigid cargo the tilt table test has been simulated whose results are reported in Figure 4.8. The SRT (solid lines) Figure 4.8

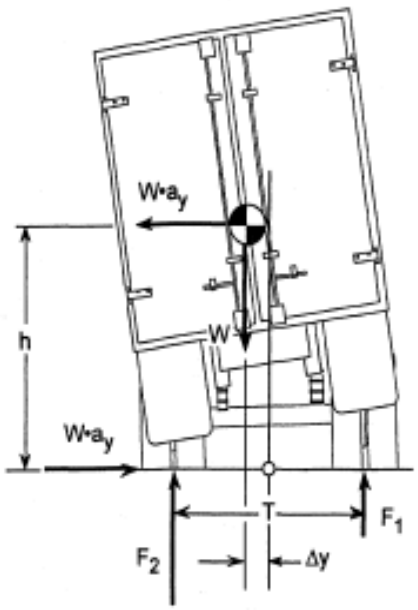

Figure 4.7: Simplified roll plain model of heavy vehicle, during steady turning.

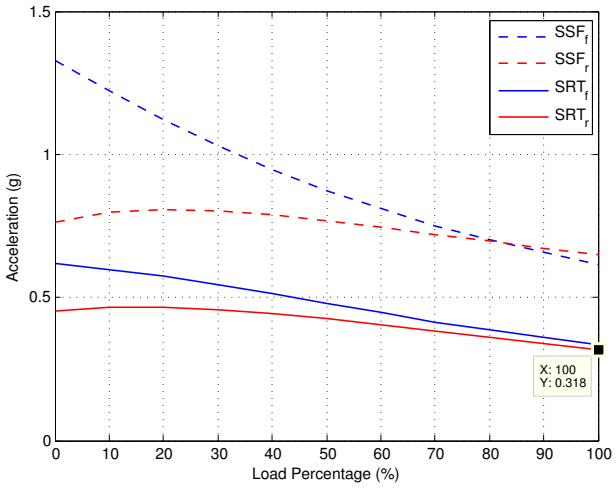

Figure 4.8: Static Stability Factor (SSF) and Static Rollover Threshold (SRT) of vehicle model, simulated with rigid load, as function of the loadcondition, for front and rear axle. The SRT characterizing the vehicle rollover stabilty is $0.381g$.

are compared with the SSF (dashed lines) and are derived as function of the load percentage defined for the front and the rear axles respectively blue and red lines. The difference between SSF and SRT is due to the lateral shift

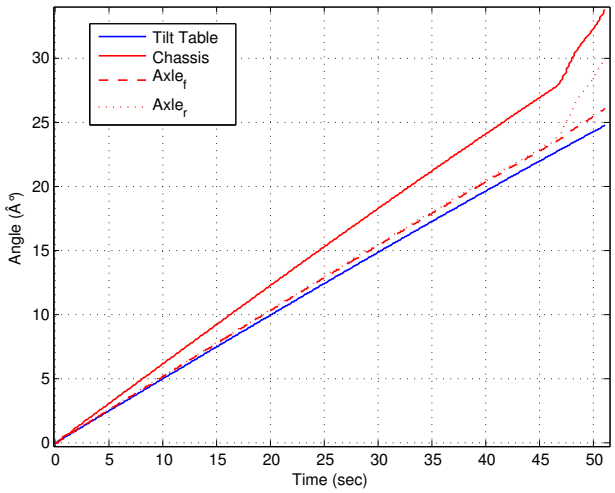

(a) Longitudinal acclerations

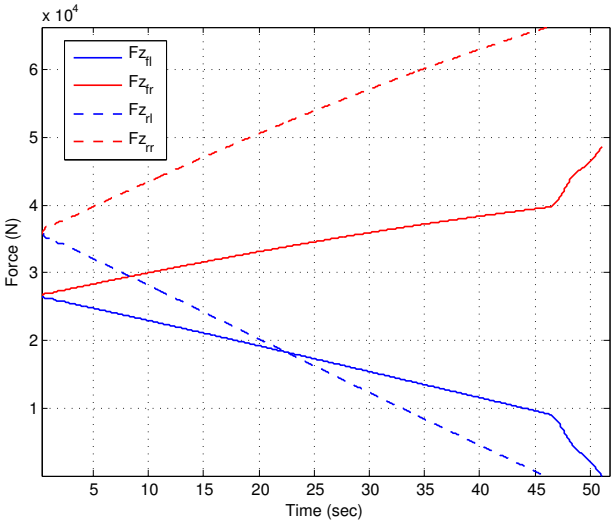

(b) Vertical contact loads

Figure 4.9: Simulation of tilt table test performed for 50,0% load condition and rigid load. (a) comparison between tilt table angle, vehicle angle and axles roll angles. (b) Time histories of vertical contact load during tilt table simulaiton.

of the vehicle cg. In first approximation exists one SSF, but being the front track width differents from the rear one as consequence two SSF are defined. As expected the lowest acceleration leading to the lift of all the wheels of one vehicle side (SRT) is obtained for 100,0% of load condition, for this vehicle the value is $0.318g$ (see Figure 4.8).

In Figure 4.9(a) are compared the roll chassis angle (solid red line) with the

tilt table angle (blue solid line), as can be observed the chassis has roll angle higher than the tilt table one as consequence of the tyres and suspensions compliance. Moreover the rear and front axles roll angle is also plotted, respectively pointed and dashed red lines. As expected both axles roll angles are smaller than the chassis angles this is due to the higher roll stiffness. In Figure 4.9(b) are reported the vertical tyres loads during titl table test, it is possible to observe as the first wheel to lose the contact with the titl table test is the rear one which confirmed to experimental tests and is due to the higher rear axles roll stiffenss.

4.4 Dynamical interaction between vehicle and sloshing cargo model

The dynamical interaction between vehicle and fluid sloshing is the key issue in modelling the dynamics of tank trucks. As has been discussed in the state of art (see chapter 1) along the years simplified models based on mechanical analogy or on quasi static fluid model have been proposed to be easily introduced within vehicle model. In the litterature review has been clarely pointed out the limitation of such techniques on accurately modelling the influence of fluid sloshing on the vehicle dynamcis. In this work the

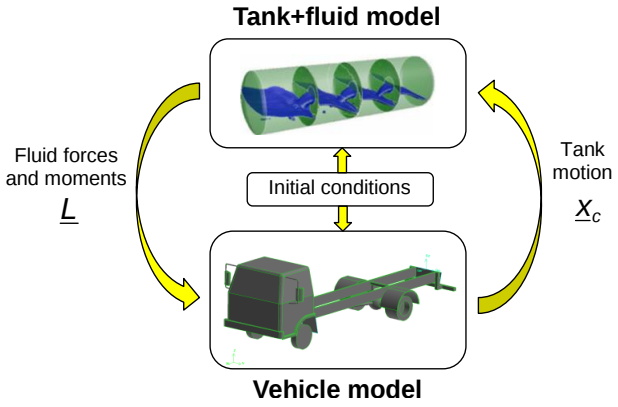

Figure 4.10: Sketch showing the subsystems interaction.

fluid-vehicle interaction has been modelled by the co-simulation technique. According to the co-simulation proposed by Rumold [202] the system of non-

linear coupled equations representing the whole non-linear system (vehicle plus fluid cargo) must be devided into two standalone subsystems which can be simulated separately, each one in a suitable computational enviroment, whose interaction is simulated by an input/output exchange process. Figure 4.10 shows a schematic picture of the subsystems interaction.

The system of equations representing the sloshing fluid cargo (Tank + fluid model in Figure 4.10) is reported in equations (4.9), (4.10):

$$\frac{\partial \rho}{\partial t} + \nabla \cdot (\rho \mathbf{v}) = 0; \tag{4.9}$$

$$\frac{\partial}{\partial t}(\rho \mathbf{v}) + \nabla \cdot (\rho \mathbf{v}\mathbf{v}) = -\nabla p + \nabla \cdot (\tau_{Re}) + \mathbf{F}; \tag{4.10}$$

where $\mathbf{v}$ and p are respectively the velocity field and the static pressure, while τ_{Re} is the Reynolds stress tensor and is defined in the equation (4.11):

$$\tau_{Re} = \mu_t \Big[(\nabla \mathbf{v} + \nabla \mathbf{v}^T) - \frac{2}{3} \nabla \cdot \mathbf{v} \mathbf{I} \Big]; \tag{4.11}$$

where μ is the dynamc viscosity, while $\mathbf{I}$ is the identity matrix. Assuming the incompressible fluid hypothesis the continuity equation read as follow:

$$\nabla \cdot (\mathbf{v}) = 0; \tag{4.12}$$

In the fluid momentum equation (equation (4.10)) the term $\mathbf{F}$ represents the external accelerations acting on the fluid volume. The expression of the external acclerations read as follow:

$$\mathbf{F} = \mathbf{g} - \frac{d\mathbf{U}}{dt} - \frac{d\mathbf{\Omega}}{dt} \times \mathbf{r} - 2\mathbf{\Omega} \times \mathbf{v} - \mathbf{\Omega} \times (\mathbf{\Omega} \times \mathbf{r}) \tag{4.13}$$

where $\mathbf{g}$ is the gravitational acceleration, whereas $\mathbf{U}$ and $\mathbf{\Omega}$ represent the linear and angular velocity of the tank wall and $\mathbf{r}$ is the distance of the considered fluid volume from the coordinate system (see Figure 4.11(a)). The quantities $\mathbf{U}$ and $\mathbf{\Omega}$ are the input of the fluid model coming from the solution of the vehicle equations of motion, which are indicated as $\underline{\dot{X}}_c$ in Figure 4.10.

The output of the fluid system of equations of motion is represented by the pressure and viscous forces acting on the wetted wall which expression reads as follow:

$$\mathbf{F}_{li} = \sum_c (f^p_{c,i} + f^\tau_{c,i}); \tag{4.14}$$

where $i = x, y, z$, c indicates the $c-th$ cell over which the pressure p and viscous stress τ are calculated. The expression of the fluid sloshing moments reads as follow:

$$\underline{\mathbf{M}_l} = \sum_c (\underline{r_c} \times \underline{f_c}); \tag{4.15}$$

where $\underline{\mathbf{M}_l} = \{\mathbf{M}_{lx}, \mathbf{M}_{ly}, \mathbf{M}_{lz}\}$ collects the components of the fluid sloshing moment, $\underline{r_c} = \{r_{cx}, r_{cy}, r_{cz}\}$ and $\underline{f_c} = \{f_{cx}, f_{cy}, f_{cz}\}$ collects respectively the components of the position vector of the $c-th$ cell and the components of the pressure and viscous force acting on the $c-th$ cell. In Figure 4.11 is reported a schematic representation of the pressure and viscous stress used to calculates the $c-th$ fluid forces and moments.

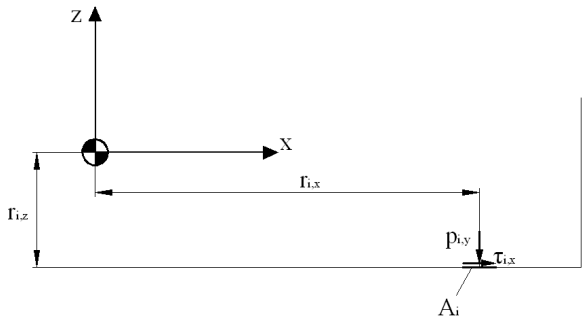

(a) 2D sketch of fluid sloshing pressure and viscous stress

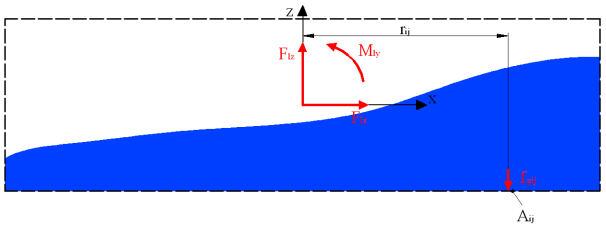

(b) 2D sketch of fluid sloshing forces and moments

Figure 4.11: 2D schematic representation of the pressure and viscous stress (a), whose integration over the wetted wall yields the sloshing forces and moments (b).

The equations of motion of the vehicle subsystem symbolically reads as follow:

$$[\mathbf{M}]\underline{\ddot{\mathbf{X}}} = \underline{\mathbf{f}_e}(\underline{\dot{\mathbf{X}}}, \underline{\mathbf{X}}) + \underline{\mathbf{f}_k}(\underline{\dot{\mathbf{X}}}, \underline{\mathbf{X}}) + \underline{\mathbf{f}_l}(\underline{\dot{\mathbf{X}}}, \underline{\mathbf{X}}, \mathbf{v}, \mathbf{p}); \tag{4.16}$$

Where $[\mathbf{M}]$ is the mass matrix and $\underline{\ddot{\mathbf{X}}}$ is the acceleration vector. The terms

$\underline{\mathbf{f}_e}$ and $\underline{\mathbf{f}_k}$ represent respectively the viscous-elastic suspension forces and the contact forces calculated using the Magic Formula tyre model (see section 4.3), both of those terms are functions of the state vector $(\underline{\mathbf{X}}, \underline{\dot{\mathbf{X}}})$. The last terms $\underline{\mathbf{f}_l}$ represents the non-linear components of fluid sloshing forces and moments derived with the equations (4.16) and (4.14), and beyond the state vector $(\underline{\mathbf{X}}, \underline{\dot{\mathbf{X}}})$ they are functions of the liquid pressure $\mathbf{p}$ and of the velocity field $\mathbf{v}$, which are obtained integrating the fluid momentum equations together with the continuity and Reynolds stress equations (4.9). (4.10) and (4.11). In Figure 4.10 the term $\underline{\mathbf{f}_l}$ is indicated with $\underline{\mathbf{L}}$ and represents the output of the subsystem fluid model and the input of the vehicle subsystem. In Figure 4.12 are schematic represented the fluid sloshing force and moments applied on the saddle supports.

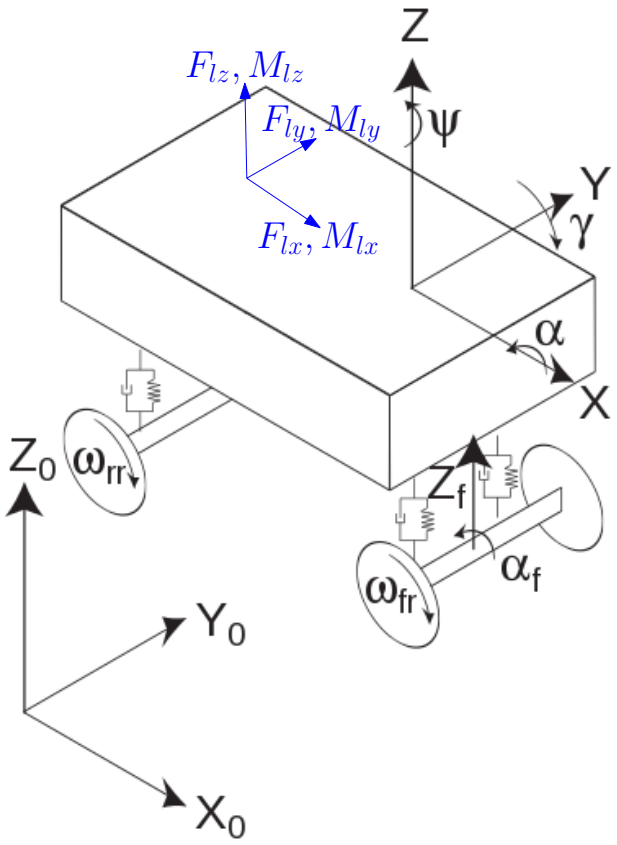

Figure 4.12: Sketch of the vehicle model showing the bodies, the degrees of freedom and the sloshing force F_{lx}, F_{ly}, F_{lz} andM_{lx}, M_{ly}, M_{lz}, applied at the saddle supports.

The whole system representing the tank truck model is developped in FLUENT. The subsystem fluid sloshing is easily implemented in FLUENT, being FLUENT a CFD code. The equations of motion of the subsystem vehicle are implemented in a routine, written in C code, introduced within the FLUENT solver process by mean of the UDF utilities, within the same routine the runge and kutta 4th order is implemented to integrate the equations of motion. Within the same routine also the sloshing forces are calculated and feeded into the vehicle of motion equation.

Chapter 5

Results

5.1 Introduction

In order to assess the effect of the fluid sloshing on the vehicle dynamics, several manoeuvres have been simulated. As already mentioned, the 3D motion of the fluid has been considered. In Section 5.2, straight line braking manoeuvres will be taken in order to evaluate the influence of sloshing on the vehicle longitudinal-pitch dynamics. In particular, the baffles influence will be investigated through simulations. In section 5.3 the Static Rollover Threshold (SRT) will be evaluated through tilt table tests simulations for different fill load percentage. The curve load percentage versus SRT obtained for vehicle-liquid cargo coupled simulations will be compared with results obtained with an equivalent rigid cargo. In Section 5.4, lane changes manoeuvres will be considered in order investigate the influence of the fluid sloshing on the roll dynamics. Only one fill level has been considered, results are compared with the one coming from an equivalent rigid cargo.

5.2 Braking manoeuvre

The effect of the fluid sloshing on the vehicle longitudinal-pitch dynamics has been assessed through straight line braking simulations. The 3D tank fluid model described in Section 3.6 has been used in co-simulation with the vehicle model described in the previous chapter in order to evaluate the effect

of baffles on the fluid motion and consequently on the vehicle dynamics. The tested tank configurations are: the cleanbore, the one closed baffle (two compartments tank) and the two closed baffles. As an example of the obtained results, Figure 5.1 and 5.2 refer to a straight line braking manoeuvre with the tank volume filled at 50,0% and a mean deceleration equal to $7m/s^2$. During the simulation, the vehicle model runs at the constant speed of $80km/h$ and at t=1s it starts braking with torques repatition between rear and front wheel (rear $6000Nm$; front $18000Nm$).

Figure 5.1 shows from the top to the bottom, the longitudinal vehicle displacement, the longitudinal velocity and the longitudinal acceleration. The colored lines refer to fluid vehicle simulation; respectively: blue line clean bore, red line one baffle, green line two baffles. While the black line is refered to the rigid cargo vehicle simulaitons.

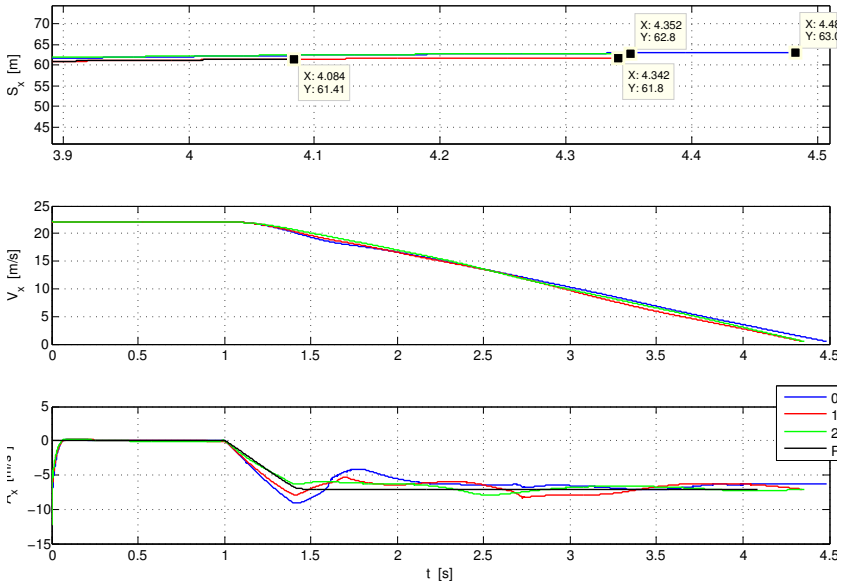

Figure 5.1: Comparison between three different baffles arrangements simulated in full brake manoeuvres with a 50,0% filled-volume. From the top to thebottom: position, velocity and acceleration.

As can be observed from Figure 5.1 the fluid sloshing increases the brake distances up to $2,5m$ in the case of the clean bore. While the sloshing mitigatin introduced by the baffles, is able to reduce up $2,0m$ the brake distances in the case of the three tank compartments. As consequece of the

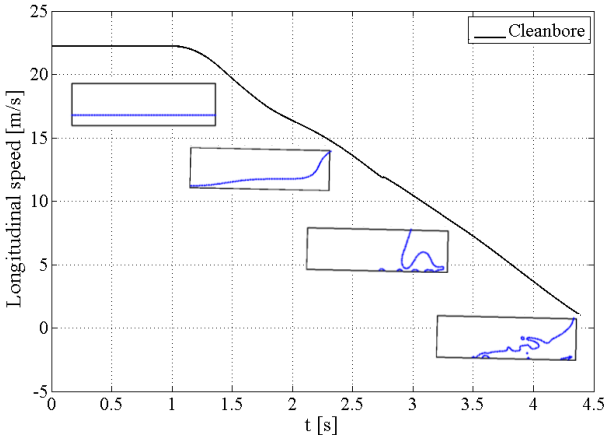

(a) Clean bore tank

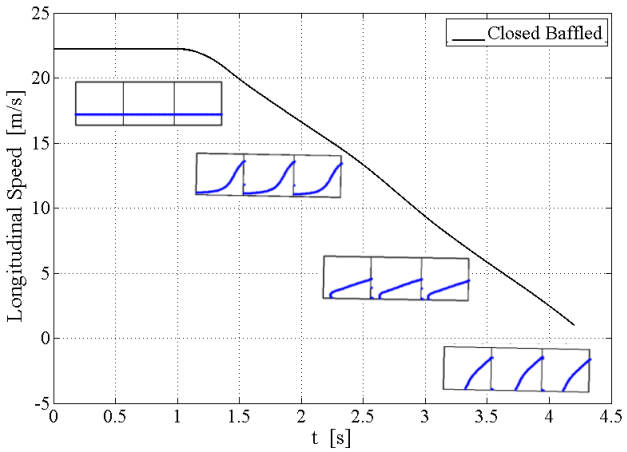

(b) Three baffles tank

Figure 5.2: Comparison of the free surface evolution of the fluid during braking manoeuvres, between a clean bore tank and a 3 compartments baffled tank.On the plot is reported also the velocity profile.

fluid sloshing the longitudinal acceleration of the vehicle in clean bore case shows big variations in amplituide compared with the rigid cargo, whose steady state value is about $7m/s^2$.

Figure 5.2 shows the evolution of the free fluid surface throughout the simulation for the three different baffles arrangements. As it can be seen, the presence of two baffles significantly reduces the fluid motion. Since the fluid has to cover a shorter distance before impacting on the walls (the tank

volume is divided into three equal parts by the baffles), the longitudinal force exerted by the fluid (Figure 5.3, at the top) in the baffled tank cases increases faster, and presents a smaller peak with respect to the cleanbore tank. This peak is reached when the fluid splashes against the front wall of the cleanbore tank (t=2s). Moreover, while the pitch moment is almost

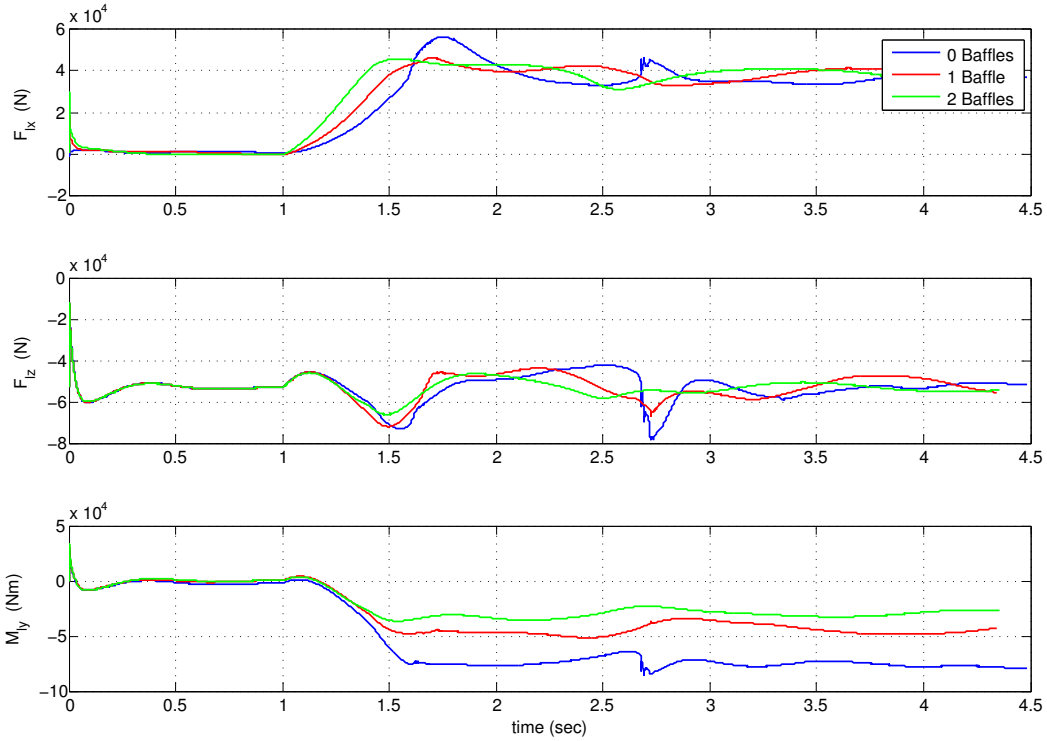

Figure 5.3: Comparison between three different baffles arrangements simulated in full brake manoeuvres with a 50,0% filled-volume. From the top to thebottom: Longitudinal fluid force, vertical force and pitch moment.

equal to zero when closed baffles are present; it increases the load transfer from the rear to the front wheels when the fluid can move through the entire tank (Figure 5.2(a)-third part), this leading to the rear wheels locking up after 2.2s in the cleanbore case (Figure 5.4(c), blue line). The presence of baffles reduces the rear-front load transfer and delays the rear wheels locking up to 2.35s in the case of one baffle (Figure 5.4(c), red line) and prevent wheel lock up in case of three baffles (Figure 5.4(c)-, green). It must be noted that, if the fluid sloshing is neglected (i.e. a rigid cargo is considered),

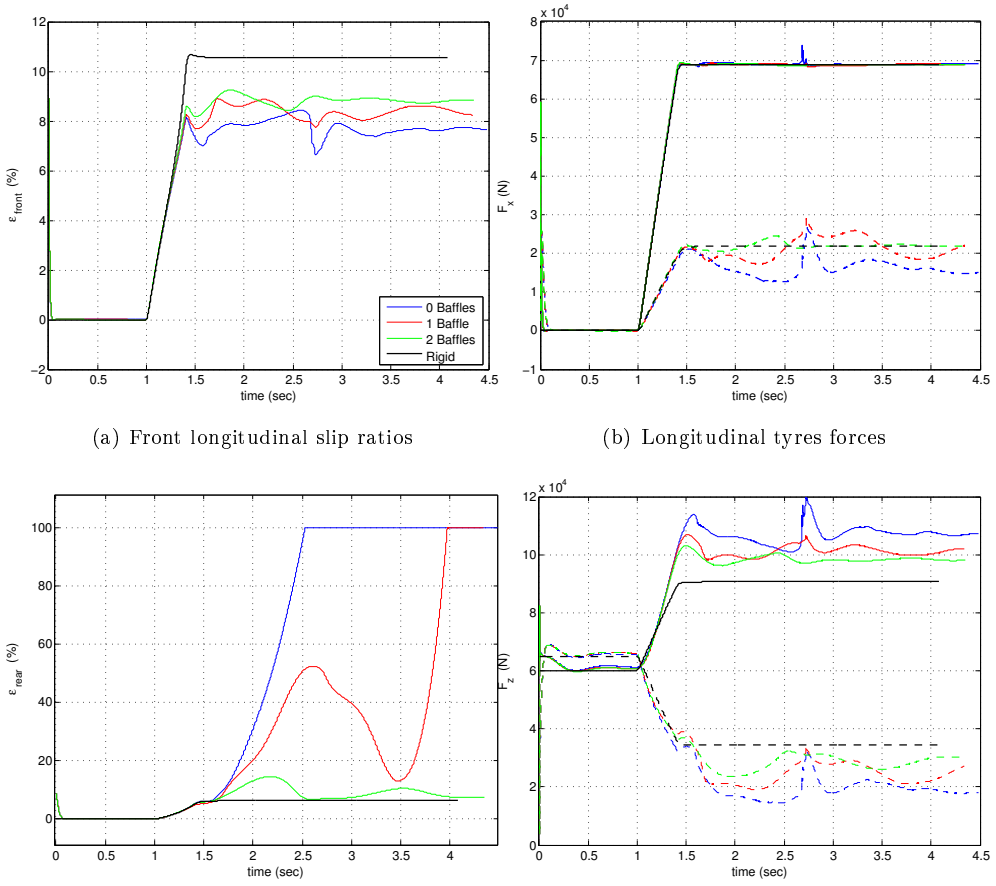

(a) Front longitudinal slip ratios

(b) Longitudinal tyres forces

(c) Rear longitudinal slip ratios

(d) Vertical tures forces

Figure 5.4: Comparison between three baffles arrangements: 0 Baffles - blue lines; 1 Baffle - red linee; 2 Baffles - green lines. With tank at 50,0% filledvolume during a full braking manoeuvre. (b) and (d): dashed lines - rear tyres forces; solid lines - front tyres forces.

the rear wheels do not lock up (Figure 5.4(c) -lower part, black line). This clearly underlines the necessity of introducing fluid-vehicle interaction when simulating tank trucks dynamics.

5.3 Static Rollover Threshold

The static rollover threshold (SRT) is used to evaluate the static lateral acceleration leading to the vehicle rollover. The SRT can be evaluated through experimental tests (tilt table test) or using simulations. In this part the cou-

pled vehicle plus fluid cargo has been used to evaluate the SRT of the road tanker for different fill level, the results are compared with those obtained with an equivalent rigid cargo.

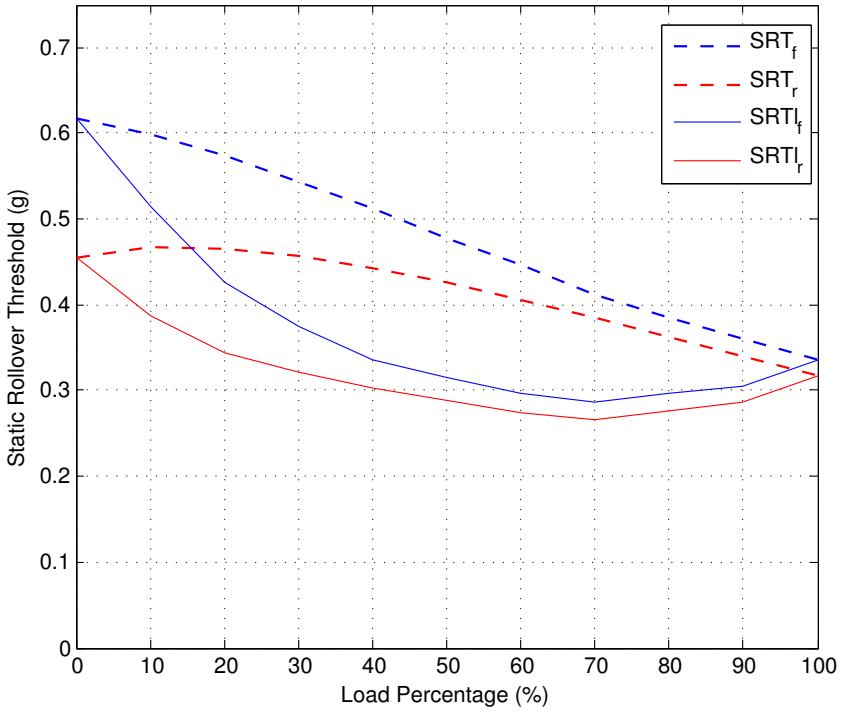

Figure 5.5: Comparison of Staic Rollover Threshold for vehicle simulated with fluid cargo and vehicle simulated with rigid cargo. The limid accelerationdefining the SRT is calculated for each axles and fro different load conditions.

In Figure 5.5 are plotted the limit static accelerations leading to the lift of one wheel of each axle. In dashed lines are reported the results related to the equivalent rigid cargo, in blue lines are reported results of the front axles whereas with red lines are reported results of the rear axles. The results in dashed line have been presented and discussed in the chapter 5. As already mentioned in chapter 5 the lowest acceleration leading to the lift of one side wheels is obtained in full load conditions (see blue dashed line Figure 5.5). As depicted in Figure 5.5 for tank truck partly filled the lowest SRT is not obtained for 100,0% of load conditions but it is obtained for 70,0%-filled volume, this is infact the lower point of the blue solid line. This results point out a limitation of the ADR discussed in paragraph concerning with ADR

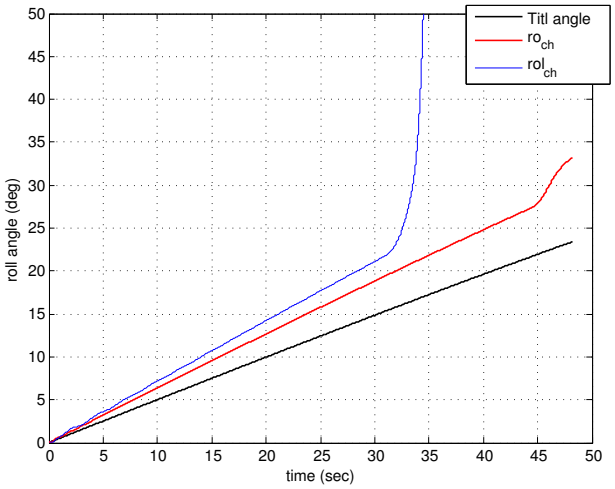

(a) Chassis roll angle and tilt angle

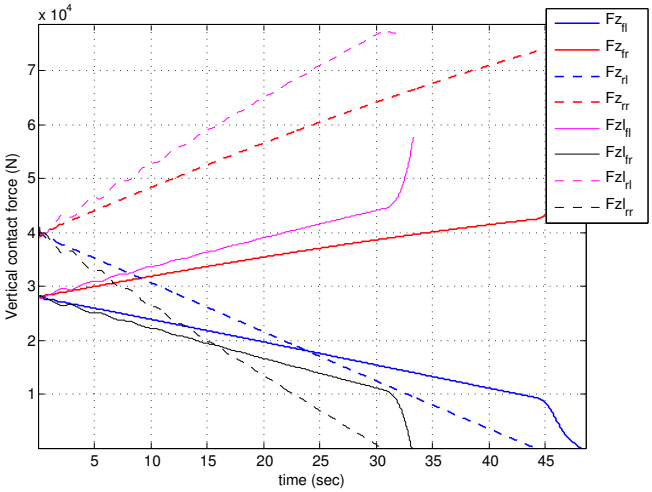

(b) Normal contact forces

Figure 5.6: Comarison of time histories of chassis roll angle (a) and vertical contact load (b), during tilt table simulation, of results obtained with vehiclesimulated with an equivalent rigid cargo and vehicle simulated with liquid sloshing cargo.

- Europe of section 2.2 which states that tilt table tests have to be made in full load condition with a total weight not exceding the allowable Gross Vehicle Weight. Only because the fluid employed during the test is imposed to be water, to comply on the limitation on the total GVW, is allowed to make a test with partly filled tank but not less than 70,0%-filled volume is allowed. While the results obtained suggest to investigate the minimum SRT as function of the fill level.

In Figure 5.6(b) are compared the vertical contact loads during tilt table simulation, magenta and black lines are refered to a vehicle-sloshing cargo coupled simulation, while the blue and red lines are refered to a vehicle simulated with an equivalent rigid cargo. Solid lines are refered to front axles vertical loads while dashed lines are refered to rear axle vertical contact loads. In Figure 5.6(b) are shown results referd to a 60,0%-filled volume. As figure shows an higer load transfer is observed in vehicle-liquid coupled simulations. This is due the lateral displacement of the fluid cargo, which leads to a reduction of the restoring arm in roll plain vehicle model. In Figure 5.6(a) are reported the time histories of the chassis roll angles, in blue line is reported the vehicle-liquid cargo coupled simulation while in red line is reported the equivalent vehicle simulated with rigid cargo. The blak line represents the roll angle imposed by the tilt table. As Figure 5.6(a) shows the greater load transfer observed for vehicle fluid coupled simulation (see Figure 5.6(b)) leads to higher chassis roll angle, this increases the negative effect due to the suspensions lash, which present also in rigid cargo simulation and was discussed in section 4.3.

5.4 Lane change

To investigate the influence of the fluid sloshing on the vehicle sideslip-yaw-roll dynamics, a lane change manoeuvre has been simulated; results are compared with an equivalent rigid cargo. The manoeuvre consists in a lateral displacement of about 3.5m operated in 30m at the constant speed of 50km/h and a steer angle frequency of 0.5 Hz; the tank volume is 50,0% filled. It is worth to point out that the manoeuvre has been simulated in open loop,

i.e. no driver model has been introduced. The considered tank section shape has been proposed in Kang [108] and is based on the Reuleaux triangle. As

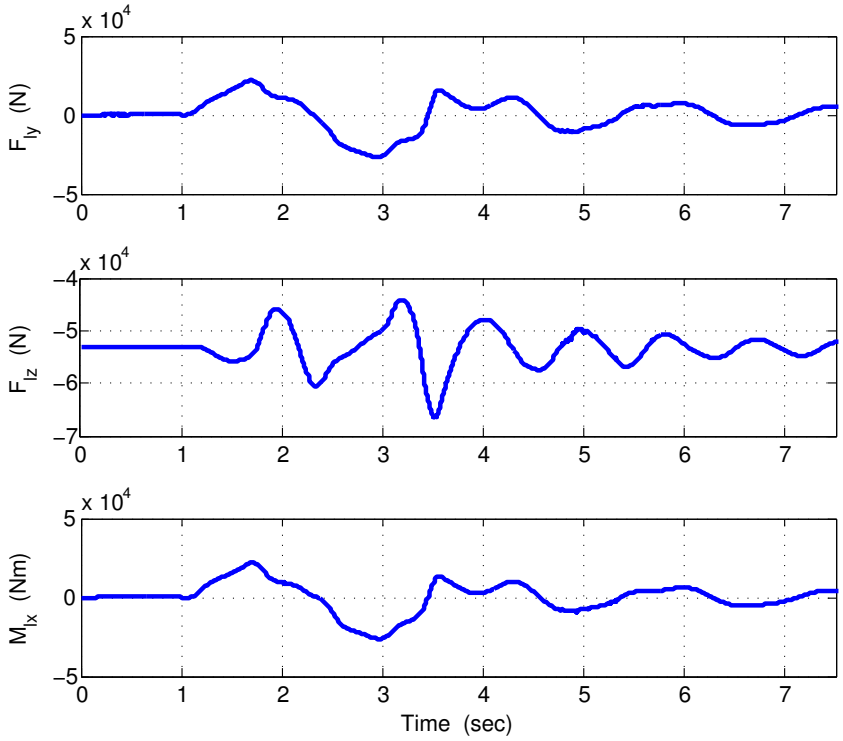

Figure 5.7: Lane change manoeuvre liquid sloshing forces: Lateral force (top), vertical force (middle) and roll moment (bottom).

mentioned before the effect of the liquid cargo is considered by mean of the forces rising from fluid sloshing and calculated by the numerical solution of the Navier-Stokes equations. In Figure 5.7 the forces rising from the fluid sloshing are plotted, from the top to the bottom are reported the lateral and the vertical force and the roll moment. The lateral force and the roll moment have the same shape as the lateral acceleration. Of course if the lateral external acceleration has a frequency close to the resonance than the lateral sloshing force can have an amplification factor up to 4 times the equivalent inertial forces due to a rigid cargo (see section 3.4). In such conditions a small laterl acceleration can lead to the rollover becouse of the sloshing forces.

During a lane change, the presence of a moving cargo, like a fluid in a tank, lead to greater lateral acceleration and roll angle compared with an

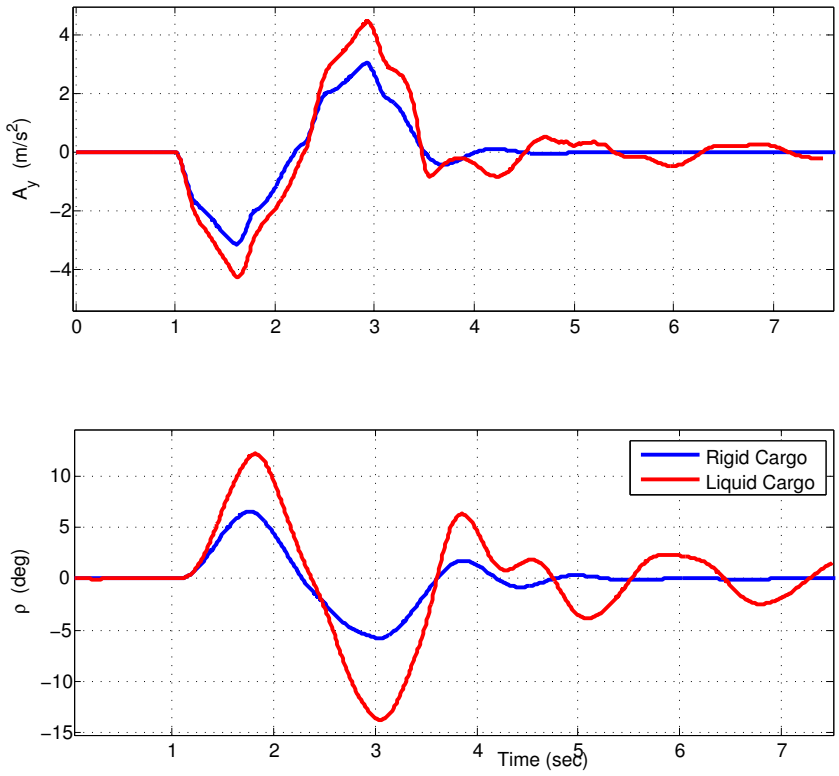

Figure 5.8: Lane change manoeuvre:comparison between liquid cargo and an equivalent rigid cargo; truck's lateral acceleration (top), truck's rollangle.

equivalent rigid cargo Figure 5.8; thus the presence of the fluid deprecate the rollover characteristics. In particular being this simulation performed in open loop (without driver model), the trajectory followed by the vehicle with rigid cargo is imposed to be the same as the one followed by the vehicle with liquid cargo. Thus if a greater lateral acceleration is required to follow the same path means that the liquid sloshing reduces the steering capability; thus increses the understeering, at the beginning of the manoeuvre and the oversteering at the end of the manoeuvre.

In Figure 5.9 are reported the tire contact forces vertical Figure 5.9(a) and 5.9(b) and lateral Figure 5.9(c) and 5.9(d) . It is evident how the motion of the liquid causes an increase of the load transfers, which affects the vertical and the lateral forces.

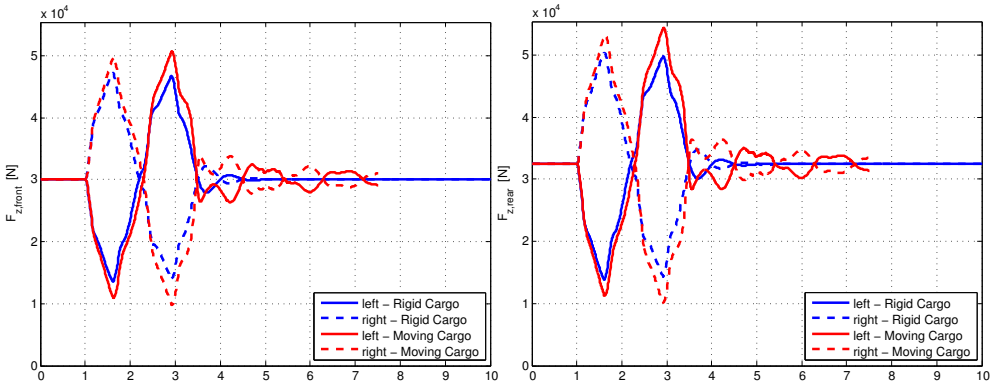

(a) Front vertical contact forces

(b) Rear vertical contact forces

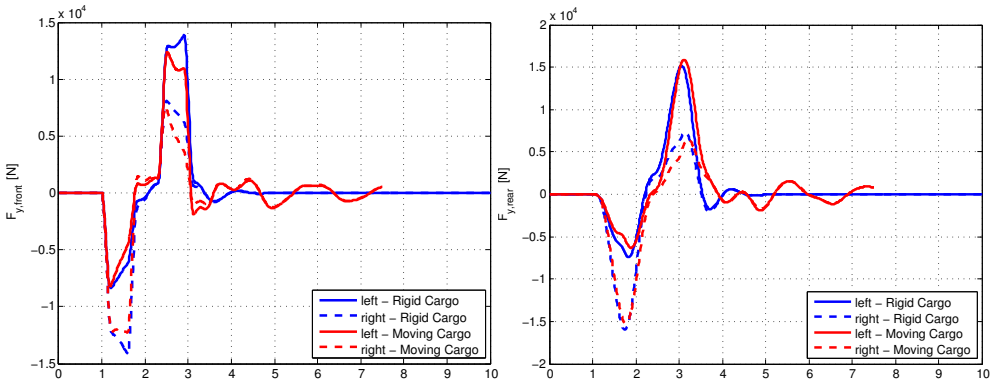

(c) Front lateral contact forces

(d) Rear lateral contact forces

Figure 5.9: Lane change manoeuvre: tires contact forces, comparison between liquid and equivalent rigid cargo; vertical contactforces (a) and (b); lateral contact forces (c) and (d).

Chapter 6

Conclusions

The hazard represented by the tank truck is well recognized all aroud the world, in special way is recognized the hazard represented by partly filled tank truck carrying hazardous materials. A lot of risk assessment projects have been issued along the years to better understand the risck associated with tank truck carrying dangeorus goods. The review of the tank truck accidents surveys, which is usually a part of the afore mensionated risk assessment projects, showed a controversial situation between European Community and North America. In fact a lot of risck assessment projects have been issued in North American countries compared with European countries. Those projects allowed a deep understanding of the rollover mechanism as well as the greater propensity to rollover showed by the partly filled tank truck. Moreover in North America exist regularly updated databases collecting accidents reports since 1970 instead in the European community only in the 1993 has been issued the CARE data base to fill up this lack. Even though the technical solutions regularly adopted by the European tank truks and trailers manufacturers and the regulations introduced by the ADR in 2003 in terms of 'lateral stability', improuves the tank trucks safety. Some of those thecnical solutions are: the use of single wheel instead of double wheels, which increase the elastic restoring moments due to the suspensions and allows the use of low profile tank (tank with low cg); The use of integrated tank-chassis design. Whereas the introduction of a minimum SRT of $0,42g$ and the forbid the circulation of tank filled in the range between 70,0%

and 30,0% are the regulations intruduced by the ADR to improve the the lateral stability.

Even if in Europe the ADR introduced some important regulations to improve the roll stability of tank trucks carrying hazardous materials, the lack of commercial software, able to easily simulate the tank truck dynamics, make really difficult the improvement of tank trucks stability in the design stage. In fact only general criteria, like lowering the cg or widing the track, have been adopted so far to comply with the regulations restriction.

In order to evaluate the effect of fluid sloshing on tank trucks dynamics and vice versa, a 3D fluid model implemented in FLUENT and a 14 dofs vehicle model have been coupled. The vehicle model has been implemented into FLUENT UDF and directly linked to the solver. Through this approach, the fluid and the vehicle models exchange input and output at predefined time steps, during the simultaneous integration of the respective equations of motion. The vehicle model imposes the motion to the tank containing the fluid, while forces due to the fluid sloshing are transferred to the vehicle model.

The performed braking manoeuvres have shown that load transfers, due to the fluid sloshing, can cause premature rear wheels locking up and then effectiveness of baffles has been investigated. The effect of sloshing is related to the amount of liquid contained and to the ratio between volume taken by the fluid and the free volume inside the tank. With applicaiton the best baffles arrangement can be easily studied in design stage. The simulation of the tilt table test allowed to make in evidence how the minimum Static Rollover Threshold is not ever in full load condition but can be in partly filled conditions like at 70,0%-filled volume for the tank considered in this study. This is due to the big lateral cg shift allowed by this tank cross section. This finding suggests that the test should be repeated for more fill levels in order to assesses the minimum value of the SRT. This can be easily done using the application developed in this work. Not only but also the investigation of new tank cross sections can be easily done. A comparison of simulations results, between liquid and an equivalent rigid cargo, in a lane change manoeuvres have allowed to evaluate how much the fluid sloshing affects the rollover in

dynamical condiitons, moreover the influence of the liquid cargo on the steering performance are also easily evaluated. Furthermore with the proposed application the effectiveness of longitudinal baffles on rollver stability can be investigated.

Appendix A

The four main USA databases of accident's reports

MCMIS: MCMIS is the official database of the Federal Motor Carrier Safety Administration (FMCSA) [153]. The data from MCMIS consist of approximately 105.000 serious crashes reported during the 2002 and collected all around US. Serious crashes are defined as those that result in: a fatality, an injury requiring transport to a facility for immediate medical attention, or at least a vehicle towed from the scene. From those accidents 2.100 were identified as involving hazmat (hazardous materials) from those a representative sample of 1.260 was selected. Of these crashes, 264 or about $21,0\%$ resulted in rollover. This database is considered the widest in the USA.

LTCCS: The LTCCS database consists of 967 crashes collected during 2001 and 2003 in 24 significant areas in 17 States of the USA. The database has been developed by a team established to study the main large truck crash causes in US. Among the 967 reported crashes 89 involved tank trucks.

TIFA: The TIFA file is produced at the Centre for National Truck and Bus Statistics [CNTBS] at [5]. The TIFA survey project has operated since 1980. In [166] a period of 5 years from 1999 to 2003 has been considered, for this period there are records of 25.704 accidents. Those records were filtered to find the records including tank trucks only. There were 1.837

accidents involving tank trucks all around the US, among which 482 resulted in rollover.

GES: The GES, General Estimates System, of the National Automotive Sampling Systems (NASS), obtains the data from a national representative probability sample of police-reported crashes. GES is based on representative sample and it is not a census. Data are reported from 1999 to 2004 for different vehicles types. Considering the 2002, a number of 891 rollovers are predicted based on 26 samples reported from the authority, with a standard deviation of 294. All the databases provide general information about the accidents collected from police.

Moreover each database has its own peculiarity: The MCMIS doesn't have many information about the vehicles involved in the accidents, on the other hand, it is a wide census; The LCCTS isn't a wide census but it has many information collected and investigated from special teams on the scene of the accident; The TIFA is based on the FARS data base, each reported accidents involves at least one fatality, moreover it has many information on roadways, vehicles, drivers and environmental conditions; The GES [2] is a statistical probability based on significant samples of accidents in the USA, it includes fatal accidents, injuries, and property damages only. Even though, databases are queried in an appropriate way in order to drawn conclusion on the influence of the sloshing on the tank truck rollover.

Appendix B

Vehicles Inventory and Use Survey data base

The greater propensity of tractor semitrailer to roll over is confirmed by **VIUS** (Vehicles Inventory and Use Survey) which is a census of tank vehicles in 2002. In table B.1 this census is reported, the $0,34\%$ of all tank trucks tractor semitrailer, or 371 rollovers from TIFA database, in 2002 have been involved in rollover, while only about the $0,05\%$, 111 rollovers from TIFA, of all the tank straight track have been involved.

Table B.1: Estimates of vehicles for tank trucks, 2002 Vehicle Inventory and Use Survey (VISU)

Tank type	**Tractor Semitrailer**		**Straight Truck**		**Total**	
	Number	%	Number	%	Number	%
Dry bulk	28.296	26,0	26.057	13,5	54.353	18,0
Liquiq/ gas	80.599	74,0	166.654	86,5	247.252	82,0
Total	108.895	100,0	192.710	100.0	301.605	100.0

Appendix C

Influece of driver age and vehicles speed on rollover frequency

Table C.1 shows how the greater part of the driver involved in rollovers were from 25 to 55 years old, moreover the percentage of the drivers age comprise between $25 - 36$ is slightly more high than the percentage of divers age comprise $45 - 55$ years old.

Table C.1: Rollover Crash Frequency vs Driver Age Category for differets data base

Driver Age	**MCMIS**	**TIFA**	**GES**	
			Estimate	**95,0% Confidence Interval**
<25	4,8 %	4,8 %	7,74 %	(2,4, 22,4)
25-36	23,0 %	75,0 %	23,97 %	(16,6, 33,3)
35-45	33,0 %		32,29 %	(14.4, 57.5)
45-55	20,6 %		24,83 %	(15.4, 37.6)
55-65	15,5 %	19,3 %	9,18 %	(5.6, 14.8)
>65	2,7 %		1,98 %	(0.7, 5.3)
Total	100,0 %	100,0 %	100,0 %	

Table C.2 reports the influence of the velocity prior to the accident, the majority of the tuck involved weren't travelling too fast. Only the 19,0 % of trucks and the 16,0 % of tank trucks were travelling too fast, instead, the 46,3 % of all trucks and the 52,0 % of the tank trucks weren't travelling too fast.

Table C.2: Rollover Crash Frequency vs Speed Category (LTCCS)

Speeding	**All Trucks**		**Cargo Tanks Only**	
	Rollover	**Percent of All Rollover**	**Rollover**	**Percent of All Rollover**
Did not realize caution required	41	19,0 %	4	16,0 %
Keeping un with traffic	3	1,4 %	0	0.0 %
Other reason	63	29,2 %	6	24,0 %
Unknown	9	4,2 %	2	8,0 %
No travelling too fast	100	46,35 %	13	52,0 %
Overall	216	100,0 %	25	100,0 %

Appendix D

Official dangerous goods classification

Table D.1: Dangerous goods classification

Classes	Material type	Material specification
Class 1	Explosive	mass explosive hazard fragment projection but no mass explosion hazard fire hazard with minor blast and or projections hazard presents no significant hazard largely confined to package insensitive substance with mass explosion hazard extremely insensitive substance without mass explosion hazard
Class 2	Gasses	2.1 flammable gasses 2.2 non-flammable, non-poisonous or non-corrosive gas 2.3 poisonous gas 2.4 corrosive gas
Class 3	Flammable liquids	A liquid with a closed-cup flash point of not greater than 61 deg. C.
Class 4	Flammable solids	4.1 A readily combustible solid, from friction or heat retained or is self reactive substance that is liable to undergo a strongly exothermic reaction 4.2 A substance liable to spontaneous combustion 4.3 A substance that, on contact with water emits flammable gasses or may ignite from spontaneous heating
Class 5	Oxidizing Substances and Organic Peroxides	5.1 A substance which causes or contributes to the combustion of other materialby yielding oxygen 5.2 A strongly oxidizing organic compound liable to explosive decomposition
Class 6	Poisonous and Infectious Substances	6.1 A poisonous solid or liquid 6.2 Infectious organism
Class 7	Radioactive materials	Radioactive materials with activity greater than 74 kB/kg
Class 8	Corrosive Substances	A substance that causes visible necrosis of skin or corrodes steel or non-clad aluminum
Class 9	Miscellaneous or Products or Substances	9.1 A dangerous substance not ascribed by any other class 9.2 An environmentally hazardous substance 9.3 A dangerous waste

Appendix E

European CARE database

The Council decided on 30 November 1993 the creation of a Community database on road accidents (Council Decision 93/704/EC, Oj No L329 of 30.12.1993, pp. 63-65). The **CARE** is a Community database on road accidents resulting in death or injury (no statistics on damage - only accidents). The major difference between CARE and most other existing international databases is the high level of disaggregation, i.e. CARE comprises detailed data on individual accidents as collected by the Member States. This structure allows for maximum flexibility and potential with regard to analysing the information contained in the system and opens up a whole set of new possibilities in the field of accident analysis.

Purpose of CARE system is to provide a powerful tool which would make possible to identify and quantify road safety problems throughout the European roads, evaluate the efficiency of road safety measures, determine the relevance of Community actions and facilitate the exchange of experience in this field.

National data sets should be integrated into the CARE database in their original national structure and definitions, with confidential data blanked out. The Commission provides a framework of transformation rules allowing CARE to provide compatible data.

Appendix F

Dangerous goods road and rail accidents in the 2001-2006 (Hazardous Cargo Bulletin-Accident Log)

Appendix F. Dangerous goods road and rail accidents in the 2001-2006 (Hazardous Cargo Bulletin-Accident Log)

	Road or rail Tanker	**Causes and accident type**	**Cargo**	**Leakage, Fire or Explosion**
2001	-	-	-	-
2002	rail tank	Derailment	Propane	
	road tanker	Overturned after driver	bitumen at 200°C lost control	
2003	road tanker	Probably driver fell asleep, hit crash barrier, overturned	gasoline and diesel	cargo lost
	road tanker	driver error hit central barrier	heating oil	oil leaked
	road tanker	Excessive speed overturned	vinyl acetate	little cargo split
	road tanker	Driver lost control taking abend too fast, overturned after a while	sulphuric acid	leaking acid to road
	road tanker	Driver lost control when approaching two car accident, truck fell off bridge	gasoline	tanker exploded
	road tanker	Truck ran off	Trichloroethylene	spilling
	road tanker	Truck ran into lorry caught	various acid solutions	acid spilt to road
	road tanker	Truck had run off road	Benzeze/methanol-based resin	leaked
2004	rail tank	Derailed	LPG and Propylene	Fire
	road tanker	Truck fell from a bridge	Fuel	Exploded
	road tanker	Truck spun out of control on railway line, overturned	Propane-butan mix	fire crews sealed pipe
2005	road tanker	Possilble driver goig too fast, lost control and overturned	VAM	Split
	road tanker	Truck ran of highway on heavy snow	Isobutyl Methacrylate	
	road tanker	Driver lost control of tanker colliding with central garrail, overturned	kerosene	Spilling
	road tanker	Truk ran off, overturned	Ammonium mitrate	Spilling
	rail tanker	Derailed	Methanol	
	road tanker	Suspected brake faliure, truck crashed into another truck	Unspecified food stuff	
2006	road tanker	Overturned after accident at roudabout	Ammunition	Splilling
	rail tanker	freight train ran into back a second freight train halted at stop signal	Hydrofluric acid and caustic soda	
	road tanker	Tanker veered across median and into ditch	kerosene	Spill

Bibliography

[1] Etac, (2006), (european truck accident causation). http://ec.europa.eu/transport/roadsafety_library/publications/etac_final_report.pdf.

[2] General estimates system (ges). http://www.nhtsa.gov/NASS.

[3] Large truck crash causation study (ltccs). http://www.fmcsa.dot.gov/facts-research/research-technology/analysis/ltccs.htmhttp://mcmiscatalog.fmcsa.dot.gov.

[4] Motor carrier management information system. http://mcmiscatalog.fmcsa.dot.gov.

[5] The transportation research institute at the university of michigan (umtri). http://www.umtri.umich.edu/news.php.

[6] Trucks involved in fatal accidents (tifa). http://www.umtri.umich.edu/expertiseSub.php?esID=29.

[7] Dagob, (2007), (dangerous goods related accidents and accidents in the baltic sea region), December 2007. htttp://www.dagob.info.

[8] Trace, (2007) (traffic accident causation in europe)), November, 2007. http://www.trace-project.org.

[9] Asteryx, (2003), (assessing the european road safety problem an exploitation study of the care database). case study: heavy goods vehicle accidents, October, 2003. http://ec.europa.eu/transport/road_safety/pdf/projects/asteryx.pdf.

[10] N. H. Abramson. *Dynamic behaviour of liquids in moving containers.* Washington, Scientific and Technical Information Division, National Aeronautics and Space Administration, 1966.

[11] T. Acarman and Ü. Özgüner. *Rollover prevention for heavy trucks using frequency?shaped sliding mode control.*

[12] H. Akyild?z and N. E. Unal. *Sloshing in a three-dimensional rectangular tank: Numerical simulation and experimental validation*, page pp. 2135?2149. Ocean Engineering, Vol. 33, 2006.

[13] Johnson A. Aliabadi, S. and J. Abedi. *Comparison of finite element and pendulum models for simulation of sloshing*, page pp. 535?545. Computers and Fluids, Vol. 32, 2003.

[14] Mucino V. H. Gautam M. Aquaro, M. and M. Salem. *A finite elemnt modeling approach for stability analysis of partially filled tanker trucks.* SAE technical paper no. 1999-01-3708, 1999.

[15] N. Aquelet and M. Souli. *A new ALE formulation for sloshing analysis*, pages pp. 423–440. Structural Engineering and Mechanics, Vol. 16, No. 4, 2003.

[16] M. Arafa. *Finite Element Analysis of Sloshing in Rectangular Liquid-filled Tanks*, page pp. 883?903.?141. Journal of Vibration and Control, Vol. 13, No. 7, 2007.

[17] M. Aslam. *Finite Element Analysis of Earthquake-Induced Sloshing in Axisymmetric Tanks*, pages pp. 159–170. International Journal for Numerical Methods in Engineering, Vol. 17, 1981.

[18] Y. BaoZeng. *Large-scale amplitude liquid sloshing in container under pitching excitation*, pages pp. 3816–3823. Chinese Science Bulletin, Vol. 53, No. 24, 2008.

[19] Gavrilyuk I. Hermann M. Barnyak, M. and A. Timokha. *Analytical velocity potentials in cells with a rigid spherical wall*, page pp. 38?45.?127? ZAMM - Journal of Applied Mathematics and Mechanics, Vol. 91, No. 1, 2011.

[20] R. Barron and S. W. R. Chng. *Dynamic analysis and measurement of sloshing of fluid in containers*, pages pp. 83–90. Journal of Dynamic Systems, Measurement, and Control, Vol. 111, 1989.

[21] Birken K. Johannsen K. Lang S. Neuß N. Rentz-Reichert H. Wieners C Bastian, P. *UG ? A flexible software toolbox for solving partial differential equations*, page pp. 27?40. Computing and Visualization in Science, Vol. 1, 1997.

[22] G. K. Batchelor. *An Introduction to Fluid Dynamics.* 1967.

[23] H. F. Bauer. Nonlinear mechanical model for the description of propellant sloshing. *AIAA Journal, Vol. 4, No. 9, pp. 1662?1668*, 1967.

[24] H. F. Bauer. Nonlinear propellant sloshing in a rectangular container of infinite length, developments in theoretical and applied mechanics. In *proceedings of the Southeastern Conference on Theoretical and Applied Mechanics, Vol. 3, pp. 725?759.?42.*, 1967.

[25] H. F. Bauer. *On the destabilizing effect of liquids in various vehicles (part 1)*, pages 227–260. Vehicle System Dynamics, 1: 3, 1972.

[26] Kadja M. Mai T. H. Belakroum, R. and C. Maalouf. *An efficient passive technique for reducing sloshing in rectangular tanks partially filled with liquid*, page pp. 341?346. Mechanics Research Communications, Vol. 37, 2010.

[27] M. Biglarbegian and J. Zu. *Tractor?semitrailer model for vehicles carrying liquids*, page pp. 871?885. Vehicle System Dynamic, Vol. 44, No. 11, 2006.

[28] J. R. Billing and J. D. Patten. An assessment of tank truck roll stability. Technical report, Transport Dangerous Goods Directorate, Ottawa, 2005.

[29] Bhattacharyya S. K. Biswal, K. C. and P. K Sinha. *Non-linear sloshing in partially liquid filled containers with baffles*, page pp. 317?337. International Journal for Numerical Methods in Engineering, Vol. 68, 2006.

[30] Foglia M. Mantriota G. Bottiglione, F. and M. Mastrovito. *Liquid sloshing in articulated tank vehicles: image-based investigation in field test*, pages pp. 441–459. International Journal of Heavy Vehicle systems, Vol. 14, Nos. 4, 2007.

[31] H. Braess and P. Wriggers. *Arbitrary Lagrangian Eulerian finite element analysis of free surface flow*, pages pp. 95–109. 2000.

[32] Savio L. Viviani M. Chen Y. Temarel P. Couty-N. Hoflack S. Diebold L. Moirod N. Brizzolara, S. and A. Souto-Iglesias. *Comparison of experimental and numerical sloshing loads in partially filled tanks*, page pp. 15?43. Ships and Offshore Structures, Vol. 6, No. 1?2, 2011.

[33] Stella F. Bucchignani, E. and F. Paglia. A partition method for the solution of a coupled liquid-structure interaction problem. 2004.

[34] B Budiansky. *Sloshing of liquids In Circular Canals and Spherical Tanks*, pages pp. 161–173. Journal of the Aerospace Sciences, Vol. 27„ 1960.

[35] A. Cariou and G. Casella. *Liquid sloshing in ship tanks: a comparative study of numerical simulation*, pages 183–198. Marine Structures, vol. 12, 1999.

[36] J. D. Casasanta. Rollover stability analysis of commercial semi?tanker trucks utilizing a trammel pendulum model to simulate fluid sloshing. Master's thesis, M.S. Thesis, Binghamton University, State University of New York, Binghamton, NY, USA, 2010.

[37] D. A. Caughey and M. M. Hafez. *Frontiers of computational fluid dynamics*. World Scientific Publishing Co. Pte. Ltd, 2006.

[38] B. Chen and H. Chiang. Complete two-dimensional analysis of seawave-induced fully non-linear sloshing fluid in a rigid floating tank. 2000.

[39] Djidjeli K. Chen, Y.G. and W.G Price. *Numerical simulation of liquid sloshing phenomena in partially filled containers*, page pp. 830?842. Computers and Fluids, Vol. 38, 2009.

[40] Hwang W. S. Chen, Y. H. and C. H. Ko. *Sloshing behaviours of rectangular and cylindrical liquid tanks subjected to harmonic and seismic excitations*, page pp. 1701?1717. Earthquake Engineering and Structural Dynamics, Vol. 36, 2007.

[41] J. R. Cho and H. W. Lee. *Non-linear finite element analysis of large amplitude sloshing flow in two-dimensional tank*, pages pp. 514–531. International Journal for Numerical Methods in Engineering, Vol. 61, 2004.

[42] Lee H. W. Cho, J. R. and S. Y. Ha. *Finite element analysis of resonant sloshing?response in 2-D baffled tank*, page 2005. Journal of Sound and Vibration, Vol. 288, pp. 829?845.

[43] Colicchio G. Lugni C. Colagrossi, A. and M. Brocchini. *A study of violent sloshing wave impacts using an improved SPH method*, page pp. 94?104. Journal of Hydraulic Research, Vol. 48, 2010.

[44] Frangi A. Cremonesi, M. and U. Perego. *A Lagrangian finite element approach for the analysis of fluid?structure interaction problems*, pages pp. 610–630. International Journal for Numerical Methods in Engineering, Vol. 84, 2010.

[45] L. Dai and L. Xu. *A numerical scheme for dynamic liquid sloshing in horizontal cylindrical containers*, pages pp. 901–918. Proceedings of the Institution of Mechanical Engineers, Part D: Journal of Automobile Engineering, Vol. 220, 2006.

[46] Xu L. Dai, L. and B. Setiawan. A new non-linear approach to analysing the dynamic behaviour of tank vehicles subjected to liquid sloshing. *Proc. IMechE Vol. 219 Part K: J. Multi-body Dynamics.?19*, 2005.

[47] J. F. Dalzell. Exploratory studies of liquid behavior in randomly excited tanks: Lateral excitation: Technical report no. 2. Technical report, NAS8-20319, SwRl Project No. 02-1869, National Aeronautics and Space Administration, George C. Marshall Space Flight Center, Huntsville, Alabama, 1967.

[48] Colagrossi A. Souto-Iglesias A. Zamora-Rodriguez R. Delorme, L. and E Botia-Vera. *A set of canonical problems in sloshing, Part I: Pressure field in forced roll?comparison between experimental results and SPH*, page pp.168?178. Ocean Engineering, Vol. 36, 2009.

[49] Z. Demirbilek. *Energy dissipation in sloshing waves in a rolling rectangular tank - I. Mathematical theory*, pages pp. 347–358. Ocean Engineering, Vol. 10, No 5, 1983.

[50] Z. Demirbilek. *Energy dissipation in sloshing waves in a rolling rectangular tank - II. Results and application*, pages pp. 375–382. Ocean Engineering, Vol. 10, No 5, 1983.

[51] Z. Demirbilek. *Energy dissipation in sloshing waves in a rolling rectangular tank - II. Solution method and analysis of numerical technique*, pages pp. 359–374. Ocean Engineering, Vol. 10, No 5, 1983.

[52] Pyles J. M. Disimile, P. J. and N. Toy. *Hydraulic jump formation in water sloshing within an oscillating tank*, pages pp. 549–556. Journal of Aircraft, Vol. 46, No. 2, 2009.

[53] F. T. Dodge. *Engineering study of flexible baffles for slosh suppression.* 1971.

[54] Durmus A. Dogangun, A. and Y. Ayvaz. *Static and dynamic analysis of rectangular tanks by using the Lagrangian fluid finite element*, page pp. 547?552. Computers and Structures, Vol. 59, No. 3, 1996.

[55] S. Dutta and M. K. Laha. *Analysis of the small amplitude sloshing of a liquid in a rigid container of arbitrary shape using a low-order boundary element method*, pages pp. 1633–1648. International Journal for Numerical Methods in Engineering, Vol. 47, 2000.

[56] R. D. Ervin and A. Mathew. Reducing the risk of spillage in transportation of chemical wastes by tuck. UMITRI-88-28.

[57] D. V. Evans and C. M. Linton. *Sloshing frequencies*, pages pp. 71–87.? Quarterly Journal of Mechanics and Applied Mathematics, Vol. 46, 1993.

[58] Firoozkoohi R. Faltinsen, O. M. and A. N. Timokha. *Analytical modeling of liquid sloshing in a two-dimensional rectangular tank with a slat screen*, pages pp. 93–109. Journal of Engineering Mathematics, Vol. 9, No. 1-3, 2010.

[59] O. M. Faltinsen and A. N. Timokha. *An adaptive multimodal approach to nonlinear sloshing in a rectangular tank*, page pp. 167?200. Journal of Fluid Mechanics, Vol. 432, 2001.

[60] O. M. Faltinsen and A. N. Timokha. *Asymptotic modal approximation of nonlinear?resonant sloshing in a rectangular tank with small fluid depth*, page pp. 319?357? Journal of Fluid Mechanics, Vol. 470, 2007.

[61] O. M. Faltinsen and A. N. Timokha. *Sloshing*. Cambridge, 2009.

[62] O. M. Faltinsen and A. N. Timokha. *A multimodal method for liquid sloshing in a two-dimensional circular tank*, pages pp. 457–479.? Journal of Fluid Mechanics, Vol. 665, 2010.

[63] Rognebakke O. F. Faltinsen, O.M. and A. N. Timokha. *Resonant three-dimensional?nonlinear sloshing in a square base basin Part3. Base ratio perturbations*, page pp. 93?116. Journal of Fluid Mechanics, Vol. 551, 2006.

[64] Rognebakke O. F. Lukovskii I. A. Faltinsen, O. M. and A. N. Timokha. *Multidimensional modal analysis of nonlinear sloshing in a rectangular tank with finite water depth*, page pp. 201?234. Journal of Fluid Mechanics, Vol. 407, 2000.

[65] Haddadpour H. Noorian M. A. Firouz-Abadi, R. D. and M. Ghasemi. *A 3D BEM model for liquid sloshing in baffled tanks*, pages pp. 1419–1433. International Journal for Numerical Methods in Engineering, Vol. 76, 2008.

[66] D'Alessandro V. Schiehlen W. Fleissner, F. and P. Eberhard. *Sloshing cargo in silo vehicles*, page pp. 968 973. Journal of Mechanical Science and Technology, Vol. 23, 2009.

[67] Lehnart A. Fleissner, F. and P. Eberhard. *Dynamic simulation of sloshing fluid and granular cargo in transport vehicles*, page pp. 3?15. Vehicle System Dynamic, Vol. 48, No. 1, 2010.

[68] United Nation Economic Commission for Europe. Uniform provision concerning the approval of tank vehicles of category n and o with regard to the roll stability, 2000. UN-ECE N° 111.

[69] Economic Commission for Europe Committee on Inland Transport. (adr 2011), european agreement concerning the international carriage of dangerous goods by road,. Volume I and II, ISBN 978-92-1-139140-4.

[70] D. W. Fox and J. R. Kuttler. *Upper and lower bounds for sloshing frequencies by intermediate problems*, pages pp. 667–682.?26? Journal of Applied Mathematics and Physics (ZAMP), Vol. 32, 1981.

[71] D. W. Fox and J. R. Kuttler. *Sloshing frequencies*, pages pp. 668–696? Journal of Applied Mathematics and Physics (ZAMP), Vol. 34, 1983.

[72] R. M. Franck and R. B. Lazarus. *Mixed Eulerian-Lagrangian method.* Methods in Computational Physics, Vol. 3, 1964.

[73] J. B. Frandsen. *Sloshing motions in excited tanks*, pages pp. 53–87. Journal of Computational Physics, Vol. 196, 2004.

[74] J. B. Frandsen and A. G. L. Borthwick. *Simulation of sloshing motions in fixed and vertically excited containers using a 2-D inviscid ?-transformed finite difference solver*, pages pp. 197–214. Journal of Fluids and Structures, Vol. 18, 2003.

[75] J. B. Frandsen and W. Peng. Experimental sloshing studies in sway and heave base excited square tanks. *Civil Engineering in the Oceans VI:Proceedings of the International Conference, pp. 504-512*, 2006.

[76] M. Funakoshi and S. Inoue. *Surface waves due to resonant horizontal oscillation*, pages pp. 219–247. Journal of Fluid Mechanics, Vol. 192, 1988.

[77] Lukovsky I. Trotsenko Yu. Gavrilyuk, I. and A. Timokha. *Sloshing in a vertical circular cylindrical tank with an annular baffle. Part 1. Linear fundamental solutions*, page pp. 71?88. Journal of Engineering Mathematics, Vol. 54, 2006.

[78] Lukovsky I. Trotsenko Yu. Gavrilyuk, I. and A. Timokha. *Sloshing in a vertical circular cylindrical tank with an annular baffle. Part 2. Nonlinear resonant waves*, page pp. 57?78. Journal of Engineering Mathematics, Vol. 54, 2006.

[79] J. Gerrits and A. E. P. Veldman. Dynamics of liquid-filled spacecraft. *Journal of Engineering Mathematics, Vol. 45, pp. 21?38.?155*, 2003.

[80] J. Gertsch and Eichelhard O. Simulation of heavy dynamic rollover threshold for heavy trucks. *SAE International 2004, 2003-01-3385*, 2004.

[81] Tan M. Turnock S. Godderidge, B. and C. Earl. *A verification and validation study of the application of computational fluid dynamics to the modelling of lateral sloshing*. University of Southampton, 2006.

[82] Turnock S. Earl C. Godderidge, B. and M. Tan. *Identification of dangerous LNG sloshing using a rapid sloshing model validated with computational fluid dynamics*, pages pp. 170–177. 18th International Offshore and Polar Engineering Conference (ISOPE 2008), International Society of Offshore and Polar Engineers (ISOPE), 2008.

[83] Turnock S. Tan M. Godderidge, B. and C. Earl. *An investigation of multiphase CFD modelling of a lateral sloshing tank*, page pp. 183?193. Computers and Fluids, Vol. 38, 2009.

[84] Sabbagh-Yazdi S. R. Goudarzi, M. A. and W. Marx. *Investigation of sloshing damping in baffled rectangular tanks subjected to the dynamic excitation*, page pp. 1055?1072. 2010.

[85] D. J. E. Harvie and D. F. Fletcher. *A New Volume of Fluid Advection Algorithm:?The Stream Scheme*, page pp. 1?32. ournal of Computational Physics, Vol. 162, 2000.

[86] S. M. Hasheminejad and M. Aghabeigi. *Liquid sloshing in half-full horizontal elliptical tanks*, pages ?pp. 332–349. Journal of Sound and Vibration, Vol. 324, 2009.

[87] S. M. Hasheminejad and M. Aghabeigi. *Transient sloshing in half-full horizontal elliptical tanks under lateral excitation*, page ?pp. 3507?3525. Journal of Sound and Vibration, Vol. 330, 2011.

[88] S. M. Hasheminejad and M. Aghabeigi. *Sloshing characteristics in half-full horizontal elliptical tanks with vertical baffles*, pages ?pp. 57–71. Applied Mathematical Modelling, Vol. 36, 2012.

[89] Hatanaka K. Hayashi, M. and M. Kawahara. *Lagrangian finite element method for free surface Navier-Stokes flow using fractional step methods*, pages pp. 805–840. International Journal for Numerical Methods in Fluids, Vol. 13, 1991.

[90] Troesch B. A. Henriei, P. and L. Wuytack. *Sloshing Frequencies for a Half-space with Circular or Strip-like Aperture*, pages ?pp. 285–318. Journal of Applied Mathematics and Physics (ZAMP), Vol. 21, 1970.

[91] Amsden A. A. Hirt, C. W. and J. L. Cook. *An arbitrary Lagrangian?Eulerian computing method for all flow speeds*, page pp. 227?253. Journal of Computational Physics, Vol. 14, No. 3, 1974.

[92] A. Huerta and W. K Liu. *Viscous Flow with Large Free Surface Motion*, pages pp. 277–324. Computer Methods in Applied Mechanics and Engineering, Vol. 69, 1988.

[93] Liu W. K. Hughes, T. J. R. and T. K. Zimmermann. *Lagrangian-Eulerian finite element formulation for incompressible viscous flows*, page pp. 329?349. Computer Methods in Applied Mechanics and Engineering, Vol. 29,, 1981.

[94] R. E. Hutton. An investigation of resonance, nonlinear and nonplanar free surface oscillations of a fluid. Technical report, NASA TN D-1870.?49, 1963.

[95] Pilipchuk V. N. Ibrahim, R. A. and T. Ikeda. Recent advances in liquid sloshing dynamics. *Applied Mechanics Reviews, Vol. 54, No. 2, pp. 133-198*, 2001.

[96] R. A. Ibrahim. Anti-slosh damper design for improving the roll dynamic behavior of cylindrical tank trucks. *SAE technical paper no.1999-01-3729*, 1999.

[97] R. A. Ibrahim. *Liquid Sloshing Dynamics - Theory and Applications*. Cambridge, 2005.

[98] Fluent Inc. *FLUENT 6.3 Documentation*, 2006.

[99] M. Isaacson. Earthquake-induced hydrodynamic forces on reservoir roofs. *Canadian Journal of Civil Engineering, Vol. 37, pp. 1107-1115*, 2010.

[100] M. Ishii and T. Hibiki. *Thermo-fluid dynamics of two-phase flow*. 2011.

[101] C. S. Jog and R. K. Pal. A monolithic strategy for fluid?structure interaction problems. 2011.

[102] D. D Kana. An experimental study of liquid surface oscillations in longitudinally excited compartmented cylindrical and spherical tanks. Technical report, NASA CR-545, Southwest Research Institute, San Antonio, Texas, 1966.

[103] D. D. Kana. *A model for nonlinear rotary slosh in propellant tanks*, page pp. 169?177. Journal of Spacecraft and Rockets, Vol. 24, No. 2, 1987.

[104] D. D. Kana. *Validated spherical pendulum model for rotary liquid slosh*, page pp. 188?195. Journal of Spacecraft and Rockets, Vol. 26, No. 3, 1989.

[105] D. D. Kana and D. J. Fox. *Distinguishing the transition to chaos in a spherical pendulum*, page pp. 298?310. Chaos, Vol. 5, No. 1, 1995.

[106] Rakheja S. Kandasamy, T. and A. K. W. Ahmed. *An Analysis of Baffles Designs for Limiting Fluid Slosh in Partly Filled Tank Trucks*, pages pp. 23–32. The Open Transportation Journal, Vol. 4, 2010.

[107] N. Kang and K. Liu. *Influence of baffle position on liquid sloshing during braking and turning of a tank truck*, pages pp. 317–324. Journal of Zhejiang University-SCIENCE A (Applied Physics and Engineering), Vol. 11, No. 5, 2010.

[108] Xiaodi Kang. *Optimal tank design and directional dynamic analysis of liquid cargo vehicles under steering and braking.* PhD thesis, Concordia University, Montreal, Quebec, Canada, 2001.

[109] Papaprokopiou D. Karamanos, S. A. and M. A. Platyrrachos. *Finite Element Analysis of Externally-Induced Sloshing in Horizontal-Cylindrical and Axisymmetric Liquid Vessels*, pages pp. 051301:1–11. Journal of Pressure Vessel Technology, Vol. 131, 2009.

[110] J. T. Katsikadelis. *Boundary Elements: Theory and Applications.* Elsevier Science Ltd.?210, 2002.

[111] G. H. Keulegan and L. H. Carpenter. *Forces on cylinders and plates in an oscillating fluid*, page pp. 423?440. 1958.

[112] R.S. Khandelwal and N.C. Nigam. *Digital simulation of the dynamic response of a vehicle carrying liquid cargo on a random uneven surface*, pages pp. 195–214. Vehicle System Dynamics, Vol. 11, No. 4, 1982.

[113] Seibi A. Khezzar, L. and A. Goharzadeh.

[114] Park J. S. Kim, M. S. and W. I. Lee. *A new VOF-based numerical scheme for the simulation of fluid flow with free surface. Part II: application to the cavity filling and sloshing problems,*, pages pp. 791–812. International Journal for Numerical Methods in Fluids, Vol. 42, 2003.

[115] Shinb Y. S. Kim, Y. and K. H. Lee. *Numerical study on slosh-induced impact pressures on three-dimensional prismatic tanks*, page pp. 213?226. Applied Ocean Research, Vol. 26, 2004.

[116] Y. Kim. *Numerical simulation of sloshing flows with impact load*, page pp. 53?62. Applied Ocean Research, Vol. 23, 2001.

[117] Y. Kim. Experimental and numerical analyses of sloshing flows. 2007.

[118] Mieda T. Shibata H. Kobayashi, N. and Y. Shinozaki. *A study of the liquid slosh response in horizontal cylindrical tanks*, pages pp. 32–38. Journal of Pressure Vessel Technology, Vol. 111, 1989.

[119] G.C. Koli and V. V Kulkarni. Simulation of fluid sloshing in a tank. In *Proceedings of the World Congress on Engineering 2010 Vol II, WCE 2010*, June 30 - July 2, 2010, London, U.K.

[120] K. Komatsu. *Nonlinear sloshing analysis of liquid in tanks with arbitrary geometries*, page pp. 193?207. International Journal of Nonlinear Mechanics, Vol. 22, No. 3, 1987.

[121] J. R. Kuttler and V. G. Sigillito. Sloshing of liquids in cylindrical tanks. In *AIAA J. 22(2)*, 1984.

[122] H. Lamb. *Hydrodynamics*. Cambridge University Press, 1975.

[123] T. A. Lance. Analysis of propellant slosh dynamics and generation of an equivalent mechanical model for use in preliminary voyager autopilot design studies. Technical report, Technical memorandum No. 33-306, Jet Propulsion Laboratory, California Institute of Technology, Pasadena, California, 1966.

[124] Kim M. H. Kwon S. H. Kim J. W. Lee, D. H. and Y. B. Lee. *A parametric sensitivity study on LNG tank sloshing loads by numerical simulations*, page pp. 3?9. Ocean Engineering, Vol. 34, 2007.

[125] Lee Y. G. Lee, S. H. and K. L. Jeong. *Numerical simulation of three-dimensional sloshing phenomena using a finite difference method with marker-density scheme*, page pp. 206?225. Ocean Engineering, Vol. 38, 2011.

[126] T. G. Lepelletier and F. Raichlen. *Nonlinear oscillation in rectangular tanks*, page pp. 1?23. Journal of Engineering Mechanics, Vol. 114, No. 1, 1987.

[127] D. Liu and P. Lin. *A numerical study of three-dimensional liquid sloshing in tanks*, page pp. 3921?3939. Journal of Computational Physics, Vol. 227, 2008.

[128] D. Liu and P. Lin. Three-dimensional liquid sloshing in a tank with baffles. *Ocean Engineering*, 2009.

[129] G. R. Liu and M. B. Liu. *Smoothed Particle Hydrodynamics*. 2003.

[130] M. Liu and D. G. Gorman. *Formulation of Rayleigh damping and its extensions,*, pages pp. 277–285. Computers and Structures, Vol. 57, No. 2,, 1995.

[131] Z. Liu and Y. Huang. *A new method for large amplitude sloshing problems*, pages pp.185–195. Journal of sound and Vibration, Vol. 175, No. 2, 1994.

[132] R. Livaoglu and A. Dogangun. Effect of foundation embedment on seismic behavior of elevated tanks considering fluid?structure-soil interaction. *Soil Dynamics and Earthquake Engineering, Vol. 27, pp. 855?863.?166*, 2007.

[133] Vaiciurgis E. Lloyd, N. and T. A. G. Langrish. *The Effect of Baffle Design on Longitudinal Liquid Movement in Road Tankers: An Experimental Investigation*, pages pp. 181–185. Trans IChemE, Vol. 80, Part B, 2002.

[134] A. Maleki and Ziyaeifar M. *Damping enhancement of seismic isolated cylindrical liquid storage tanks using baffles*, pages pp. 3227–3240. Engineering Structure, Vol. 29, 2007.

[135] Arribas D. Vicente M.T. Aparicio F. Martin, A. Rollover stability of tank trucks, test and calculation requirements based on ece 111 regulation. *In. J. Heavy Vehicle Systems, Vol. 17, Nos. 3/4*, 2010.

[136] Rossow G. Mayenburg, M. and C. Patterson. *Truck Safety Technology for the 21st Century.* SAE Paper No. 952260, 1995, 1995.

[137] J. L. McCarty and D. G. Stephens. Investigation of the natural frequencies of fluids in spherical and cylindrical tanks. Technical report, NASA TN D-252, 1960.

[138] P. McIver. *Sloshing frequencies for cylindrical and spherical containers filled to as arbitrary depth*, pages pp.243–257. Journal of Fluid Mechanics, vol. 201,, 1988.

[139] P. McIver and M. McIver. *Sloshing frequencies of longitudinal modes for a liquid contained in a trough*, pages pp. 525–541.?219. Journal Fluid Mechanics, Vol. 252, 1993.

[140] J. W. Miles. *Resonantly forced surface waves in a circular cylinder*, page pp. 15?31. Jurnal of Fluid Mechanics, Vol. 149, 1984.

[141] P. Ming and W. Duan. *Numerical simulation of sloshing in rectangular tank with VOF based on unstructured grids*, pages pp. 856–864. Journal of Hydrodynamics, Vol. 22, No. 6, 2010.

[142] Upadhyay P. P. Mitra, S. and K. P. Sinhamahapatra. *Slosh dynamics of inviscid fluids in two-dimensional tanks of various geometry using finite element method*, pages pp. 1625–1651. International Journal for Numerical Methods in Fluids, Vol. 56, 2007.

[143] Rakheja S. Modaressi-Tehrani, K. and R. Sedaghati. *Analysis of the overturning moment caused by transient liquid slosh inside a partly filled moving tank*, pages pp. 289–301. Proceedings of the Institution of Mechanical Engineers, Part D: Journal of Automobile Engineering, Vol.220, No.3, 2006.

[144] V. J. Modi and S. R. Munshi. An efficient liquid sloshing damper for vibration control. 1998.

[145] N. N Moiseev. *On the theory of nonlinear vibration of a liquid of finite volume*, pages pp. 860–872. Journal of Applied Mathematics and Mechanics, Vol. 22, No.5, 1958.

[146] N. N. Moiseev. *Introduction to the Theory of Oscillations of Liquid-Containing Bodies*, pages 233–289.?230. Advances in Applied Mechanics, Vol. 8, pp, 1964.

[147] J. J. Monaghan. *Smoothed particle hydrodynamics*, page pp.1703?1759. Reports on Progress in Physics, Vol. 68, 2005.

[148] de Pont J.J. Bass P.H. Mueller, T.H. Heavy vehicle stability versus crash rates. Technical report, TERNZ, 1999.

[149] Moiseev N. N. and A. A. Petrov. *The Calculation of Free Oscillations of a Liquid in a Motionless Container*, pages pp. 91–154. Advances in Applied Mechanics, Vol. 9, 1966.

[150] T. Nakayama and K Washizu. *The boundary element method applied to nonlinear sloshing problems the analysis of two-dimensional*, pages pp. 1631–1646. International Journal for Numerical Methods in Engineering, Vol. 17, 1981.

[151] T. Nakayama and W. Washizu. *Nonlinear analysis of liquid motion in a container subjected to forced pitching oscillation*, pages pp. 1207–1220. International Journal for Numerical Methods in Engineering, Vol. 15, 1980.

[152] W. F. Noh. *CEL:A time-dependent two-space dimensional coupled Eulerian-Lagrangian code*, pages pp. 117–179. Methods in Computational Physics, Vol. 3, 1964.

[153] US Department of Transportation.

[154] US Department of Transportation.

[155] US Department of Transportation. Code of federal regulation title 49: Transportation part 178 specifications for packaging. http://ecfr.gpoaccess.gov/cgi/t/text/text-idx?sid=f88d1f012b3f3b4021b4a0a80b3d2f1e&c=ecfr&tpl=/ecfrbrowse/Title49/49tab_02.tpl

[156] Suzuki H. Ohno, K. and T. Sawada. Analysis of liquid sloshing of a tuned magnetic fluid damper for single and co-axial cylindrical containers. 2011.

[157] K. Okamoto and M. Kawahara. *Two-dimensional sloshing analysis by Lagrangian finite element method*, page pp. 453?477. International Journal for Numerical Methods in Fluids, Vol. 11, 1990.

[158] T. Okamoto and M. Kawahara. *3-D Sloshing Analysis by an Arbitrary Lagrangian-Eulerian Finite Element Method*, page pp. 129 ? 146. International Journal of Computational Fluid Dynamics, Vol. 8, No. 2, 1997.

[159] J. L. Ortiz and A. A. Barhorst. *Large-displacement non-linear sloshing in 2-D circular rigid containers - prescribed motion of the container*, pages pp. 195–210. International Journal for Numerical Methods in Engineering, Vol. 41, 1998.

[160] Hans B. Pacejka. *Tyre and vehicle dynamics.* SAE International and Elsevier, 2002.

[161] P. Pal. *Sloshing of Liquid in Partially Filled Container-An Experimental Study.* International Journal of Recent Trends in Engineering, Vol. 1, No. 6, 2009.

[162] Zhang H. Pan, X. and Y. Lu. *Numerical simulation of viscous liquid sloshing by moving-particle semi-implicit method*, pages pp. 184–189. Journal of Marine Science and Application, Vol. 7, 2008.

[163] Saha U. K. Panigrahy, P. K. and D. Maity. *Experimental studies on sloshing behavior due to horizontal movement of liquids in baffled tanks*, page pp. 213?222. Ocean Engineering, Vol. 36, 2009.

[164] Karamanos S. A. Papaspyrou, S. and D. Valougeorgis. *Response of half-full horizontal cylinders under transverse excitation*, pages pp. 985–1003. Journal of Fluids and Structures, Vol. 19, 2004.

[165] Valougeorgis D. Papaspyrou, S. and S. A. Karamanos. *loshing effects in half-full horizontal cylindrical vessels under longitudinal excitation*, pages pp. 255–265. Journal of Applied Mechanics, Vol. 71, 2004.

[166] Harback K. McMillan N. Greenberg A. Mayfield H. Pape, D. B. and J. C. Chitwood. Cargo tank roll stability study. Technical report, U.S. Department of Transportation Federal Motor Carrier Safety Administration, April 30, 2007.

[167] L. A. Patkas and S. A. Karamanos. *Variational Solutions for Externally Induced Sloshing in Horizontal-Cylindrical and Spherical Vessels*, pages pp. 641–655? Journal of Engineering Mechanics, Vol. 133, No.6, 2007.

[168] W. G. Penney and A. T. Price. *Finite periodic stationary gravity waves in a perfect liquid, part II*, pages pp. 254–284. Philosophical Transactions of the Royal Society of London. Series A, Mathematical and Physical Sciences, Vol. 244, No. 882, 1952.

[169] V. N. Pilipchuk and R. A. Ibrahim. *The dynamics of a nonlinear system simulating liquid sloshing impact in moving structures*, page pp. 593?615. Journal of Sound Vibration, Vol. 205, No. 5, 1997.

[170] G. Popov. *Dynamics of liquid sloshing in road containers.* PhD thesis, PhD Thesis, Concordia University, Montreal, Quebec, Canada, 1991.?11, 1991.

[171] Sankar S. Popov, G. and T. S. Sankar. Dynamics of liquid sloshing in baffled and compartmented road containers. 1993.

[172] Sankar S. Popov, G. and T. S. Sankar. Optimal shape of a rectangular road container. 1993.

[173] Sankar S. Popov, G. and T.S. Sankar. Shape optimization of elliptical road containers due to liquid load in steady-state turning. 1996.

[174] Sankar S. Sankar T. S. Popov, G. and G. H. Vatistas. Dynamics of liquid sloshing in horizontal cylindrical road containers. In *Proceedings of the Institution of Mechanical Engineers. Part C: Mechanical engineering science, Vol. 207, pp. 399-406*, 1993.

[175] Sankar S. Sankar T. S. Popov, S. and G. H. Vatistas. Liquid sloshing in rectangular road containers. 1992.

[176] Vatistas G. H. Sankar S. Popov, G. and T. S. Sankar. Numerical simulation of viscous liquid slwuoshing in arbitrary shaped reservoirs. 1993.

[177] El-Gindy M. Preston-Thomos, J. Static rollover thresholds of heavy vehicles. In *Proceedings of CSME Forum, Montreal, pp. 946-951, 1992*, 1992.

[178] W. G. Price and Y. G. Chen. *A simulation of free surface waves for incompressible two-phase flows using a curvilinear level set formulation*, page pp. 305?330. International Journal for Numerical Methods in Fluids, Vol. 51, 2006.

[179] Berlot R. R. *Production of rotation in a confined liquid through translational motion of the boundaries*, page pp. 513?516. Journal of Applied Mechanics, 1959.

[180] Garza L. R. and H. N. Abramson. Measurements of liquid damping provided by ring baffles in cylindrical tanks, technical report no. 5. Technical report, Contract No. NAS8-1555, SwRI Project No. 6-1072-2, 1963.

[181] R. Radovitzky and M. Ortiz. *Lagrangian finite element analysis of Newtonian fluid flows*, pages pp. 607–619. International Journal for Numerical Methods in Engineering, Vol. 43, 1998.

[182] Pistani F. Rafiee, A. and K. Thiagarajan. *Study of liquid sloshing: numerical and experimental approach*, pages pp. 65–75. Computational Mechanics, Vol. 47, 2011.

[183] Ranganathan R. Rakheja, S. and S. Sankar. *Field testing and validation of directional dynamics model of a tank truck*, pages pp. 251–275. International Journal of Vehicle Design, vol. 13, no. 3,, 1992.

[184] S. Rakheja, S. Sankar and R. Ranganathan. *Roll plane analysis of articuated tank vehicles during steady turning*, pages 81–104. Vehicle System Dynamics, vol. 17, 1988.

[185] Sankar S. Rakheja, S. and R. Ranganathan. Influence of tank design factors on the rollover threshold of partially filled tank vehicles. 1989.

[186] Stiaharu G.-Richard M. Rakheja, S. Évaluation de la problématique reliée à l instabilité en roulement des véhicules routiers de type citerne, transportant des produits liquids. Technical report, Le Ministe're des Transport du Quebec, Aout, 2003.

[187] B. Ramaswamy and M. Kawahara. *Lagrangian finite element analysis applied to viscous free surface fluid flow*, pages pp. 953–984. International Journal for Numerical Methods in Engineering, Vol. 7, 1987.

[188] R. Ranganathan, S. Rakheja, and S. Sankar. *Influence of liquid load shift on the dynamic response of articuated tank vehicles*, pages 177–200. Vehicle System Dynamics, vol. 19, 1990.

[189] R. Ranganathan and Y.S. Yang. *Impact of Liquid Load Shift on the Braking Characteristics of Partially Filled Tank Vehicles*, pages pp. 223–240.?6. Vehicle System Dynamics, 26: 3, 1989.

[190] Rakheja S.-Sankar S. Ranganathan, R. *Kineto-static roll plane analysis of articulated tank vehicles with arbitrary tank geometry.* International Journal of Vehicle Design, vol. 10, no.1, 1989.?9, 1989.

[191] Rakheja S.-Sankar S. Ranganathan, R. *Directional Response of a B-Train Vehicle Combination Carrying Liquid Cargo,.* Journal of Dynamics Systems, Measurement, and Control Vol. 115.?8, 1993.

[192] Ying Y. Ranganathan, R. and J. B. Miles. Analysis of fluid slosh in partially filled tanks and their impact on the directional response of tank vehicles. 1993.

[193] Ying Y. Ranganathan, R. and J. B. Miles. Development of a mechanical analogy model to predict the dynamic behavior of liquids in partially filled tank vehicles. 1993.

[194] S. Rebouillat and D. Liksonov. *Fluid?structure interaction in partially filled liquid containers: A comparative review of numerical approaches*, page pp. 739?746. Computers and Fluids, Vol. 39, 2010.

[195] Shin Hyung Rhee. *Unstructured Grid Based Reynolds-Averaged Navier-Stokes Method for Liquid Tank Sloshing*, pages 572–582. Journal of Fluid Engineering, 2005.

[196] Basurto E. R. Roberts, J. R. and Chen P. Y. Slosh design handbook i. Technical report, NASA CR-406, 1966.

[197] Ram?rez O . Fortanell J. M. Martinez M. Romero, J. A. and A. Lozano. *Analysis of lateral sloshing forces within road containers with high fill levels*, pages pp. 303–312. Proceedings of the Institution of Mechanical Engineers, Part D: Journal of Automobile Engineering, Vol. 220, 2006.

[198] V. J. Romero and M. S. Ingber. A numerical model for 2-d sloshing of pseudo-viscous liquids in horizontally accelerated rectangular containers. In *Proceedings of 17th International Conference on Boundary Elements, Madison, Wisconsin*, 1995.

[199] Hopfinger E. J. Royon-Lebeaud, A. and A. Cartellier. *Liquid sloshing and wave breaking in circular and square-base cylindrical containers*, pages pp. 467–494. Journal of Fluid Mechanics, Vol. 577, 2007.

[200] F. Ru-De. *Finite element analysis of lateral sloshing response in axisymmetric tanks with triangular elements*, pages pp. 51–58. Computational Mechanics, Vol. 12, 1993.

[201] M. Rudman. *Volume-tracking methods for interfacial flow calculations*, pages pp. 671–691. International Journal for Numerical Methods in Fluids, Vol. 24, 1997.

[202] W. Rumold. *Modeling and Simulation of Vehicles Carrying Liquid Cargo*, page pp. 351?374. Multibody System Dynamics, Vol. 5, 2001.

[203] Celebi M. S. and Akyildiz H. *Nonlinear modelling of liquid sloshing in a moving rectangular tank*, pages 1527–1552. Ocean Engineering, vol. 29, 2002.

[204] Mucino V. H. Saunders E. Salem, M. I. and M. Gautam. Lateral sloshing in partially filled elliptical tanker trucks using a trammel pendulum. *In. J. Heavy Vehicle Systems, Vol. 16, Nos. 1/2, pp. 207-224*, 2009.

[205] Rakheja S. Sankar, S. and R. Ranganathan. Directional response of partially filled tank vehicles. *SAE technical paper no.892481.?15*, 1989.

[206] Rakheja S. Sankar, S. and R. N. Sabounghi. Stability analysis of liquid tank vehicle. In *International Symposium on Heavy Vehicle Weights and Dimensions, June 8-13, 1986, ?Kelowna, British Columbia*, 1986.

[207] Ranganathan R. Sankar, S. and S. Rakheja. Impact of dynamic fluid slosh loads on the directional response of tank vehicles. pages 385–404, 1992.

[208] B. A. Sayar and J. R. Baumgarten. *Pendulum analogy for nonlinear fluid oscillations in spherical containers*, page pp. 769?772. Journal of Applied Mechanics, Vol. 48, 1981.

[209] P. Gwehenberger J. Schieder, U. and K. Langwieder. Load and load securing for trucks, influences and concequences in accidents situation.

[210] S. E. Semercigil and O. F. TURAN. An improved standing-wave-type sloshing absorber. 2000a.

[211] H. Shakib and F. Omidinasab. Effect of earthquake characteristics on seismic?performance of rc elevated water tanks considering fluid level within the vessels. *Arabian Journal for Science and Engineering, Vol. 36, pp. 227-243*, 2011.

[212] P. N. Shankar. A simple method for studying low-gravity sloshing frequencies. *Proceedings: Mathematical, Physical and Engineering Sciences, Vol. 459, No. 2040, pp. 3109-3130.?157.*, 2003.

[213] P. N. Shankar and R. Kidambi. *A modal method for finite amplitude nonlinear sloshing*, page pp. 631?651. Pramana-Journal of Physics, Vol. 59, No. 4, 2002.

[214] Khaji N. Shekari, M. R. and M. T. Ahmadi. A coupled be?fe study for evaluation of seismically isolated cylindrical liquid storage tanks considering fluid?structure interaction. 2009.

[215] T. W. H. Sheu and S. M. Lee. *Large-Amplitude Sloshing in an Oil Tanker with Baffle-Plate/Drilled Holes*, pages pp. 45–60. International Journal of Computational Fluid Dynamics, Vol. 10, No. 1, 1998.

[216] Stephens D. G. Silveira, M. A. and H. W. Leonard. An experimental investigation of the damping of liquid oscillations in cylindrical tanks with various baffles. Technical report, NASA TN D-715, Langley Research Center, Langley Field, Va, 1961.

[217] A. Slibar and H. Troger. *Dynamic Steady State Behavior of a Tractor-Semitrailer-System Carrying Liquid Load*, pages 110–114. Vehicle System Dynamics, 4: 2, 1975.

[218] A. Slibar and H. Troger. *The Steady-State-Behavior of a Truck-Trailer-System Carrying Rigid or Liquid Load*, pages 167–169. Vehicle System Dynamics, 6, 1977.

[219] M. Souli and J. P Zolesio. *Arbitrary Lagrangian-Eulerian and free surface methods in fluid mechanics*, pages pp. 451–466. Computer Methods in Applied Mechanics and Engineering, Vol. 191, 2001.

[220] Ruhl R. L. Southcombe, E. and E. Kuznetsov. Fluid load analysis within the static roll model. *SAE technical paper no. 2000-01-3476*, 2000.

[221] A. Souto-Iglesias. Impact pressure test case description, 2010. Available from http://canal.etsin.upm.es/papers/SAOS2010/.

[222] D. G. Stephens and H. F. Scholl. Effectiveness of flexible and rigid ring baffles for damping liquid oscillations in large-scale cylindrical tanks. Technical report, NASA TN D-3878, Langley Research Center, Langley Station, Hampton, Va, 1967.

[223] Leonard H. W. Stephens, D. G. and M. A. Silveira. An experimental investigation of the damping of liquid oscillations in an oblate spheroidal tank with and without baffles. Technical report, NASA TN D-808.?290, 1961.

[224] I. E. Sumner. Experimental investigation of slosh-suppression effectiveness of annular-ring baffles in spherical tanks. Technical report, NASA TN D-2519, 1964.

[225] I. E. Sumner. Experimentally determined pendulum analogy of the liquid sloshing in spherical and oblate-spherical tanks. Technical report, NASA TN D-2737, 1965.

[226] R. Sygulski. *Boundary element analysis of liquid sloshing in baffled tanks*, page pp. 978?983. Engineering Analysis with Boundary Elements, Vol. 35, 2011.

[227] Li J. Tang, B. and T. Wang. *The least square particle finite element method for simulating large amplitude sloshing flows*, page pp. 317?323. Acta Mechanica Sinica, Vol. 24, 2008.

[228] Zhao M. Teng, B. and G. H. He. *Scaled boundary finite element analysis of the water sloshing in 2D containers*, page pp. 659?678. International Journal for Numerical Methods in Fluids, Vol. 52, 2006.

[229] Wendel G. R. Green S. T. Thomassy, F. A. and A. C. Jank. Coupled simulation of ?vehicle dynamics and tank slosh: Phase 2 interim report, tflrf no. 368. Technical report, U.S. Army TARDEC Fuels and Lubricants Research Facility (SwRI), Southwest Research Institute, San Antonio, TX, 2003.

[230] Bouazara M. Toumi, M. and M. J. Richard. *Impact of liquid sloshing on the behaviour of vehicles carrying liquid cargo*, page pp. 1026?1034. European Journal of Mechanics A/Solids, Vol. 28, 2009.

[231] Kana D. D. Dodge F. T. Unruh, J. F. and T. A. Fey. *Digital data analysis techniques for extraction of slosh model parameters*, page pp. 171?177. Journal of Spacecraft and Rockets, Vol. 23, No. 2, 1986.

[232] S. Ushima. *Three-dimensional arbitrary Lagrangian?Eulerian numerical prediction method for nonlinear free surface oscillations*, page pp. 605?623. International Journal for Numerical Methods in Fluids, Vol. 26, 1998.

[233] S. Ushima. *Numerical Visualization of Free Surface Oscillation Predicted with Arbitrary Lagrangian-Eulerian Method*, pages pp. 237–244. Journal of Visualization, Vol. 3, No. 3, 2000.

[234] M. Utsumi. A mechanical model for low-gravity sloshing in an axisymmetric tank. *Transactions of the ASME, Vol. 71, pp. 724-730.?156*, 2004.

[235] A. E. P. Veldman and M. E. S. Vogels. Axisymmetric liquid sloshing under low-gravity conditions. *Acta Astronautica, Vol. II, No. 10/11, pp. 641-649*, 1984.

[236] Hirt C. W. and Nichols B. D. *Volume Of Fluid (VOF) Method for the Dynamics of Free Boundaries*, pages 209–225. Journal of Computational Physics, 1981.

[237] C. Z. Wang and B. C Khoo. *Finite element analysis of two-dimensional nonlinear?sloshing problems in random excitations*, pages Ocean Engineering, Vol. 32. pp. 107?133, 2005.

[238] O?Kins J. Wasfy, T. M. and S. Smith. Experimental validation of a time-accurate finite element model for coupled multibody dynamics and liquid sloshing. 2007.

[239] O?Kins J. Wasfy, T. M. and S. Smith. Experimental validation of a coupled fluid-multibody dynamics model for tanker trucks. 2008.

[240] Green S. T. Wendel, G. R. and R. C. Burkey. *Coupled Simulation of Vehicle Dynamics and Tank Slosh: Phase 1 Report Testing and Validation of Tank Slosh Analysis, Interim Report, TFLRF No. 364*. 2002.

[241] P. Wesseling. *An introduction to multi-grid methods*. 1992.

[242] S. Wiesche. Sloshing dynamics of a viscous liquid in a spinning horizontal cylindrical tank. *Aerospace Science and Technology, Vol. 12, pp. 448?456*, 2008.

[243] Blower D. F. Ervin R. D. Winkler, C. B. and Chalasani R. M. Rollover of heavy commercial vehicles. *Heavy Vehicle Systems, Research report RR-04, Society of Automotive Engineering*, 2004.

[244] J. Woodrooffe. Evaluation of dangerous goods vehicle safety performance. Technical report, Transport Dangerous Goods, Safety and Security, Transport Canada, March 31, 2000.

[245] C. H. Wu and B. F. Chen. *Sloshing waves and resonance modes of fluid in a 3D tank by a time-independent finite difference method*, page pp. 500?510. Ocean Engineering, Vol. 36, 2009.

[246] Ma Q. W. Wu, G. X. and R. E. Taylor. *Numerical simulation of sloshing waves in a 3D tank based on a finite element method*, page pp. 337?355. Applied Ocean Research, Vol. 20, 1998.

[247] Taylor R. E. Wu, G. X. and D. M. Greaves. *The effect of viscosity on the transient free-surface waves in a two-dimensional tank*, page pp. 77?90. Journal of Engineering Mathematics, Vol. 40, 2001.

[248] Dai L. Dong M. Xu, L. and B. Setiawan. *Influence of liquid slosh on ride quality of liquid cargo tank vehicles*, pages pp. 675–684. Proceedings of the Institution of Mechanical Engineers, Part D: Journal of Automobile Engineering, Vol. 218, 2004.

[249] G. Yan and S. Rakheja. Straight-line braking dynamic analysis of a partly filled baffled and unbaffled tank trucks. 2009.

[250] Guorong Yan. *Liquid slosh and its influence on braking and roll responses of partly filled tank vehicles.* PhD thesis, Concordia university, Montreal, Quebec, Canada, 2008.

[251] Rakheja S. Yan, G. and K. Siddiqui. *Experimental Study of Liquid Slosh Dynamics in a Partially-Filled Tank*, pages pp. 071303: 1–14. Journal of Fluids Engineering, Vol. 131, 2009.

[252] Rakheja S. Yan, G.R. and K. Siddiqui. Baffle design analysis for a road tanker: Transient fluid slosh approach. *SAE International*, 2008.

[253] Rakheja S. Yan, G.R. and K. Siddiqui. Analysis of transient fluid slosh in partly-filled tanks with and without baffles: Part 1 model validation. *Int. J. Heavy Vehicle Systems, Vol. 17, Nos. 3/4, 2010*, 2010.

[254] Rakheja S. Yan, G.R. and K. Siddiqui. Analysis of transient fluid slosh in partly-filled tanks with and without baffles: Part 2 role of baffles. *Int. J. Heavy Vehicle Systems, Vol. 17, Nos. 3/4, 2010*, 2010.

[255] Siddiqui K. Rakheja S. Yan, G. and K. Modaressi. Transient fluid slosh and its effect on the rollover-threshold analysis of partially filled conical and circular tank trucks. *Int. J. Heavy Vehicle Systems, Vol. 12, No. 4, 2005*, 2005.

[256] Z. Ye and A. M. Birk. *Fluid pressures in partially liquid-filled horizontal cylindrical vessels undergoing impact acceleration*, pages pp. 449–458. Journal of Pressure Vessel Technology, Vol. 116, 1994.

[257] Wang B. Ma X. Yin, L. and J. T. Zou. *he nonlinear sloshing of liquid in tank with pitching*, page pp. 1032?1034. Journal of Applied Mechanics, Vol. 66, 1999.

[258] Li J. F. Zhou, H. and T. S. Wang. *Simulation of liquid sloshing in curved-wall containers with arbitrary Lagrangian?Eulerian method*, page pp. 437?452. International Journal for Numerical Methods in Fluids, Vol. 57, 2007.

[259] Richard M. J. Ziarani, M. M. and S. Rakheja. Optimizations of liquid tank geometry for enhancement of static roll stability of partially-filled tank vehicles. *Heavy Vehicle Systems, Int. J. of Vehicle Design, Vol. 11, No. 2, 2004*, 2004.